AUGMENTATION OF HEAT TRANSFER DURING CONDENSATION OVER FINNED TUBES

A THESIS

submitted in fulfilment of the
requirements for the award of the degree
of
DOCTOR OF PHILOSOPHY
in
MECHANICAL ENGINEERING

By

RAVI KUMAR

DEPARTMENT OF MECHANICAL AND INDUSTRIAL ENGINEERING
UNIVERSITY OF ROORKEE
ROORKEE-247 667 (INDIA)

FEBRUARY, 1998

CANDIDATE'S DECLARATION

I hereby certify that the work which is being presented in the thesis entitled **'AUGMENTATION OF HEAT TRANSFER DURING CONDENSATION OVER FINNED TUBES'** in fulfilment of the requirement for the award of the Degree of Doctor of Philosophy and submitted in the Department of Mechanical and Industrial Engineering of the University is an authentic record of my own work carried out during a period from September,1992 to February,1998 under the supervision of Professor H.K.Varma, Professor K.N.Agrawal and Dr. Bikash Mohanty.

The matter presented in this thesis has not been submitted by me for the award of any other degree of this or any other university.

Ravi Kumar

(RAVI KUMAR)

This is to certify that the above statement made by the candidate is correct to the best of our knowledge.

(H.K.VARMA)	**(K.N.AGRAWAL)**	**(BIKASH MOHANTY)**
Director	Professor	Assistant Professor
Moradabad Institute of Technology	Mech. & Ind. Engg. Deptt.	Chem. Engg. Deptt.
Moradabad	University of Roorkee	University of Roorkee
	Roorkee	Roorkee

Date: 17.02.98

The Ph.D. Viva-Voce examination of **Ravi Kumar**, Research Scholar, has been held on. 8th April, 2000

Signature of supervisor(s)	**Signature of H.O.D.**	**Signature of External Examiner**
	Prof. & Head	
	Deptt. of Mech. and Indl Engineering	
	University of Roorkee	
	Roorkee-247667	

ABSTRACT

The surface condensers are widely used in the refrigeration and air-conditioning, petro chemical and process industries, thermal and atomic power plants and allied industries. Many augmentation techniques, to improve the vapour to coolant heat transfer rate, have been reported in literature. These techniques can reduce the size of condensers in a significant manner. A thorough review of literature shows that the enhancement in condensing side heat transfer coefficient will augment the heat transfer in the surface condensers. The heat transfer coefficient can be enhanced many folds by the simple technique of providing integral-fins over the tube surface. Therefore, an experimental investigation has been planned and carried out to study the augmentation of heat transfer by enhancing the condensing side heat transfer coefficient and heat flux during condensation of the saturated vapour of steam, refrigerant R-12 and R-134a over 14 horizontal tubes including 11 integral-fin tubes with different fin geometries. R-134a is a new environment friendly refrigerant with thermo-physical properties closer to those of R-12. R-134a has zero ozone depletion potential and ten percent global warming potential in comparison to R-12. Hence, R-134a is seen as a suitable replacement of R-12.

The investigation was initiated by acquiring data for the condensation of steam, R-12 and R-134a over a plain tube in two experimental set-ups(set-up #1 for steam and set-up #2 for R-12 & R-134a). The results for the condensation over a plain tube established the integrity of each of the experimental set-up. The plain tube results are also used as reference data for the comparison of the performance of other finned tubes.

In past, several investigations have been carried out to find the optimum fin density(fin-spacing) for the condensation of steam over circular integral-fin tubes(CIFTs) and it has been established by these investigators that a CIFT with 390 fpm fin density and 1.5 mm fin spacing produces maximum

increase in heat transfer rates and yields 2 to 3 times augmentation in heat transfer coefficient. The R-134a is a new refrigerant in the market and the information regarding the thermal performance of R-134a during condensation over horizontal tubes is not available in the literature. Therefore, the experiments have been conducted for the condensation of steam over a CIFT with 390 fpm fin density and in the case of R-134a the fin density was systematically varied to establish the best value by four CIFTs (934 fpm, 1250 fpm, 1560 fpm and 1875 fpm). The 1560 fpm fin density tube turned out to be the best performing tube with an enhancement factor, EF, equal to 5.63. For the condensation of steam over 390 fpm tube the enhancement factor, EF, has been found to be 2.27.

All the data for the condensation of steam have been acquired by varying the temperature of saturated steam in a range of 373K-395K. The cooling water flow rate was varied from 8.0 litres per minute to 28.0 litres per minute (or approximately 480 kg/hr to 1680 kg/hr). However, for the condensation of R-134a the temperature of condensing fluid has been kept at 312±0.5K (approximate temperature of refrigerant in the condenser of a refrigeration plant) and cooling water flow rate was varied from 400 kg/hr to 1050 kg/hr.

In order to further increase the heat transfer coefficient, the spine integral-fin tubes(SIFTs) are introduced. The spines are generated by cutting axial slots on the surface of best performing CIFT. The depth of slots is purposely kept less than the height of the circular fins to ensure the proper drainage of the condensate from the tube surface. The experiments for the condensation of steam and R-134a vapours over these tubes are performed. It is discovered that in comparison to CIFT the SIFTs further increase the heat transfer coefficient by approximately thirty percent for the condensation of steam and fifteen percent for the condensation of R-134a. Later, to investigate the position on the tube surface where spines are most effective, partially-spined circular integral-fin tubes(PCIFTs) are manufactured. These tubes have the spines either on the upper half or on the lower half of the surface of the best performing CIFT. The dividing plane lies on the axis of the tube.

For the condensation of R-134a the spines in the lower half of the tube surface have enhanced the heat transfer coefficient by 11 percent in comparison to the best performing CIFT. Similarly, for the condensation of steam the spines in the lower half of the tube have enhanced the heat transfer coefficient by approximately 20 percent in comparison to the best performing CIFT. For the condensation of R-134a the spines are not effective in the upper half of the tube. However, to some extent, these are effective in the upper half of the tube for the condensation of steam and provide five percent enhancement in comparison to the best performing CIFT.

An uncertainty analysis of the experimental results has also been carried out. The uncertainty in condensing side heat transfer coefficient for the condensation of steam has remained in the range of 2-4 percent. Whereas, the uncertainty in the condensing side heat transfer coefficient for the condensation of R-134a falls in a range of 4-8 percent.

The experimental results have been compared with those predicted by several analytical models. The experimental data are in best agreement with the widely accepted Honda and Nozu model. Approximately 80 percent of experimental data agree with this model in an error band of ±20 percent.

From the present experimental results a correlation has also been developed between different dimensionless numbers to find the condensing side heat transfer coefficient . The dimensionless heat transfer coefficient is expressed in the form of Condensation number(CN) and has been correlated with the condensate Reynolds number(Re), condensate Weber number(We) and non-dimensional tube geometry(Y).

$$CN = 0.024 Re^{-1/3} We^{0.3} Y^{1.4}$$

$$\text{Where, } CN = h_o \left[\frac{\mu^2}{k^3 \rho^2 g} \right]^{1/3}$$

$$Re = \frac{4\dot{m}}{\mu P_f}$$

$$\dot{m} = \rho . AF . V_f$$

$$\text{Weber number}(We) = \frac{\partial p / \partial x}{\rho g} = \frac{\frac{2\sigma}{ef}\left(\frac{1}{rt} + \frac{1}{rb}\right)}{\rho g}$$

$$Y = \frac{4AF}{D_r P_f}$$

and $$AF = \pi\left[\left(\frac{D_o^{\,2} - D_r^{\,2}}{2}\right) + D_o tt + D_r(P_f - tb)\right]$$

The correlation has predicted approximately 90 percent of experimental data for the condensation of steam and R-134a over CIFTs and SIFTs in a range of ±15 percent. The correlation is recommended up to a fin density of 1560 fins per meter for the condensation of R-134a over CIFTs. It has also been validated by the experimental results of other investigators for the condensation of steam and different refrigerants. The developed correlation has predicted the experimental results of other investigators for the condensation of refrigerants in a range of ±30% and those for the condensation of steam in a range of ±35 percent.

ACKNOWLEGMENTS

The author takes this opportunity to express his deep gratitude to all those, who have made it possible for him to submit this work in the hands of learned elite.

The author expresses his deep sense of gratitude and indebtedness to his revered guides Professor H.K.Varma, Diroctor, Moradabad Institute of Technology, Dr. K.N.Agrawal, Professor, Mechanical and Industrial Engineering Department, University of Roorkee, Roorkee and Dr. Bikash Mohanty, Assistant Professor, Chemical Engineering Department, University of Roorkee, Roorkee who provided whole hearted co-operation, never ending inspirations and guidance, all blended with the personal touch throughout the duration of this work. Their painstaking efforts during experimentation, invaluable suggestions and thorough discussions have immensely contributed towards the completion of this work.

Thanks are also due to Professor J.S.Saini, Head, Mechanical and Industrial Engineering department, and Professor S.C.Gupta, officer-in-charge, Heat Transfer Research Laboratory, Chemical Engineering Department for providing various facilities and help during the completion of this work.

Sincere thanks are also due to Prof. B.S.Varshney, Director, Meerut Institute of Engineering & Technology, Meerut, for his suggestions and help during this work.

The author sincerely acknowledges the help rendered by M/s Du Pont Inc., United States of America, for providing a free of cost sample of refrigerant R-134a to carry out the present research work. Thanks are extended to Mr. Jugjiv Singh and Mr. K. Ganesh of Du Pont South Pacific for expediting the supply of R-134a.

The thanks are also due to M/s Gaurav Reprographic Ltd., Dehradun for their assistance during initial investigations of this work.

The author wishes to thank his colleague in the Mechanical and Industrial Engineering Department, Mr. R.M.Sarviya and Mr. Mahesh Kumar Gupta and in the Heat Transfer Research Laboratory, Chemical Engineering Department, Mr. B.B. Gulyani, Mr. Sailander Kumar, Mr. Anuj Jain and Mr. C.B.V. Vittal for their advice and help during this work.

The author also extends his thanks to Mr.Loti Ram and Mr.P.S.Dhiman of Instrumentation laboratory of Mechanical and Industrial Engineering Department for their help in machining, manufacturing and installation of experimental set-ups and test-sections. The thanks are also due to Mr.S.P.Garg, Mr. Mukhtar, Mr. Surendra Kumar, Mr. Satyaveer, the staff of Refrigeration and Air-Conditioning Laboratory, Mechanical and Industrial Engineering Department for their help in the commissioning of the experimental set-up for the condensation of refrigerants and Late Sri J.P. Varma, Mr. Suresh Sharma, Mr. Rajkumar and Mr. Puran Singh of Heat Transfer Research Laboratory, Chemical Engineering Department for their assistance in the commissioning the experimental set-up for the condensation of steam. Author also wishes to thank Mr Umesh and Mr. Harbans Singh for operating the steam boiler.

Finally, the author wishes to express his handful of regards towards his esteemed father Late Mr.M.N. Kulshrestha for his endless motivations and thanks his mother, sister Rachana and wife Shikha who stood with him when he was dealing with the problem.

(RAVI KUMAR)

CONTENTS

LIST OF FIGURES

LIST OF PHOTOGRAPHS

LIST OF TABLES

NOMENCLATURE

avg.	average
a.d.	average deviation
A	total surface area of the test-section surface, m^2
AF	area of the test-section surface for one pitch length, m^2
A_i	inside tube surface area, m^2
AMTD	arithmetic mean temperature difference, $T_s - (T_{ci}+T_{co})/2$, K
A_f	fin surface area, m^2
A_r	area at fin root diameter, $\pi D_r L$, m^2
A_t	area od fin tip, $\pi D_o tt.L.P_f^{-1}$, m^2
A_o	test-section area at the fin tip, $\pi D_o L$, m^2
A_p	fin cross section area, m^2
A_r	outside tube surface area, $\pi D_r L$, m^2
C_i	Sieder-Tate type correlation coefficient
CIFT	circular integral-fin tube
C_o	Nusselt's model coefficient
Cp	specific heat, $kW.kg^{-1}.K^{-1}$
C_b	fraction of flooded tube surface
CN	condensation number
D	diameter of test-section, m
D_H	hydraulic diameter, m
ef	height of the circular fin, m
EF	enhancement factor, $(h_o)_{finned\ tube}/(h_o)_{plain}$ at same ΔT_f
emf	electro motive force, mVolts

es	height of spine fin, m
fpm	fins per meter, m^{-1}
f_m	coolant flow rate, $kg.hr^{-1}$
f_q	coolant flow rate, litres per minute
g	acceleration due to gravity, ms^{-2}
h	heat transfer coefficient, $kWm^{-2} K^{-1}$
h_b	heat transfer coefficient in the flooded region, $kWm^{-2} K^{-1}$
h_{fc}	heat transfer coefficient due to fin conduction, $kWm^{-2} K^{-1}$
h_i	inside tube heat transfer coefficient , $kWm^{-2} K^{-1}$
h_o	outside tube heat transfer coefficient, $kWm^{-2} K^{-1}$
k	thermal conductivity of condensate, Wm^{-2}-K^{-1}
k_t	thermal conductivity of fin tube material, Wm^{-2}-K^{-1}
k_b	thermal conductivity of coolant bulk, Wm^{-2}-K^{-1}
L	tube length, m
LMTD	log mean temperature difference, K
lpm	litres per minute
$\dot{m}$	condensate flow rate, $kg.sec^{-1}$
max.	maximum
$\dot{m}_c$	coolant flow rate, $kg.sec^{-1}$
min.	minimum
N	total number of fins
Nu	Nusselt's number, $h_o D_r k^{-1}$
Pr	Prandtl number, $\mu C_p k^{-1}$
P	pressure of condensing steam, kPa
P_e	perimeter of the fin, m
PCIFT	partially-spined circular integral-fin tube
P_f	Fin Pitch, m

q	Heat flux, kWm^{-2}
$\dot{Q}$	rate of heat transfer, kW
r^2	sum of the residues in regression
rb	$(P_f-tb)/2$
Re	Reynolds number
rt	tt/2
R_w	thermal resistance of tube wall
S_f	fin spacing, m
SF	correction factor
SIFT	spine integral-fin tube
S_m	length of condensate profile on the fin surface, m
tt	fin thickness at the tip of the fin, m
tb	fin thickness at the root of the fin, m
T	temperature
T_b	bulk temperature of cooling water, $(T_{ci}+T_{co})/2$, K
T_c	cooling wate temperature, K
T_{ci}	cooling water inlet temperature, K
T_{co}	cooling water outlet temperature, K
T_s	vapour saturation temperature, K
T_{wi}	inside tube average wall temperature, K
T_{wo}	outside tube average wall temperature, K
U_o	Over all heat transfer coefficient, kW/m^2-K
V	Cooling water velocity, ms^{-1}
V_f	velocity of condensate on the tube surface, ms^{-1}
We	Weber number
Y	$4AF.D_r^{-1}P_f^{-1}$

SUBSCRIPTS

AW	Adamek and Webb
b	coolant bulk
BK	Beatty and Kadz model
HN	Honda and Nozu
I	inside
o	outside
Owen	Owen Sardesai Smith an Lee
r	fin root
RW	Rudy and Webb
suh	spines in upper half of test-section
slh	spines in lower half of test-section
Webb	Webb et al.

SYMBOLS

ρ	density of condensate, kgm^{-3}
ρ_b	density of cooling water, kgm^{-3}
λ	latent heat of vaporisation, $kJ.kg^{-1}$
μ	dynamic viscosity, Pa-s
ν	kinematic viscosity, m^2s^{-1}
ΔT_f	temperature drop across the condensate film (T_s-T_{wo}), K
η_f	fin efficiency
σ	surface tension
θ	half angle at the fin tip, radian
θ_c	half angle at the spine tip, radian

θ_m	angular change along the fin surface
ϕ	angle of condensate retention, radian
ς	fin profile factor

CHAPTER #1

Introduction

The enhancement in heat transfer has concerned the research scientists since the earliest documented studies of heat transfer. In his pioneering paper directed towards development of a temperature scale, Newton in the year 1701 A.D. suggested an effective way of increasing the convective heat transfer, '.... not in a calm air, but in a wind that blew uniformly upon it....'. Joule in the year 1861 A.D. reported significant improvement in the 'conductivity' or overall heat transfer coefficient for in-tube condensation of steam when a wire, spiralled around the condenser tube, was inserted in the cooling water jacket. In spite of these earlier efforts, this aspect of heat transfer received a little attention until about thirty years ago. In fact, the field begun to develop in the mid-1950s in response to the need for more efficient heat exchangers in the power generation, the advent of commercial nuclear power plants and space flight systems. Another factor associated with the sharp increase in activity with the heat recovery and alternate energy systems was stimulated by the 1973 oil crisis.

Inside surface condensers, the condensation of vapour takes place over the horizontal tubes. The condensation of vapour over horizontal tubes has an academic as well as industrial importance. The largest present-day use of surface condensers is in refrigeration & air-conditioning, petro-chemical and other process industries, thermal & atomic power plants and other allied industries. With rapid growth in industrialisation, the surface condensers will continue to have more and more applications in various industrial processes.

For many years, surface condensers were designed with smooth horizontal tubes and there was a little motivation for improving heat transfer in the condensers. The energy crisis and the requirement

of compact design of condensers were the major driving forces behind the use of finned tubes in place of plain tubes inside the condensers. These tubes were initially used to increase the heat transfer by increasing the surface area and thus, increasing the tube surface area per unit length of the tube. Later on, it was discovered that the circular integral-fin tubes enhance the condensing side heat transfer coefficient more than that the increase in surface area due to finning. This phenomenon is primarily due to the surface tension of the condensate, which helps in thinning of the condensate film on the fin surface.

A review of literature reveals that concerted efforts have been made by different research workers to acquire experimental data and to develop theoretical models for the prediction of condensing side heat transfer coefficient of a single horizontal low integral-fin tube. However, many of these investigations are reported only for the low surface tension fluids such as refrigerants. The condensation of high surface tension fluids viz. steam, also takes place in many industrially important heat transfer applications. The geometric factors which influence the performance of integral-fin tubes involve fin pitch, fin thickness, fin shape and fin size.

It has been observed in almost all the investigations that the condensate is retained in the inter-fin spacing due to the capillary action and as the fin spacing is reduced the angle of condensate retention is increased. The retained condensate hampers the heat transfer. With the further increase in fin density the surface area also increases, which provides more area for heat transfer. Therefore, if the fin density is systematically increased a fin spacing is attained when the heat transfer coefficient is maximum. This optimum fin spacing is a function of the thermo-physical properties of condensing fluid. A review of literature shows that optimum fin spacing for a large number of fluids is not known and hence, research efforts are needed to bridge the gap.

The augmentation in the heat transfer during condensation of the vapour of low surface tension fluids viz. refrigerants is also important to refrigeration and air-conditioning industry. Many investigations have been carried out to find an optimum fin density for the condensation of low pressure refrigerants

viz. R-11 and R-113. However, the data during condensation of high pressure refrigerants e.g. R-12, R-21 and R-22 are scarce and no systematic approach has been made to find the optimum fin density for the condensation of these refrigerants. A little and scattered information is available about the condensation of these refrigerants over horizontal integral-fin tubes. Therefore, there is a need for an orderly investigation of the condensation of these fluids over the finned tubes.

Some investigators have found that the spine fins, generated by cutting the axial slots of the depth of fin height on the surface of the horizontal circular integral-fin tube with the optimum fin spacing can further enhance the condensing side heat transfer coefficient. However, investigations related to condensation of different fluids on spine fins or other configurations which give better performance than finned tube are hardly available and thus call for research efforts.

When the condensation of vapour takes place over a horizontal tube, the surface temperature of the tube fluctuates. Therefore, the determination of condensing side heat transfer coefficient by the wall temperature measurement technique is considered quite difficult. To cope-up with this problem, many investigators have also recommended the use of modified Wilson plot technique for the computation of condensing heat transfer coefficient. However, the data on comparison of the direct measurement and the modified Wilson plot for the prediction of condensing side heat transfer coefficient are available for a limited number of fluids and tube-geometries.

It would be of industrial importance if a correlation is developed between the condensing side heat transfer coefficient in the form of Condensation Number and the different dimensionless numbers containing the thermo-physical properties of condensing fluid and the geometry of the finned tube.

A decade ago, it was discovered that the cholorofluorocarbons(CFC's) such as R-11, R-12, R-113 etc. and hydrcholorofluorocarbons(HCFC's) viz. R-22 cause damage to the ozone layer in the atmosphere. In 1987, an international group of scientists and government officials established the Montreal protocol- an agreement to control the use and release of CFC's and to schedule the

time-table for eliminating their production. This agreement was a historic step in the ongoing process of building consensus regarding environmental impacts of CFC's. Therefore, nowadays, there is a serious concern among the scientists and engineers to find a suitable replacement of CFC's. The R-134a, a hydrofluorocarbon(HFC), has been recommended as a replacement of R-12. In hydrofluorocarbons(HFCs) the chlorine molecules of CFC's has been replaced by the hydrogen molecule because the chlorine molecule in the CFC's is responsible for the ozone depletion.

The greenhouse gases allow solar radiation to pass through the earth's atmosphere, but limit the amount of energy which can later be radiated back into the space. The greenhouse effect helps maintaining a temperature on earth consistent with the needs of living things. However, lately, higher concentration of certain gases like carbon dioxide in atmosphere has resulted in global warming due to excessive greenhouse effect. The cholofluorcarbon(CFC) group of refrigerants has also been implicated for its bad effects on the global environment because they belong to a category of chemicals known as the greenhouse gases. The global warming potential of R-134a is very low and is only ten percent of that of R-12.

Keeping the above enunciated facts in view, an experimental investigation has been carried out to study the heat transfer during condensation of a high surface tension fluid i.e. steam and a low surface tension fluid i.e. R-134a over horizontal finned tubes. Well instrumented experimental apparatus were designed and fabricated to carry out the present investigation with the following objectives.

OBJECTIVES:

1. To study the heat transfer characteristics during condensation of steam and refrigerants over single horizontal tubes, both plain and with different geometries of fins.

2. To compare the performance of R-12 and R-134a during condensation over a horizontal plain tube followed by an experimental investigation to determine the optimum fin density for the condensation of R-134a over horizontal circular integral-fin tubes(CIFTs).

3. To compare the performance of a spine-integral fin tube(SIFT) with a circular integral-fin tube(CIFT) of optimum fin density for the condensation of steam and R-134a. In case, the SIFT outperforms the CIFT then determination of better position of spine fins on the tube surface (upper half or lower half of the tube) for the condensation of steam and R-134a.

4. To explore the validity of modified Wilson plot technique for the determination of condensing side heat transfer coefficient for the condensation of steam, R-12 and R-134a over horizontal plain and finned tubes.

5. To Scrutinise the available models to identify the best model for the prediction of condensing side heat transfer coefficient for the condensation over circular integral-fin tubes with the help of present experimental data.

6. To develop an empirical correlation for the condensing side heat transfer coefficient as a function of dimensionless numbers consisting of the thermo-physical properties of condensing fluids (steam and R-134) and the tube geometry.

CHAPTER #2

Literature Review

A literature review has been carried out regarding the condensation of pure vapours over a horizontal integral-fin tube. The literature review facilitates a clear insight of the phenomenon of the condensation of saturated pure vapours over horizontal integral-fin tubes.

2.1 CONDENSATION OF PURE VAPOURS OVER A HORIZONTAL INTEGRAL-FIN TUBE

The condensation of pure vapours inside a surface condenser takes place when the saturated vapour comes in contact with the cold surface of the condenser tubes and exchange heat with the tube wall. Subsequently, the heat from the tube wall is carried away by the coolant flowing inside the tube. The augmentation in heat transfer from vapour to cooling water can reduce the size of condensers in a significant manner. The heat transfer rate from vapour to the tube wall can be improved either by lowering temperature of tube surface or by enhancing the condensing side heat transfer coefficient at constant vapour to tube wall temperature difference. A survey of literature shows that the heat transfer coefficient during condensation over horizontal tube can be augmented by providing circular integral-fins over the tube surface. The literature review presented here has been summarised in two categories, viz. the theoretical models to predict the condensing side heat transfer coefficient and the experimental investigations to determine the heat transfer coefficient during condensation of pure vapours over a horizontal integral-fin tube.

2.2 DETERMINATION OF CONDENSING SIDE HEAT TRANSFER COEFFICIENT DURING CONDENSATION OF PURE VAPOURS OVER A HORIZONTAL CIRCULAR INTEGRAL-FIN TUBE BY ANALYTICAL MODELS

In the last fifty years several analytical models have been developed to compute the condensing side heat transfer coefficient during condensation of pure vapours over a horizontal integral-fin tube. Some important models have been discussed below in details :

2.2.1 Beatty and Katz Model

Kenneth O. Beatty and Donald L. Katz[4] were the pioneers in presenting a theoretical model for the condensation of pure vapours over a horizontal circular integral-fin tube. They assumed the gravity-driven condensate drainage on the tube surface. The tube was divided into two parts viz. fins and the horizontal cylinder. During condensation of vapour, the heat transfer coefficient of the fins was calculated with the Nusselt's theory for a vertical plane and the heat transfer coefficient of horizontal cylinder was determined using the Nusselt's theory for a horizontal cylinder. At last, these heat transfer coefficients were added on the basis of their proportional contribution in the total tube surface area. The analysis arrived at the following equation to calculate the outside tube heat transfer coefficient during condensation of pure vapours over a horizontal circular integral-fin tube(CIFT).

$$h_{BK} = 0.725\left(\frac{k^3\rho^2 g\lambda}{\mu\Delta T_f}\right)^{0.25}\left(\frac{A_r}{A_{ef}D_r^{0.25}} + 1.3\eta_f\frac{A_f}{A_{ef}L_f^{0.25}}\right) \qquad (2.1)$$

Where, L_f is the characteristic length of fin and A_{ef} is the equivalent area of the tube. Both have been calculated by the following equations (2.2) and (2.3) respectively.

$$L_f = \left(\frac{D_o^2 - D_r^2}{4D_o}\right) \qquad (2.2)$$

$$A_{ef} = A_r + \eta_f A_f \tag{2.3}$$

Equation (2.1) was used successfully in refrigeration and air-conditioning industries for many years. However, it was confirmed only by the experimental data for low fin density and low surface tension fluids. The surface tension brings forth the retention of condensate in the inter-fin spacing at the bottom of the tube which hampers the vapour to tube wall heat transfer and simultaneously, helps in thinning the condensate film on the unflooded fins surface. The thinner film on the unflooded fin surface yields higher heat transfer coefficient. These two opposite trends due to surface tension cancel out each other, thereby, unintentionally extending the range of validity of the expression. Although, it was also observed that the condensate retention between the fins is high for the higher surface tension fluids yet the flooding of inter-fin space at the bottom of the tube was not taken into account while developing the model. The effect of surface tension on condensate drainage was also neglected.

Besides developing theoretical model, Beatty and Katz also conducted experiments using Methyl chloride, Sulphur dioxide, R-22, Propane, n-butane and n-pentane as condensing fluids. Investigations for the condensation of R-22 were made on a series of tubes with different fin heights and tube materials. The condensing side heat transfer coefficients were determined by the Wilson plot. The experimental data matched with their own developed model in a range of +7.2% to -10.5% by modifying constant 0.725 in equation (2.1) to 0.689.

The geometry of the test-section tubes used by Beatty and Katz has been shown in Table-2.1.

Table-2.1

dimensions of test-sections used by Beatty and Katz[4]

s.no.	fin thickness inches			fin height inches	tube diameter inches		
	base	middle	top		inside	root	top
1	0.023	-	0.013	0.0575	0.5274	0.625	0.740
2	-	-	0.013	0.063	0.5430	0.622	0.748
3	0.037	-	0.013	0.341	0.6510	0.750	1.450
4	0.037	-	0.029	0.136	0.6810	0.768	1.040
5	0.041	0.026	0.016	0.295	0.6827	0.757	1.347
6	0.037	0.025	0.013	0.321	-	0.768	1.410
7	0.037	-	0.021	0.243	-	0.768	1.254

2.2.2 Karkhu and Brovkov Model

V.A. Karkhu and V.P. Borvkov[35] were first to realize the importance of surface tension for the condensation of pure vapours over horizontal integral-fin tubes. They studied the film-wise condensation of pure vapours on a finned tube with trapezoidal shaped fins. The fin surface was divided into two regions viz. fin crest and fin trough. It was assumed that the condensate flows along the fin side walls to the fin root under the influence of surface tension only. As the condensate touches the trough region, its starts flowing along the tube circumference only under the influence of gravity. The heat transfer in trough region due to large fin thickness was neglected. It was also proposed that the 1/6th of the tube circumference was flooded with condensate for all the cases. In order to develop the model, a uniform radial pressure gradient along the fin flank was given by the equation (2.4).

$$\frac{\partial p}{\partial x} \approx \frac{\Delta p}{\Delta x} \approx \frac{\sigma \cos\theta}{rt(ef - \Delta)} \qquad (2.4)$$

Where, 'Δ' is the local thickness of the condensate in the channel and 'rt' is the radius of curvature of the condensate at the fin tip. The 'rt' was determined by the following equation

$$rt = \frac{tt}{2}(1+\tan\theta) \tag{2.5}$$

Finally, the following equation was proposed to determine condensing side heat transfer coefficient

$$h_{KB} = \frac{G(Z_b)\lambda}{A_s \Delta T_f} \tag{2.6}$$

Where,

$$Z_b = 1.6H^{0.2}(1-0.35H^{-0.3}\dot{m}) \tag{2.7}$$

$$\dot{m} = \frac{tb}{2.ef.\tan\theta} \tag{2.8}$$

and

$$H = \frac{1.4\sigma^{1/4}\mu^{3/4}k^{3/4}D_o(T_s - T_{wo})^{3/4}}{\rho^{7/4}ef^{7/2}\left((tt+tb)/4\right)^{1/4}\lambda^{3/4}(\sin\theta)^3(1+\tan\theta)^{1/4}(\cos\theta)^{1/4}} \tag{2.9}$$

The experiments on finned tubes were also conducted during condensation of pure vapours of steam and R-113. The geometry of test-section has been shown in Table-2.2. The brass tube showed 50 to 100 percent improvement in heat transfer coefficient, whereas, the copper tube did not show any improvement in heat transfer coefficient during condensation. All the experiments were carried out at an absolute vapour pressure of 110 kPa and their model agreed with their own experimental data in the range of ±5 percent.

Table-2.2

dimensions of test-sections used by Karkhu and Brovkov[35]

material	fin-density fpm	fin height mm	semi-vertex angle degree	tube diameter mm
Brass	1238	0.92	16	18
	782	0.92	28.5	18
	1224	1.32	11.5	18
Copper	487	2.05	16.5	17

2.2.3 Rudy and Webb Model

T.M.Rudy and R.L.Webb[73] developed an analytical model to predict the condensing side heat transfer coefficient for a horizontal circular integral-fin tube. They modified the Beatty and Katz model[4] and incorporated the effect of surface tension which has hostile as well as beneficial effects on the performance of integral-fin tubes. Due to surface tension, the condensate is retained in the inter-fin spacing at the bottom of tube and hence, hampers the heat transfer. On the other hand, the surface tension tends to reduce the thickness of condensate film in the non-flooded region of the tube which results in the enhancement in heat transfer coefficient. An insignificant heat transfer in the flooded portion was assumed and therefore, it was neglected in the analysis. The flooding of the bottom of the tube by the condensate has been shown in Figure 2.1. The 'ϕ' is the angle of condensate retention.

The basic model form has been created in two parts (part-1. model for condensate flooding, and part-2. model for the condensation over unflooded surface area) and is represented by the equation (2.10).

$$h_{RW} = \left[\frac{A_b}{A_o}0.725\left(\frac{J\sigma g}{D_r \Delta T_f}\right)^{0.25} + 0.943\eta_f \frac{A_b}{A_o}\left(\frac{J\sigma}{ef^2}\left(\frac{rt+rb}{rt.rb.\Delta T_f}\right)\right)^{0.25}\right]\left[\frac{360-2\phi}{360}\right] \quad (2.10)$$

Where, $A_o=\pi D_o L$ and $A_b=\pi D_r S_f N$ The 'ϕ' have been calculated by the following equation.

$$\phi = \cos^{-1}\left(\frac{D_o - 2.0H_{avg}}{D_o}\right) - \left(\frac{\phi_1+\phi_2}{2}\right) \quad (2.11)$$

and

$$H_{avg} = \frac{\sigma\left(2.0ef - \frac{(tt+tb)}{2.0}\right)}{ef.\rho.g.S_f} \quad (2.12)$$

They conducted experiments to validate the model using R-11 as a condensing fluid for the condensation over circular integral-fin tubes(CIFTs). The fin geometry of these tubes are shown in Table-2.3.

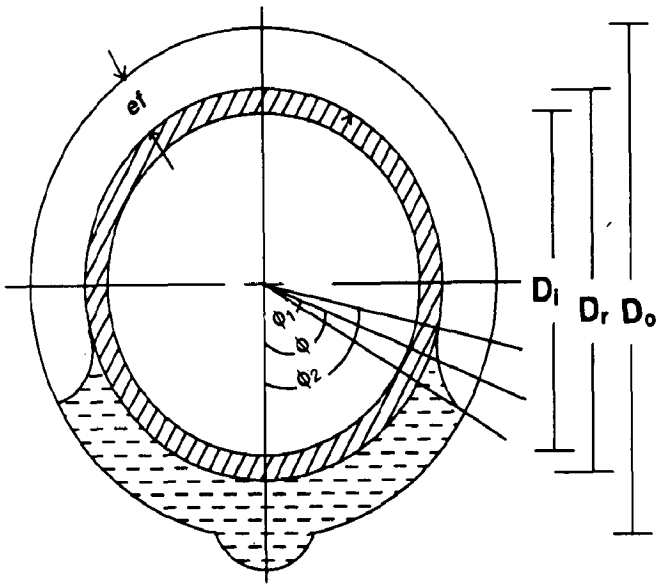

Figure 2.1

The condensate retention in the bottom of a circular integral-fin tube

Table-2.3

fin-geometry used by Rudy and Webb[73]

fin density fpm	**fin thickness** mm		**fin spacing** mm	**fin height** mm
	top	**average**		
748	0.1	0.3	1.0	1.5
748	-	0.4	0.9	0.85
1024	0.1	0.3	0.7	1.53
1378	0.1	0.2	0.5	0.89

The integral-fin tube with fin density of 1378 fpm showed the best performance. In fact, the performance of tubes increases with the fin density, obviously, because of this reason the tube of 748 fpm fin density produced the poorest results. It was realised that the model starts underpredicting the heat transfer coefficient as the fraction of flooded surface increases. For example, during condensation of R-11 over the 1378 fpm fin density tube, the model underpredicted the heat transfer coefficient by 10%. The model overpredicted the test data of 1024fpm tube by 25% and those for 748fpm tube by 30%. They improved predictions in condensing side heat transfer coefficient based on the linear pressure gradient from top of the fin to the root of the fin and indicated that integral-fin geometry could be conceived to enhance the heat transfer coefficient and would display better performance than the plain tube at the same vapour to tube wall temperature difference.

2.2.4 Owen, Sardesai, Smith and Lee Model

Owen et al. model[63] considered the heat transfer in the flooded portion of the tube as well, contrary to Rudy and Webb[1983], who considered the flooded part of the tube inactive in heat transfer which resulted the underprediction of heat transfer coefficient for higher fin density tubes. According to Owen et al., heat is also transferred in the region of retained condensate. The following equation was evolved to predict the heat transfer coefficient

$$h_{Owen} = (1 - C_b)h_{BK} + C_b\left(\frac{1}{h_{fc}} + \frac{1}{h_o}\right)^{-1} \tag{2.13}$$

Where,

$$C_b = \frac{\cos^{-1}\left(1 - \frac{4\sigma}{\rho g D_r S_f}\right)}{\pi} \tag{2.14}$$

and

$$h_{fc} = \left(1 - \frac{S_f}{P_f}\right)k_f + \left(\frac{S_f}{P_f}\right)k \tag{2.15}$$

This extended model predicted the heat transfer coefficient for all the experimental data of Beatty and Katz within 30%. This model proved more accurate in situations where appreciable fraction of tube surface was flooded with the condensate fluid. The model also concluded that not only the surface tension but also the ratio of surface tension to gravity force, i.e., σ/ρ, quantify the degree of condensate retention on the integral-fin tube.

2.2.5 Webb, Rudy and Kedzierski Model

R.L.Webb, T.M.Rudy and M.A.Kedzierski[92] developed a model to predict the condensation heat transfer coefficient on a horizontal circular integral-fin tube. Their model included surface tension-drainage on the fin surface and gravity drainage on the inter-fin surface. The heat transfer in the flooded part of the tube was also considered. Their proposed model is valid for high surface tension fluids and low surface tension fluids as well.

$$h_{WRK} = (1 - C_b)\left[h_h \frac{A_r}{A_o} + \eta_f h_f \frac{A_f}{A_o}\right] + C_b h_b \tag{2.16}$$

The value of C_b has been calculated by the following equation

$$C_b = \cos^{-1}\left[1 - \frac{2\sigma(P_e - tb)}{\rho g D_o (P_f - A_p)}\right] \tag{2.17}$$

The, h_h is calculated from the Nusselt's equation for heat transfer taking into account the additional condensate film thickness because of the condensate drainage from the fins.

The Nusselt's equation can be written in the form of condensate Reynolds Number as

$$h_h = 1.514\left(\frac{\mu^2}{k^3\rho^2 g}Re\right)^{-1/3} \tag{2.18}$$

and

$$Re = \frac{4.0\dot{m}_r}{\mu(P_f - tb)} \tag{2.19}$$

The h_h has been determined by employing the iterative method given below.

1. calculate the condensation rate on the fin surface by

   $\dot{m} = \eta_f h_f A_f \Delta T_f / \lambda$

2. take initial value of $\dot{m}_r = \dot{m}$

3. determine h_h from equation (2.18) and simultaneously calculate the condensate Reynolds number from equation (2.19)

4. calculate q_h by the equation $q_h = h_h . A_r . \Delta T_f$

5. calculate $\dot{m}_r = \dot{m} + q_h / \lambda$

6. iterate till the value of $\dot{m}_r$ converge

The heat transfer coefficient in the flooded region, h_b, was calculated as, $h_b=\varphi k/ef$. Where, $\varphi=qb_2/qb_1$ and $qb_1=kA\Delta T_f/ef$ and $qb_2=h_bA\Delta T_f$.

The condensing heat transfer coefficient on fin surface, h_f, has been calculated by the following equation.

$$h_f = 2.149\left(\frac{k}{S_m}\right)\left(\frac{\sigma\lambda\theta_m S_m(\zeta+1)}{\nu k\Delta T_f(\zeta+2)^3}\right)^{0.25} \qquad (2.20)$$

The parameters 'ζ' characterises the aspect ratio of the fin cross-section. The aspect ratio (height/thickness) increases as ζ decreases. The S_m is the length of the convex surface on which the condensate film flows over and θ_m is the angle through which the convex surface turns from its origin to S_m. As value of 'ζ' becomes higher on negative side e.g. -0.9, the fin profile is more "flat-sided" over a large portion of fin length. The value of 'ζ' between -0.77 and -0.85 was chosen to approximate the shape of the fins. It was suggested that a special precisely defined curvature on the fin side is not necessary. The model clearly established that surface tension controls the condensate drainage from the fins and that surface tension is responsible for the condensate bridging(retention) in the bottom part of the tube. This model predicted the heat transfer coefficient within ±20 percent of experimental value obtained by condensing R-11 on finned tubes of 748 fpm, 1024 fpm and 1378 fpm fin density.

2.2.6 Honda and Nozu Model

A complete approach to develop a model for the condensation over horizontal finned tubes was given by Honda and Nozu[25]. The tube was divided into unflooded(u) and flooded(f) regions. The unflooded region was devided in thin film region towards the fin tip and thick film region towards the

bottom. In thick film region, it was assumed that the radius of curvature of the liquid- vapour interface, r_b, varies with position around the tube according to following equation:

$$r_b = \frac{\sigma}{\rho g z} \tag{2.21}$$

$$\text{Where,} \quad z = \frac{D_o}{2}(1+\cos\phi) \tag{2.22}$$

Based on their numerical results, approximate expressions for the Nusselt's numbers in both the unflooded (Nu_{du}) and flooded(Nu_{df}) regions were obtained. Their final expression came into the following form.

$$Nu_{HN} = \frac{Nu_{du}\eta_u\left(1-\bar{T}_{wu}\right)\bar{\varphi}_f + Nu_{df}\bar{\eta}_f\left(1-\bar{T}_{wf}\right)\left(1-\bar{\varphi}_f\right)}{\left(1-\bar{T}_{wu}\right)\bar{\phi}_f + \left(1-\bar{T}_{wf}\right)\left(1-\bar{\phi}_f\right)} \tag{2.23}$$

Where, $\bar{\phi}_f = \frac{\phi}{\pi}$ and the dimensionless temperature is equal to $\frac{T-T_c}{T_s-T_c}$

The results predicted by the model were compared with the experimental data of various investigators (11 fluids and 22 tubes). Most of the data agreed with the model in a range of ±20 percent.

2.2.7 Adamek and Webb Model

Adamek and Webb model[2] accounts for condensation on all surfaces in the flooded and unflooded regions of the finned tube. The model is applicable to fins of two different basic profile shapes: the special continuous profile shape and fins with a rectangular or trapezoidal shape. In this model, the fin surface was divided in the different segments and the condensate generated on each segment was calculated. It was considered that the condensate on the tube surface drain either under gravity

or under surface tension of condensate. The effectiveness of these forces on different segments was determined and followed by the determination of film thickness associated with the particular segment. For laminar film condensation, the local condensation was computed as the ratio of the thermal conductivity of condensate and the thickness of the condensate film.

For gravity drained laminar film condensation in a particular segment, the thickness of condensate film was determined by the following equation

$$\delta(l) = \left[\frac{F_p . l_{ik}}{\rho g . \cos\theta}\right] \tag{2.24}$$

Where l_{ik} is the length of a particular segment on the fin surface.

and

$$F_p \equiv \frac{4k\nu\Delta T_f}{\lambda} \tag{2.25}$$

The condensate drainage from the length l_{ik} has been calculated as

$$\dot{m}(l_{ik}) = 0.943\left[\left(k\Delta T_f . l_{ik}/\lambda\right)^3\left(\rho g/\nu\right).\cos\theta\right]^{1/4} \tag{2.26}$$

If the surface tension is the dominant drainage force in a particular region l_{ik}, the surface tension induced pressure gradient is

$$\partial p/\partial s = -\sigma.\frac{\partial(1/r)}{\partial s} \tag{2.27}$$

Where, 'r' is the local radius of the condensate interface and 's' is the distance along the fin contour. It was assumed that a linear pressure gradient exists in all such surface tension drained region. Hence, for a generalised region l_{ik}

$$\partial p/\partial s \equiv -\sigma\left[1/r_k - 1/r_i\right]/l_{ik} \tag{2.28}$$

r_i and r_k are the radii at the beginning and end of the length l_{ik}, respectively.

The condensate drainage under the surface tension was calculated by the following equation

$$\dot{m}(l_{ik}) = \frac{\Delta T_f}{\lambda} \int_0^{ik} \frac{k}{\delta_{ik}(x)} dx \tag{2.29}$$

The heat transfer coefficient has been computed by the following equation

$$h_o = \frac{\lambda \sum \dot{m}}{A \Delta T_f} \tag{2.30}$$

$$A = \frac{L}{P_f}(A_f + A_r + A_t) \tag{2.31}$$

The model also predicted the experimental data of other investigators in a range of ±15 percent for the condenation of refrigerants and steam.

2.3 EXPERIMENTAL DETERMINATION OF HEAT TRANSFER COEFFICIENT DURING CONDENSATION OF PURE VAPOURS OVER A HORIZONTAL CIRCULAR INTEGRAL-FIN TUBE

In actual practice, the analytical models have often failed to predict accurately the condensing side heat transfer coefficient during condensation over a horizontal integral-fin tube. Therefore, several experimental investigations were carried out to find the condensing side heat transfer coefficient during condensation of pure vapours over a horizontal integral-fin tube. The experiments carried out with the different condensing fluids can be classified as follows:

2.3.1 High Surface Tension Fluids

High surface tension fluids are assumed to be those fluids which have the surface tension more than 0.05 Pa-m. The steam falls under this category and all the investigations discussed hereunder have been carried out only for the condensation of steam.

Katz and Geist[36] studied the condensation of steam over a vertical grid of six horizontal finned tubes and the Wilson plot technique was applied to determine the condensing side heat transfer coefficient. The difference between the predicted and experimental values of heat transfer coefficient was not more than 14 percent and the average heat transfer coefficient for the six tubes was approximately ten percent less than that for the top most tube.

Bromley[10] carried out experiments on a 300 fpm fin density tube with a fin profile chosen to yield a very high heat transfer along the top portion of the fins. However, he did not report his heat transfer results. In the following years, Karkhu and Brovkov[35] discovered an increase of 50-100 percent in the heat transfer coefficient for the condensation of steam over horizontal finned tubes. The condensation took place on copper and brass finned tubes of trapezoidal fin shape. In fact, a significant enhancement in heat transfer coefficient was attained by Mills et al.[53]. They conducted experiments for the condensation of steam on grooved tubes of 19.0 mm diameter with a fin density of 1420 fpm and a fin height of 0.46 mm. The enhancement up to 5.5 times over the smooth tube was obtained. The investigations were carried out over copper, brass, silver and stainless steel tubes. It was reported that the thermal conductivity has a significant effect on enhancement in the heat transfer coefficient. Rifert[69] investigated the condensation of steam on four integral-fin tubes with rectangular fins, four tubes with trapezoidal fins and one tube with small wavy fins. He observed that enhancement in heat transfer depends upon fin geometry and fin spacing to a very high extent. He varied the fin spacing systematically and came to the conclusion that as the fin spacing is reduced the heat transfer increases. He noticed the enhancement in heat transfer coefficient two times as compared to a smooth tube.

In fact, Yau et al.[96,97,98], Wanniacachchi et al.[86,87,88] and Marto et al.[44] made a systematic approach to augment the condensing side heat transfer coefficient during condensation of steam and renewed the interest in using the circular integral-fin tubes for high surface tension fluids viz. steam.

Yau et al.[97] conducted experiments on thirteen copper integral-fin tubes with rectangular cross section and identical fin height and fin thickness i.e. 1.59 mm and 0.5 mm, respectively. All the tubes had 12.7 mm fin root diameter. They changed the fin spacing from 20 mm to 0.5 mm. Data were collected on three different vapour velocities of 0.5, 0.7 and 1.1 m/s. It was found that a fin spacing of 1.5 mm is an optimum fin spacing giving an enhancement factor of the magnitude of 3.5 in comparison to a plain tube. The heat transfer coefficient increased with velocity of condensing vapours and at 1.1 m/s vapour velocity, it was 15 to 20 percent more than that at the vapour velocity of 0.5m/s.

Wanniarachchi et al.[86,87,88] conducted experiments on thirty copper tubes of root diameter 19.0 mm. All the tubes had rectangular shape fins and the fin spacing varied from 0.5 mm to 9.0 mm. The fin height and the fin thickness also varied from 0.5 mm to 2.0 mm and 0.5 mm to 1.5 mm respectively. The data were acquired at 1m/s and 2 m/s vapour velocity. The pressure of condensing steam remained atmospheric pressure and 85 mm Hg vacuum. It was reported that the enhancement was most sensitive to the fin spacing which was found to be 1.5 mm for the condensation of steam. The fin height and the fin thickness also influenced the performance of the tube and their optimum values were 2.0 mm and the 1.0 mm, respectively. They discovered the augmentation in heat transfer coefficient of the order of 6.5 in comparison to a plain tube at 100 kPa, 450 kPa and 85 mm Hg vacuum.

Marto et al.[44] reported that parabolic fin profile can enhance the performance of tube by 10 to 15 percent for the same fin spacing, fin height and fin thickness. They concluded that the effect of fin shape is not as profound as the fin spacing.

Mitrou[54] also conducted experiments for condensation of steam on spirally threaded tubes of copper, aluminium, copper-nickel and stainless steel and showed that tube wall material could alter the results considerably, which is in general agreement with the findings of Shklover et al.[76] and Mills et al.[53] From these results it is clear that decreasing thermal conductivity of the fin creates an increased thermal resistance in the fin, hence, a lower fin efficiency. This, in turn, leads to lower values of film condensation heat transfer over the finned tubes.

2.3.2 Medium Surface Tension Fluids

Medium surface tension fluids are those fluids which have surface tension between 0.05 to 0.025 Pa-m. Masuda and Rose[50] studied the condensation of ethylene glycol on thirteen finned tubes at atmospheric pressure. The tube with 1.0 mm fin spacing was found to be the best performing tube.

2.3.3 Low Surface Tension Fluids

Those fluids which have surface tension less than 0.025 Pa-m are regarded as the low surface tension fluids. Almost all the Chlorofluorocarbons(CFCs) fall under this category. Out of these, most of the investigations have been carried out only for the condensation of R-11 and R-113.

Carnavos[11] carried out investigations for the condensation of R-11 on a number of copper finned tubes having fin density between 1060 fpm to 1650 fpm and fin heights between 0.37 mm to 1.32 mm. Heat transfer enhancements over the smooth tube at the same temperature difference of 10K across the condensate film was about 3-4 times. The specially manufactured N-2 tube with fin density of 1260 fpm and fin height 0.508 mm with trapezoidal cross section produced the best results.

Webb et al.[89] and Rudy & Webb [73,74] conducted experiments for the condensation of R-11 on copper tubes having fin density of 748, 1024 and 1378 fpm with trapezoidal fin cross section. The best performance was displayed by the 1378 fpm tube at vapour to tube wall temperature difference

of 3K. The tube had a fin spacing of 0.513 mm at the fin tip and a fin height of 0.89 mm. The performance of this tube was superior to 748 fpm tube by 45 percent. Sukhatme and co-workers[83] reported the results of an extensive experimental investigations for the film-wise condensation of R-11 over enhanced tubes. They did experimental investigations during condensation of R-11 on trapezoidal shape integral-fin tubes. The fin density, the fin height and the semi-vertex angle, θ, of fins were varied systematically. The fin density was varied from 945 fpm to 2205 fpm with a constant vertex angle, θ, of 30 degree. In fact, the fins were cut as American Standard Screw Threads with a semi-vertex angle of 30 degree. Therefore, the fin height varied from 0.69 mm for 945 fpm to 0.29 mm for 2205 fpm tube. The 1417 fpm tube displayed the best performance by enhancing the heat transfer coefficient by approximately 10 times that of a plain tube. For the 1417 fpm fin density tube, the semi-vertex angle was changed from 30 degree to 10 degree and the fin height from 0.46 mm to 1.22 mm. The heat transfer coefficient was found to be a function of the fin height. The semi-vertex angle had an insignificant affect on the heat transfer coefficient. On the 1417 fpm tube eighty axial 'V' shape grooves were cut. The depth of grooves was varied from 0.7 to 1.22 mm. The semi-vertex angle of grooves was 10 degree. These grooves generated pyramadical shape spines on the tube surface. It was resolved that the fin of pyramadical shape further enhanced the heat transfer coefficient by approximately twenty percent. They explained it to occur by thinning the condensate film on the crest of the fin due to the surface tension pull in two directions.

Experimental studies have also been conducted on the condensation of R-113 on a horizontal integral-fin tube. Honda et al.[21] conducted experiments on three low integral-fin tubes of 1020, 1563 and 2000 fpm fin density, and a thermoexcel-C tube. The 2000 fpm tube had rectangular fins and remaining two tubes had the trapezoidal shaped fins. The 2000 fpm tube was found to enhance the heat transfer coefficient 8.8 times than that for a plain tube and the thermoexcel-C tube enhanced the same by 9 folds. The superior performance of 2000 fpm tube may be due to low fin spacing. Honda et al.[21] also acquired data for the condensation of R-113 vapour over a specially enhanced thermoexcel-C surface which handed out the maximum augmentation in heat transfer

coefficient of the order of 9.0. Some tubes were also fitted with the drainage strips to attain further improved performance. Masuda and Rose[49] entered into the investigation on fourteen integral-fin tubes having rectangular shape fins with the same tube diameter, fin thickness and fin height. The fin spacing was systematically varied from 20 mm to 0.25 mm. The fin spacing of 0.5 mm was found to be the optimum fin spacing. At this fin spacing, the augmentation in heat transfer coefficient of 7.3 was yielded. Marto et al.[46] have reported a study for the condensation of R-113 over rectangular integral-fin tubes. They conducted experiments on a tube of fin root diameter of 19.05 mm and the fin spacing was varied from 4.0 mm to 0.25 mm. They also reported that the optimum spacing existed between 0.25 mm to 0.5 mm and the augmentation in heat transfer coefficient ranged between 4-7 times of that for the plain tube.

Katz et al.[37] measured the condensing side heat transfer coefficient during condensation of R-12 on six different finned copper tubes and a plain copper tube. The fin density varied from 151 fpm to 630 fpm, the fin height from 8.28 mm to 1.42 mm and the tube diameter from 9.47 to 19.63 mm. The enhancement in heat transfer coefficient was reported to vary between 0.77 to 1.5. The fin density of 630 fpm having a fin height of 1.4 mm was concluded as the best performing tube.

Ivanov[31] conducted the experiments for the condensation of R-12 vapour on the bundle of plain tubes and finned tubes of 500 fpm and 1111 fpm fin density. They found the heat transfer coefficient for the finned tubes much higher than that for the plain tubes. Kabov[34] measured the heat transfer coefficient for the condensation of R-12 on 1333 fpm brass finned tube and he used eight copper finned tubes of 385 to 1875 fpm fin density for the condensation of R-21. The fin spacing was varied from 0.75 mm to 2.0 mm and fin height between 0.87mm and 2.5mm. He found that fin spacing was one of the principal parameters controlling the heat transfer.

Dorokhov[15] studied experimentally the condensation of R-21 on finned horizontal tubes with fin densities of 800 to 500 fpm and fin height of 0.62 mm, 1.5 mm and 2.2 mm, respectively. He indicated a rise in the heat transfer coefficient with increase in vapour velocity, but the improvement

for tubes with fin density of 800 fpm did not exceed 30 percent at a maximum vapour velocity of 5.2 m/s. Gogonin and Dorokov[18] reported experimental results for the condensation of R-21 on two different 800 fpm copper tubes over a range of vapour velocities, operating pressure and heat fluxes. They compared their results with those for a plain tube and reported that the enhancement in the condensing side heat transfer coefficient for the finned tubes was very small in comparison to that for smooth tubes.

Beatty and Katz[4] have reported the condensation of R-22 on a series of specially machined tubes of 15.9 mm to 19.5 mm fin root diameter, 1.5-6.2 mm fin height and 272 fpm to 608 fpm fin density. The data were not collected for the condensation over the plain tube. In fact, the data were acquired only for the validation of their theoretical model with which the experimental results agreed in a range of +7.2 to -10.2%.

2.4 EFFECT OF DIFFERENT PARAMETERS ON HEAT TRANSFER COEFFICIENT

The effect of different parameters on condensing side heat transfer coefficient have been discussed below in details.

2.4.1 Effect of Fin Geometry

Several investigators have accomplished experiments by varying the fin geometry (i. e. fin spacing, fin height, fin thickness and fin-shape) with a variety of condensing fluids including steam and refrigerants (specially R-11 and R-113). It has been found that the value of condensing side heat transfer coefficient is most sensitive to fin density vis a vis fin spacing. As the fin spacing is reduced, the heat transfer coefficient is enhanced significantly and also with reduction in the fin spacing, the inundation angle, ϕ, is increased resulting a reduction in the fractional tube surface area available for heat transfer. Hence, an optimum fin spacing was always concluded when the fin density was varied systematically. For the condensation of steam the value of optimum fin spacing was found to be nearly 1.5 mm. The 0.62 mm fin spacing at the fin tip for the condensation of R-11 and fin

spacing between 0.25 mm and 0.5 mm for the condensation of R-113, have been found optimum for the best performing tubes. Next to fin density, the heat transfer coefficient is sensitive to the fin height and the fin thickness.

As the fin height increases, the condensing side heat transfer coefficient also increases. After a certain value, the increase in the fin height does not contribute in the improvement of condensing side heat transfer coefficient. For steam, a fin height of 1.0 mm with 1.0 mm fin thickness for the best performing tube has been recommended[87]. The shape of the fin also has a considerable affect on the heat transfer coefficient. The experimental results of Marto et al.[44] showed that the performance of a parabolic shape fin was about fifteen percent better than that of rectangular shape fin for the same fin density (fin spacing). The very precise parabolic fin shapes were manufactured by electric discharge machining.

2.4.2 Effect of Tube Material

Most of the experimental studies for the condensation of the pure vapours over horizontal tubes have been made on copper tubes. Majority of theoretical models do not show any effect of thermal conductivity of the tube material in the prediction of condensing side heat transfer coefficient. However, the model by Owen et al.[63] shows that the value of condensing side heat transfer coefficient increases marginally with increase in thermal conductivity of tube material. Same trend can also be inferred from Honda and Nozu model[25]. Whereas, the effect of the thermal conductivity of tube material by Honda and Nozu modal is quiet appreciable as compare to Owen et al. model. In fact, the thermal conductivity of the tube material influences the fin efficiency as well as the circumferential heat transfer and hence, affects the condensing side heat transfer coefficient.

2.4.3 Effect of The Surface Tension of Condensate

The surface tension of condensate is a very important factor not only for determining the condensing side heat transfer coefficient but also to decide optimum fin density. For the same fin density, the condensing fluids of different surface tensions will yield different heat transfer coefficients. The surface tension causes the thinning of the condensate film on the fin surface. The condensate film is thinner for the high surface tension fluids. That is why, the augmentation in heat transfer coefficient is always more than the tube surface area increase due to finning.

The surface tension is also responsible for the flooding of the bottom of the finned tube with the condensate. The inundation angle, ϕ, is a function of σ/ρ[63]. Normally, for a higher surface tension fluid, the inundation angle is high. It is also high for high fin densities. Since, the flooded zone of tube hampers the heat transfer, the value of heat transfer coefficient is reduced. Therefore, the effect of surface tension force is predominant at the high fin density as on high fin density.

2.4.4 Effect of The Thermal Conductivity of Condensate

It is a known fact that the thermal conductivity of condensate plays an important role in determining the condensing side heat transfer coefficient, as the heat transfer coefficient is approximated by the ratio of thermal conductivity of the condensate and the condensate film thickness on the fin surface. The thermal conductivity of condensate is, therefore, incorporated in every analytical model. In fact, the condensing side heat transfer coefficient increases with the rise in thermal conductivity of condensate.

2.4.5 Effect of The Viscosity of Condensate

There are no experimental studies available to study the effect of the viscosity of a condensing fluid. Simultaneously, all theoretical models have included the viscosity of condensate for predictiing heat transfer coefficient. This can be understood by the physics of viscous fluids. Since, the flowability of high viscous fluids is low, it retards the drainage of condensate from the tube surface which in turn

increases the thickness of condensate layer on the fin surface. All this results in the lower value of condensing side heat transfer coefficient.

2.5 INDIRECT DETERMINATION OF CONDENSING SIDE HEAT TRANSFER COEFFICIENT

The condensing side heat transfer coefficient can also be determined without measuring the wall temperature of the test-section. Wilson[94], has devised such a technique as described below:

2.5.1 Wilson Plot Technique

Wilson has recommended a method to determine the condensing side heat transfer coefficient without measuring the tube wall temperature. The over all thermal resistance is given in the following equation (2.32).

$$\frac{1}{U_o A_r} = \frac{1}{h_i A_i} + \frac{1}{h_o A_r} + R_w \tag{2.32}$$

The over all heat transfer coefficient, U_o, can also be calculated from the respective equations for the heat balance and the heat transfer rate as shown below:

$$\dot{Q} = \dot{m}_c Cp_b (T_{co} - T_{ci}) \tag{2.33}$$

$$\dot{Q} = U_o A_r LMTD \tag{2.34}$$

Where,

$$LMTD = \frac{T_{co} - T_{ci}}{\ln\left(\frac{T_s - T_{ci}}{T_s - T_{co}}\right)} \tag{2.35}$$

Therefore, for a known value of tube wall thermal resistance, R_w, the condensing side heat transfer coefficient, h_o, can be calculated and the value of inside tube heat transfer coefficient, h_i, is obtained from the Sieder-Tate equation[78].

Further, based on the analysis of experimental data, Wilson[94] concluded that for a small range of cooling water temperature rise the inside tube heat transfer coefficient, h_i, is proportional to $V^{0.8}$. He also noted that a plot for U^{-1} as abscissa and $V^{-0.8}$ as ordinate is a straight line. Thus, he recommended that the intercept of Y-axis of this straight line depicts the sum of the resistances due to tube wall and condensing steam. Since, at the infinite cooling water velocity, the $V^{-0.8}$ will be zero and so the inside tube thermal resistance will turn zero.

The Wilson plot is based on the tacit assumption that the condensing side film resistance remains constant even when water velocity and thereby coolant side thermal resistance changes. During condensation, it is only possible when heat flux has been maintained constant while varying the cooling water velocity. In fact, this can be realised by varying vapour saturation temperature such that heat flux remains constant even as the water velocity is changed. It is very difficult to attain this type of condition. To cope with the difficulty of maintaining constant heat flux at different cooling water velocities, Briggs and Young[9] recommended an extensive modification to this technique.

2.5.2 Modified Wilson Plot Technique

The Briggs and Young[9] modified the Wilson plot technique. The equation (2.32) has been modified as follows

$$\left(\frac{1}{U_o} - R_w\right)G = \frac{A_r G}{C_i A_i F} + \frac{1}{C_o} \tag{2.36}$$

Where,

$$G = \left(\frac{k^2 \rho^2 g \lambda}{\mu D_r (T_s - T_{wo})}\right)^{0.25} \tag{2.37}$$

$$F = \frac{k_b}{D_i} Re_b^{0.8} Pr_b^{1/3} \left(\frac{\mu_b}{\mu_w} \right)^{0.14} \tag{2.38}$$

In fact, the equation (2.36) is a simple linear form of

$$Y = \left(\frac{1}{C_i} \right) X + \frac{1}{C_o} \tag{2.39}$$

With a change in cooling water velocity, the value of Y and X changes. The inverse of the slope of the best fit line at different values of Y and X yields the C_i which is subsequently used to determine the inside tube heat transfer coefficient. The inverse of Y-axis intercept gives the value of C_o. The condensing side heat transfer coefficient is determined by the following equation

$$h_o = C_o G \tag{2.40}$$

The detailed procedure to determine the condensing side heat transfer coefficient by modified Wilson plot technique has been discussed in Appendix-D.

2.6 COOLING WATER SIDE THERMAL STABILIZATION

In case of forced convection heat transfer inside a tube, the rate of heat transfer varies along the length of the tube. The heat transfer coefficient is maximum at the inlet and then it drops sharply to a certain limit value which remains constant as shown in Figure 2.2. Such a change in heat transfer coefficient is dependent upon the thermal conductivity of the fluid flowing inside the test-section. For a value of high value of thermal conductivity, fluids demand low stabilisation length.

In Figure 2.3 the shape of the characteristic curve shows that the local heat transfer coefficient decreases with the tube length asymptotically. The asymptotic value h_∞ is equal to the average heat transfer coefficient for a tube of infinite length. To obtain the average heat transfer coefficien, h_i, for

any tube length, the graphical integration of the curve of local heat transfer coefficient, h_x, and the tube length is done up to that length. Mohanty[57] has suggested an equation of the following from

$$\frac{h_i}{h_\infty} = 1 + SF\frac{x}{D_i} \tag{2.41}$$

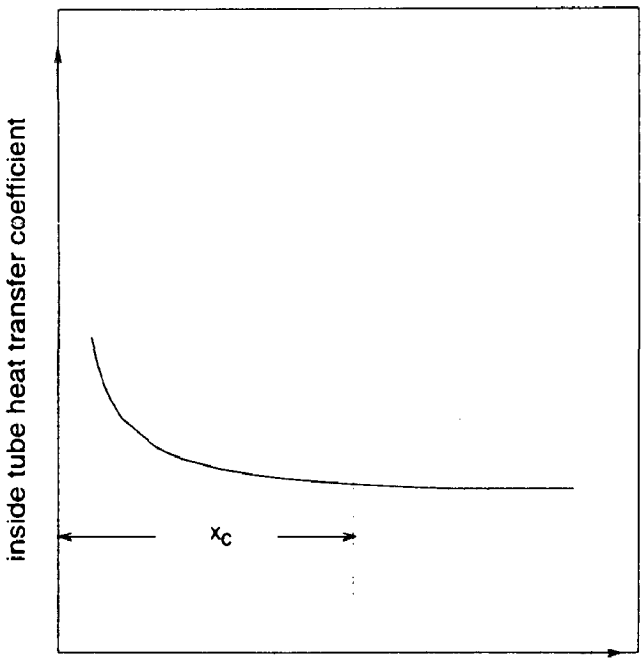

Figure 2.2
Variation of inside tube heat transfer coefficient
along the tube from the tube entrance

For $x/D_i \geq 50$ the value of SF has been considered constant. Al-Arabi[3] analysed data of seven investigators, generated for air, water and oil for Reynolds number ranging from 5,000 to 100,000 and Prandtl number 0.7 to 75. He proposed the following equation for the estimation of SF for the short tubes ($l/D_i \leq 50$).

$$\frac{SF.Pr_b^{1/6}}{(L/Di)^{0.1}} = 0.68 + \frac{3000}{Re_b^{0.81}} \tag{2.42}$$

Sieder-Tate equation[78] suggested the following equation for the initial value of cooling ware side heat transfer coefficient.

$$h_i = \frac{C_i k_b}{D_i} Re_b^{0.8} Pr_b^{1/3} \left(\frac{\mu_b}{\mu_w} \right)^{0.14} \qquad (2.43)$$

The heat transfer coefficient, h_i, from equation (2.43) should be corrected for the thermal entrance consideration. The correct value of inside heat transfer coefficient be estimated by the following equation suggested by [3].

$$h_i = h_i \left(1 + SF \left(\frac{L}{D_i} \right) \right) \qquad (2.43)$$

The thermo-physical properties of cooling water are to be determined at mean temperature of cooling water.

2.7 EFFECT OF CHOLOROFLUOROCARBONS(CFCs) ON ENVIRONMENT

Some 15 km above the earth surface approximately 24 km thick mist of ozone gas in the stratosphere prevents the ultra violet radiation in the sun rays to enter the atmosphere of the earth. Currently, it has been discovered that cholorofluorocarbons(CFCs), the commonly used refrigerants viz. R-11, R-12, R-113 etc. damage the ozone layer of the earth atmosphere. Therefore, nowadays, there is a serious concern among the scientists and engineers to find a suitable replacement of CFCs. Recently, the R-134a, a hydrocholorofluorocarbons(HFC), has been recommended as a replacement of R-12. In HFCs, the chlorine molecule of CFCs has been replaced by the hydrogen molecule because the chlorine molecule in the CFCs is responsible for the ozone depletion and the global warming characteristic of the CFCs.

The greenhouse gases allow solar radiation to pass through the earth's atmosphere, but limit the amount of energy which can later be radiated out into space. The greenhouse effect helps

maintaining a temperature on earth consistent with the needs of living things. Higher concentration of certain gases like carbon dioxide in atmosphere has resulted in global warming due to excessive greenhouse effect. Certain gases, like carbon dioxide and the refrigerants i.e. CFCs or cholofiocarbons(CFCs) have been implicated for their effects on the global environment because they belong to a category of chemicals known as the greenhouse gases. In Table-2.4 a comparison has been made between the different CFCs for their global warming potential(GWP) and ozone depletion potential(ODP). The global warming of carbon dioxide has been regarded a unit of the global warming potential and the ozone depletion potential of R-11 has been taken as a reference to compare the ODP of other refrigerants.

Table-2.4

ozone depletion potential and global warming potential of refrigerants

s.no.	chemical	chemical formula	ozone depletion potential	global warming potential	estimated atmospheric life (years)
Cholorofluorocarbons					
1	R-11	CCl_3F	1.00	1300	59
2	R-12	CCl_2F_2	0.93	3700	122
3	R-113	CCl_2FCClF_2	0.83	1900	98
Hydrochlorofluorocarbons					
1	R-22	$CHClF_2$	0.05	510	18
2	R-123	$CHCl_2CHF_2$	0.02	28	2
Hydrofluorocarbon					
1	R-134a	CF_3CH_2F	0	400	18

Though, the CFCs account only for 0.004% of the total mass of greenhouse gas emissions compared to 93.6% for carbon dioxide. Their relative contribution to global warming potential are 9.5% and 71.5%, respectively. Therefore, CFCs have much higher potential as global warming gases per unit mass. The use of R-134a in place of R-12 will reduce much concerned ozone depletion by CFCs to zero, whereas, the global warming will be reduced to approximately 10 percent of that by R-12.

2.8 CONCLUDING REMARKS

There has been consistent efforts to augment the heat transfer during condensation over horizontal tubes by enhancing the condensing side heat transfer coefficient for the condensation of a number of fluids. Most of the work has concentrated on the condensation of steam and refrigerants because they carry a lot of importance in the industrial applications. The optimum fin density for the condensation of steam has been discovered by many investigators but no work has been reported for the condensation of steam on the spine fins. Since, steam is a high surface tension fluid. This type of fins may be very useful for further augmentation in heat transfer coefficient.

The most of the investigators have concentrated their research efforts for the augmentation of heat transfer coefficient during condensation of low pressure refrigerants i.e. R-113 and R-11. A little and scattered published work is available regarding the condensation of high pressure refrigerants i.e. R-22 and R-12. The information about the optimum fin density for these refrigerants is not available in the literature.

As the conventional refrigerants are going to be phased-out due to their bad effect on the environment, the new substitutes of these refrigerants have entered the market. The R-134a is one of the alternative environment friendly refrigerants and has been regarded a suitable substitute of R-22 and R-12[17]. Since, R-134a is a new refrigerant in the market, the optimum fin spacing of R-134a has yet to be known and at the same time the performance of R-134a during condensation over spine fins is required to be investigated.

CHAPTER #3

Experimental Set-up and Instrumentation

The present investigation has been carried out for the condensation of steam, R-12 and R-134a with the objectives detailed in Chapter #1. Two separate experimental set-ups were designed and installed. One for the condensation of steam and the another for the condensation of refrigerants. The data for the condensation of steam over horizontal tubes were acquired using experimental set -up #1, for the condensation of R-12 and R-134a vapours the data were acquired using experimental set-up #2. In this Chapter, the design considerations, details of set-up #1, set-up #2 and instrumentation used, are described.

3.1 DESIGN CONSIDERATIONS

To obtain accurate and reliable experimental data, keeping the test-section tube in horizontal orientation was one of the most important design considerations. To ensure this, the test-section was held inside the test-condenser shell by specially manufactured chuck-nuts and the horizontal orientation of test-section was checked with a spirit level.

The hydrodynamic stabilisation of cooling water flow inside the test-section was another important design criterion. This was achieved by fixing a tube length more than $50D_i$ on upstream side of the test-section and more than $20D_i$ on downstream side of test-section. The inside diameter of the tube and that of test-section were equal.

An inverted U-bend beyond the outlet of the test-section was provided to make sure that the test-section was fully flooded with cooling water during the test-runs. To measure the cooling water

temperatures at the inlet and the exit of the test-section, the thermocouple pockets were installed ahead of the upstream-calming section($\geq 50D_i$) and after the down stream calming section($\geq 20D_i$). This was done so as to avoid any change in the flow pattern of the cooling water and subsequently, the inside tube heat transfer coefficient. Further, these calming sections were thermally insulated to prevent the heat exchange between cooling water and the ambience.

The presence of non-condensables i.e. air in the condensing vapour, even though in a very small quantity, alters the condensing side heat transfer coefficient significantly. Therefore, keeping the condensing vapour free from air or other non-condensables was very important. This was accomplished by providing a purge valve in the test-condenser. As the complete removal of air from the experimental set-up is imperative, an auxiliary condenser in addition to the purge valve was also employed.

To avoid the vapour shear effect on the test-section a near zero momentum of vapour is desired in the test-condenser. For the condensation of steam it was achieved by providing a perforated plate in the top portion of the test-condenser with several small holes. The nascent momentum of the entering steam was reduced significantly by positioning a cup on the perforated plate just below the inlet port of steam. This reduces the steam velocity practically to a negligible value and it was uniformly distributed throughout the test-condenser. Moreover, the steam inlet port was located away from to the vertical plain of the test-section tube.

The total test-scheme incorporated several test-sections with different fin spacings and configurations. This involved repeated replacements of test-section tubes. Therefore, the test apparatus were designed for easy removal of one tube and installation of the replacement tube. In case of refrigerants(R-12 and R-134a) in experimental set-up #2, this would result in loss of certain amount of refrigerant in replacing tubes, in checking and repairing leakages. This was a tedious job and special care was taken for good workmanship during the initial setting up of the test apparatus. The test-condenser was made as a compact entity so that when the test-section was changed the

loss of refrigerant was minimum. Keeping in view the compactness of the test-condenser, a blind ended tube of 6.5 mm diameter parallel and 35 mm above the test-section was connected to the vapour inlet port. This tube had 125 holes of 1.0 mm diameter along the tube length facing the roof of the test-condenser. So that the vapour coming out from these holes struck the roof of the test-condenser. The vapour lost its initial momentum and was distributed uniformly throughout the length of the test-section.

It was thus ensured that the velocity of the condensing vapour was less than 0.1m/s for the condensation of steam as well as R-134a. Which is much below the velocity of condensing vapour required to make the vapour shear effective(0.5m/s).

3.2 EXPERIMENTAL SET-UP FOR THE CONDENSATION OF STEAM [Set-Up #1]

The experimental set-up for data acquisition during condensation of steam over a plain tube and horizontal integral-fin tubes has been described below:

3.2.1 General Layout

Photo 3.1 and Figure 3.1 stand for the photographic and schematic views of experimental set-up. The set-up consists of a test-condenser(5). Inside the test-condenser, the test-section(9) was fixed with the help of two chuck nuts(8). The steam was generated in an oil fired boiler from demineralised water and was supplied to the test-condenser via valve V3. The test-condenser was connected to the condensate vessel(16) to collect the condensate and remove the air from the test-condenser through a vent(14). The excess steam was condensed in the auxiliary condenser(11), connected with the condensate vessel. The cooling water was supplied from a water tank(3). The water inside the test-section was circulated using a centrifugal pump(18), installed between the water tank and the test-section(9). A by pass line from pump outlet to water tank(3) with a valve V14 was provided to achieve better cooling water flow control.

The rotameters(12) were mounted at the discharge line after the centrifugal pump to measure the cooling water flow rate. A hot water tank(20) was provided to collect and subsequently drain the cooling water emerging out from the test-section.

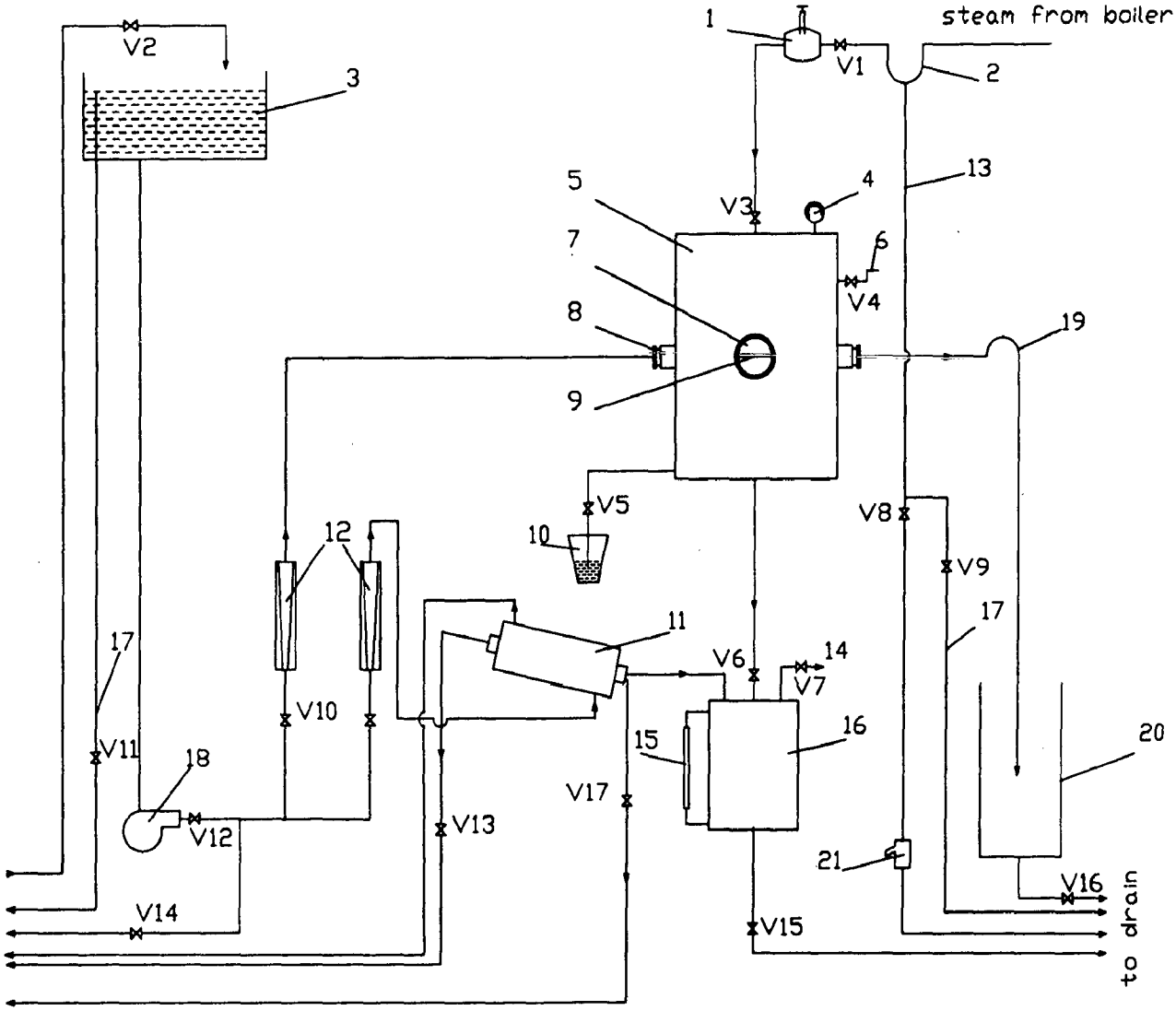

1.pressure regulator, 2.U-bend, 3.cooling water tank, 4.pressure gauge, 5.test-condenser, 6.purging port, 7.viewing window, 8.chuck-nuts, 9.test-section, 10.condensate pot, 11.auxiliary condenser, 12.rotameters, 13.condensate drainage pipe, 14.vent, 15.condensate level indicator, 16.condensate vessel, 17.over flow pipe, 18.centrifugal pump, 19.inverted U-bend, 20.hot water tank, 21.steam trap

Figure 3.1

Schematic diagram of experimental set-up for the condensation of steam(set-up #1)

Photo 3.1

Experimental set-up for the condensation of steam (set-up #1)

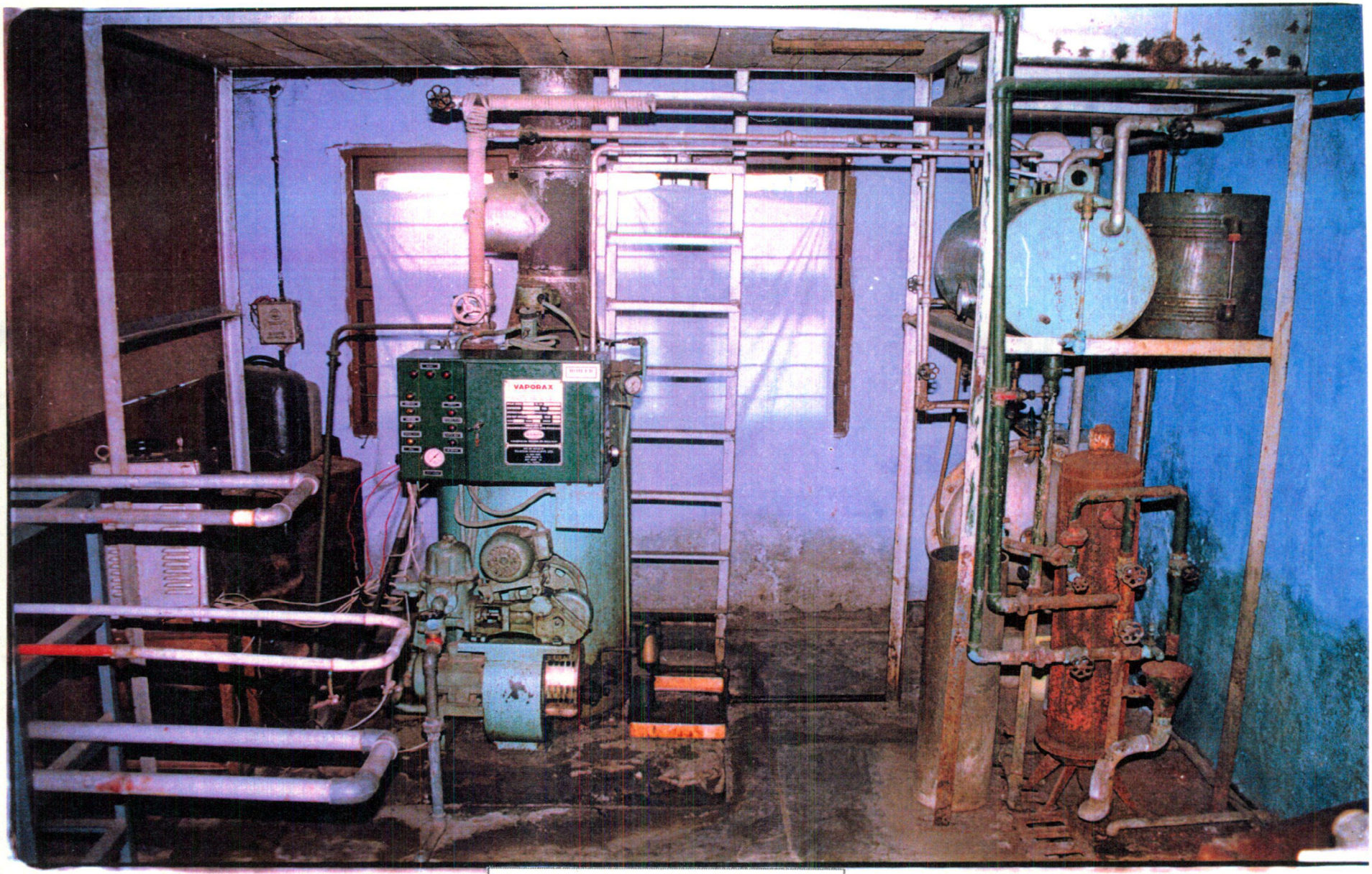

Photo 3.2

Steam generator(boiler)

3.2.2 Steam Generation and Supply

The steam was generated in an oil fired boiler. The photographic view of the oil fired boiler has been shown in Photo 3.2. As shown in Figure 3.1, the steam from boiler was supplied to the test-condenser(5) through an insulated pipe. Further, to remove condensate from the supply line a U-bend(2) was provided. At the lowest point of the U-bend, a drain-pipe(13) was fixed. This pipe was equipped with a steam trap(21) and valves V8 and V9. This arrangement assisted in removal of condensate and dirt from the steam line so that they do not enter the test-condenser. A pressure regulator(1) was installed in between valves V1 and V3 to maintain the steam pressure inside the condenser shell at a desired value. The minor adjustments in the steam pressure were carried out with the help of valve V3.

3.2.3 Test -Condenser

The details of the test-condenser are shown in Figure 3.2. The condenser shell was a rectangular vessel made up of stainless steel with height, length, and breath equal to 750 mm, 300 mm, and 310 mm respectively. On the right hand side of the test-condenser a flange(13) was provided to facilitate an access to the inside of the test-condenser. A perforated plate(3) with a cup(2) was fixed on the top portion of the test-condenser in order to dissipate any velocity component of the flow of steam over the test-section(8). The perforated plate had many holes such that the sum of the flow area of the holes was several times greater than that of steam inlet port(1). The cup was positioned on the perforated plate just below the steam inlet port(1).

The entering steam struck the cup and after dissipating the momentum it was deflected towards the top wall of the test-condenser. Finally, after passing through the holes of the perforated plate it came in contact with the test-section. During the above course, the velocity of the entering steam was apt to reduce to an insignificant value.

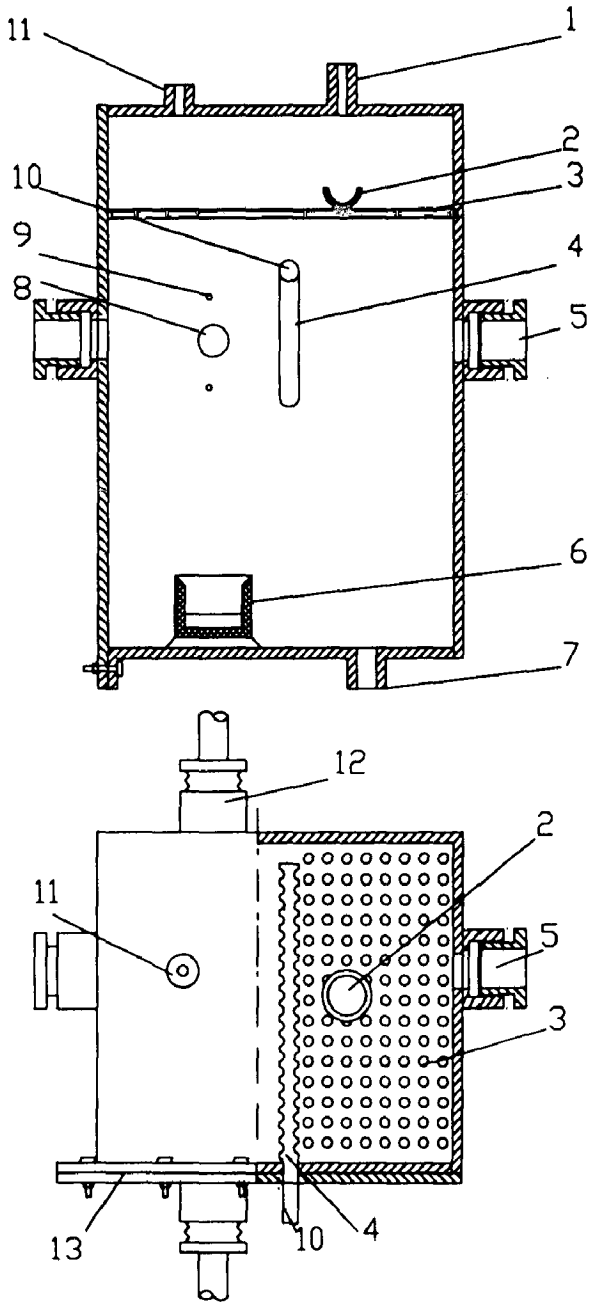

1. steam inlet port
2. cup
3. perforated plate
4. S-shape pipe
5. viewing window
6. condensate tray
7. condensate outlet
8. test-section
9. thermocouple probe
10. purging port
11. pressure gauge port
12. chuck nut
13. flange

Figure 3.2

Schematic diagram of Test-Condenser[set-up #1]

In order to prevent heat dispersion from the condensing steam to atmosphere, the test-condenser was insulated with glass wool. The test-section inside the test-condenser was held in a horizontal position with the help of chuck-nuts(12). The details of chuck-nuts are shown in Figure 3.3. The stainless steel washers(3) facilitated to accommodate any tube diameter equal to or smaller than 40 mm. A packing of asbestos rope(6) was provided between the washers to prevent any leakage of steam to the ambiance.

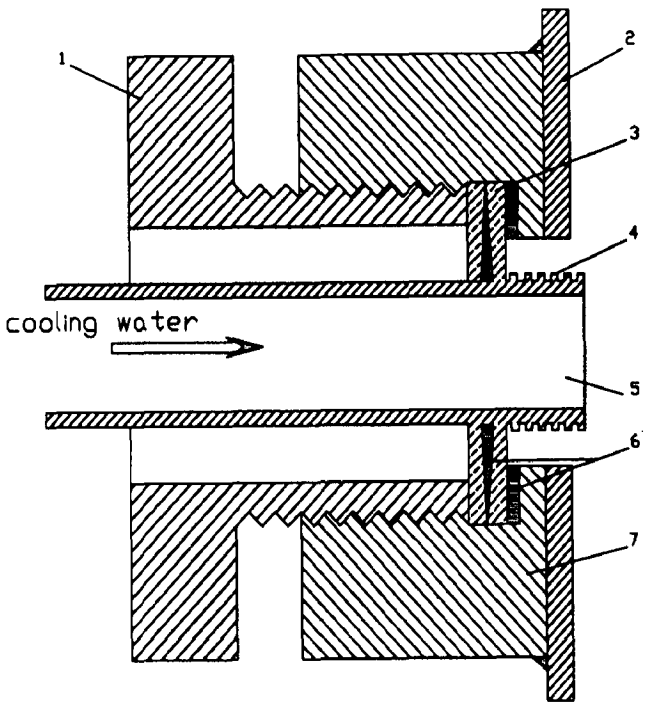

1.nut
2.test-condenser wall
3.stainless steel washer
4.test-section
5.cooling water side
6.asbastos rope packing
7.hub

Figure 3.3

Chuck-nut assembly

As shown in Figure 3.2, the condensate drained off the test-section tube surface was collected in a condensate tray(6) placed on the bottom of the test-condenser. The tray was inclined from the horizontal plane for easy removal of condensate. Being denser than steam, the air was likely to accumulate in the lower half of the test-condenser. Therefore, to remove the air from the test-condenser a S-shaped copper pipe(4) was provided. The top and the bottom portion of this pipe

3.2.4 Test-Section

The plain tube and the finned tube test-sections were all 340 mm long copper tubes of 24.0 mm outside diameter and 18.4 mm inside diameter. The test-section tube was placed 130 mm below the perforated plate, one at a time.

Three teflon coated 36 SWG copper-constantant thermocouples were fixed on the test-section. These thermocouples were placed at the top, side and bottom positions on the outside surface of the tube in a vertical plane on the mid point of the test-section. Before fixation inside the test-condenser, the test-section tubes were cleaned with hot detergent solution using clean cloth and bristle brush followed by a thorough wash with distilled water. The tubes were further rinsed using ethyl alcohol and sodium hydroxide in distilled water at about 80 °C. In fact, this chemical treatment has been found adequate by the investigators[45] to attain the film-wise condensation of steam over the tubes. A very thin oxide film around the tube is created by this chemical treatment. The increase in wall resistance due to this oxide film is negligible as reported by Wanniarachchi et al.[88].

The data were acquired for the condensation of steam over a plain tube replaced by four other finned tubes one at a time. The dimensions of the test-section tubes are shown in Table-3.1 in Section 3.4 and the photographs of the test-sections have been shown in Photo 3.4.

3.2.5 Condensate Vessel

The condensate vessel was a thermally insulated stainless steel vertical cylinder of 250 mm inside diameter and 450 mm height. The condensate vessel was installed below the test-condenser to collect the condensate from the test-condenser under gravity. The excess steam also passed through the condensate vessel before its final condensation in the auxiliary condenser.

3.2.6 Auxiliary Condenser

The purging port(6) in Figure 3.1 was expected to remove all the air from test-condenser before the start of a test-run. It has often been realised that traces of the non-condensables i.e. air and carbon dioxide may remain in the test-condenser and therefore, for the complete removal of non-condensables, an auxiliary condenser(11) was also installed in the experimental set-up. The auxiliary condenser was made up of stainless steel cylinder with 130 mm diameter and 360 mm length. It was surroundend by a water jacket of diameter 170 mm and length 320 mm. At the bottom of the auxiliary condenser the valve V17 was provided to facilitate the condensate drainage. The low pressure of condensing steam inside the auxiliary condenser provided freedom for excess steam and air to flow down to the auxiliary condenser, from where the air was vented off. Therefore, the auxiliary condenser plays an important role in making the condenser shell free from air.

3.2.7 Cooling Water Tank

The cooling water tank, as shown in Figure 3.1, was a mild steel rectangular tank(3) of 900 mm length, 450 mm breadth and 450 mm height with an overflow pipe(17) of 75 mm diameter fixed through the bottom of the tank. The pipe was protruded 380 mm above the bottom of the tank so that it maintained a constant water level inside the tank by draining the extra water. A centrifugal pump(18) connecting the over head tank to the rotameter(12) by a 50 mm diameter pipeline circulated the cooling water through the test-section.

3.2.8 Hot Water Tank

The hot water tank is a mild steel cylindrical tank with a diameter and height of 580 mm and 900 mm respectively. The hot water emerging out from the test-section was collected in this tank and was subsequently drained via valve(V16).

3.3 EXPERIMENTAL SET-UP FOR THE CONDENSATION OF R-134a [Set-Up #2]

The experimental set-up for the condensation of R-134a vapour was designed and fabricated in the laboratory. The salient features of the set-up have been discussed below:

3.3.1 General Layout

The Photo 3.3 depicts the photographic view of the experimental set-up used to study the condensation of R-12 and R-134a vapour over horizontal plain tube and the condensation of R-134a vapour over horizontal integral-fin tubes. A schematic diagram of experimental set-up has also been shown in Figure 3.4. The experimental set-up at the first place consists of a test-section(12) fixed inside the test-condenser(15). The vapour to the test-condenser was supplied by a 19 mm diameter copper tube connected to an evaporator(6), where the vapour of refrigerant was generated by electrically heating the pool of liquid refrigerant.

An auxiliary condenser(10) was also connected to the test-condenser to condense the excess vapour and to remove the non-condensables i.e. air from the set-up. The consensate from the test-condenser and from the auxiliary condenser was drained back to the evaporator through a 12.5 mm diameter copper pipe. A sight glass(19) was provided In the condensate flow line to view the condensate flow.

Prior to charging the refrigerant, a reciprocating compressor(1) was connected to test any leakage. The refrigerant was charged in the set-up with the help of a charging unit(8) connected to the evaporator. A discharging unit(20) was also provided to remove the refrigerant from the system. The discharging unit was also connected to the evaporator. The test-section was fixed inside a test-condenser and after condensation of vapour the heat was transferred to the cooling water flowing inside the test-section. From the cooling tower the cooling water was circulated inside the test-section by a centrifugal pump(2). The cooling water emerging from the exit of test-section and from the auxiliary condenser was sent back to the cooling tower. G10,187

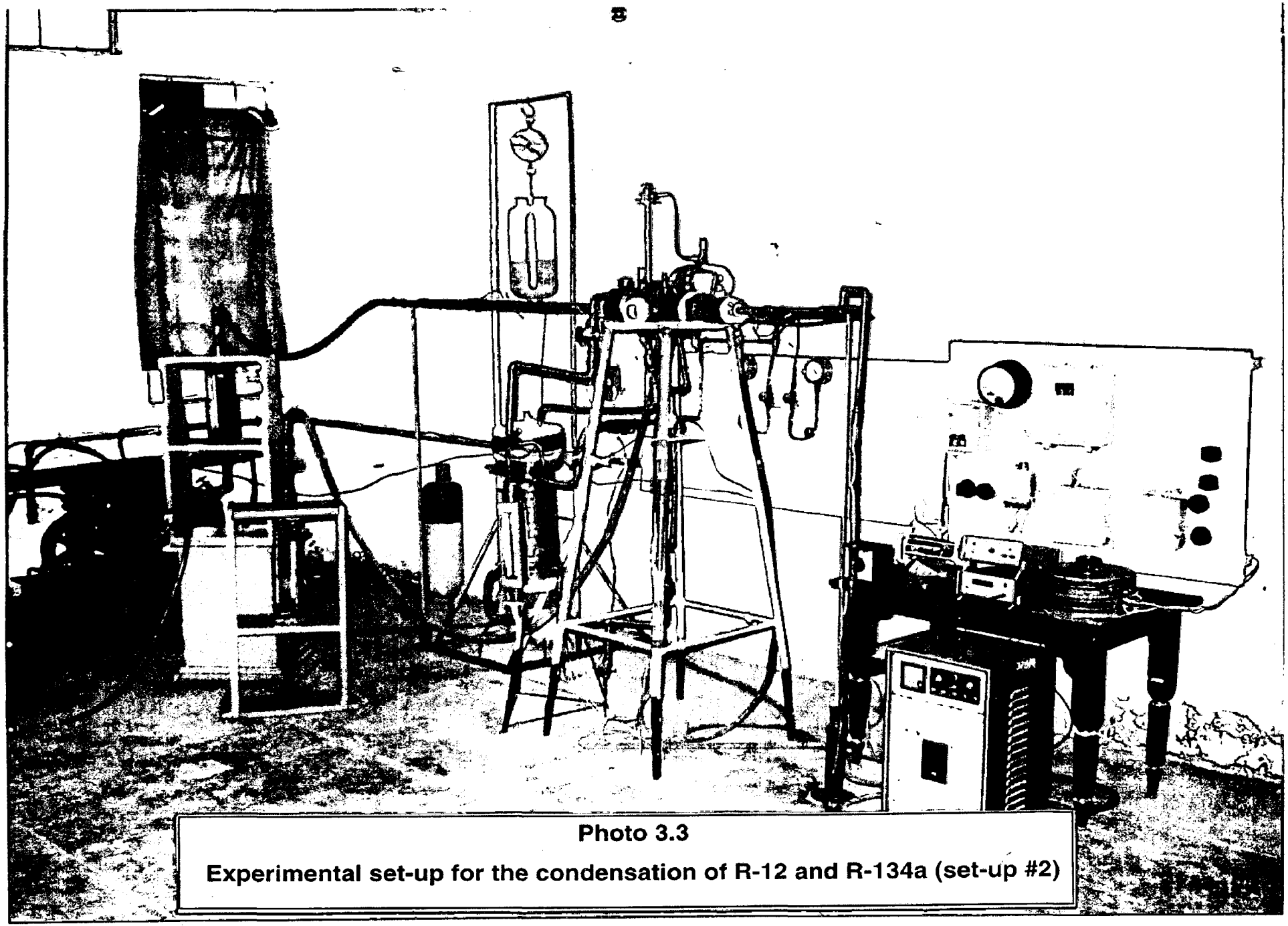

Photo 3.3

Experimental set-up for the condensation of R-12 and R-134a (set-up #2)

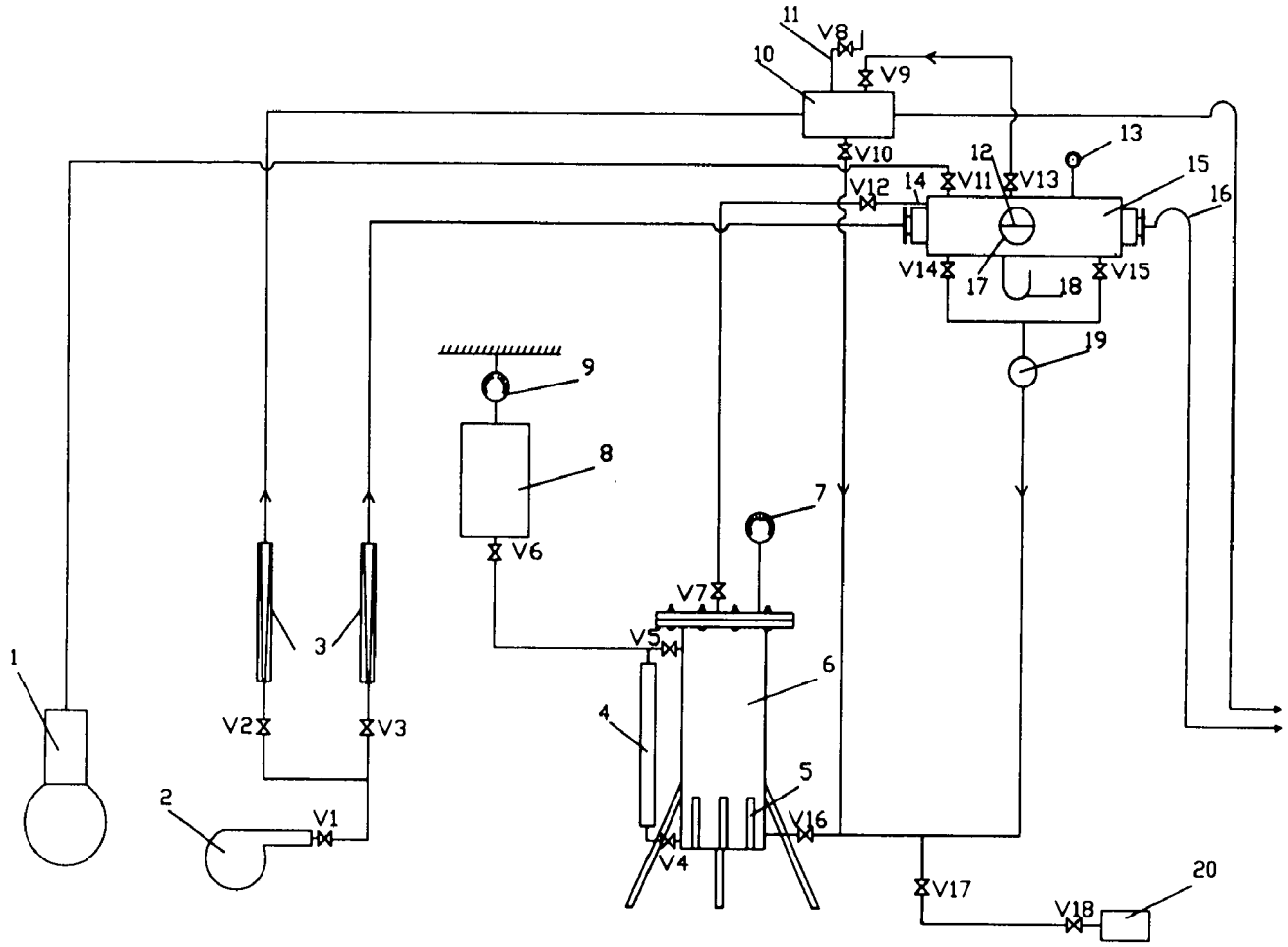

1.reciprocating compressor, 2.centrifugal pump, 3.rotameters, 4.refrigerant level indicator, 5.heaters, 6.evaporator 7.pressure gauge, 8.refrigerant charging cylinder, 9.spring balance, 10.auxiliary condenser, 11.purging pipe, 12.test-section, 13.pressure gauge, 14.perforated pipe, 15.test-condenser, 16.inverted U-bend, 17.viewing window, 18.thermocouple exit port, 19.sight glass, 20.refrigerant discharging cylinder

Figure 3.4

Schematic diagram of experimental set-up for the condensation of R-12 and R-134a [set-up #2]

3.3.2 Evaporator

The vapour of liquid refrigerant was generated in an evaporator(6). The details of the evaporator are shown in Figure 3.5. The evaporator was a mild steel cylinder of 155mm diameter and 600mm height. Three immersion heaters(7) of 3 kW each were fixed at the bottom of the evaporator to transfer heat directly to the liquid refrigerant. The top portion of the cylinder was closed with the help of a flange sealed with a 12 mm diameter hardened rubber O-ring and 8 bolts. At the top of the flange, a port(1) was provided to supply vapour to the test-condenser. To measure the pressure inside the evaporator and to check the unproportionate rise in pressure, a pressure gauge was fixed inside the adopter(2). At the bottom of evaporator, another port(6) was provided to feed back the condensate from the test-condenser to the evaporator. The refrigerant charging and discharging units were also connected to evaporator as shown in Figure 3.4.

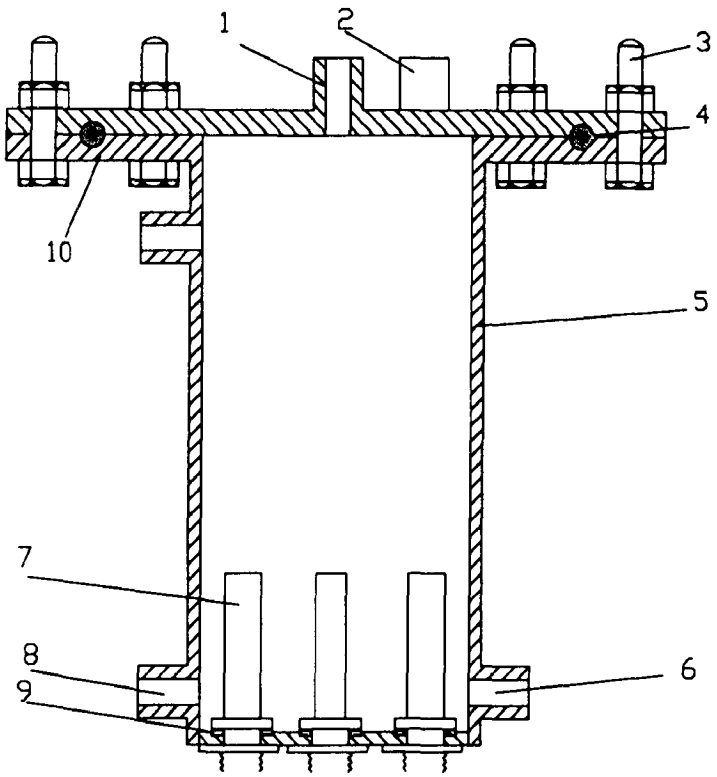

1.vapour exit port, 2.pressure gauge adopter, 3.bolt, 4.O-ring, 5.evaporator shell, 6.condensate inlet port, 7.heaters, 8.refrigerant level indicator port, 9.packing

Figure 3.5

Schematic diagram of evaporator

3.3.3 Test-Condenser

The test-condenser was an integral part of the experimental set-up. Inside the test-condenser, the condensation of refrigerant vapour over horizontal plain and finned tubes was studied. The details of test-condenser have been shown in Figure 3.6.

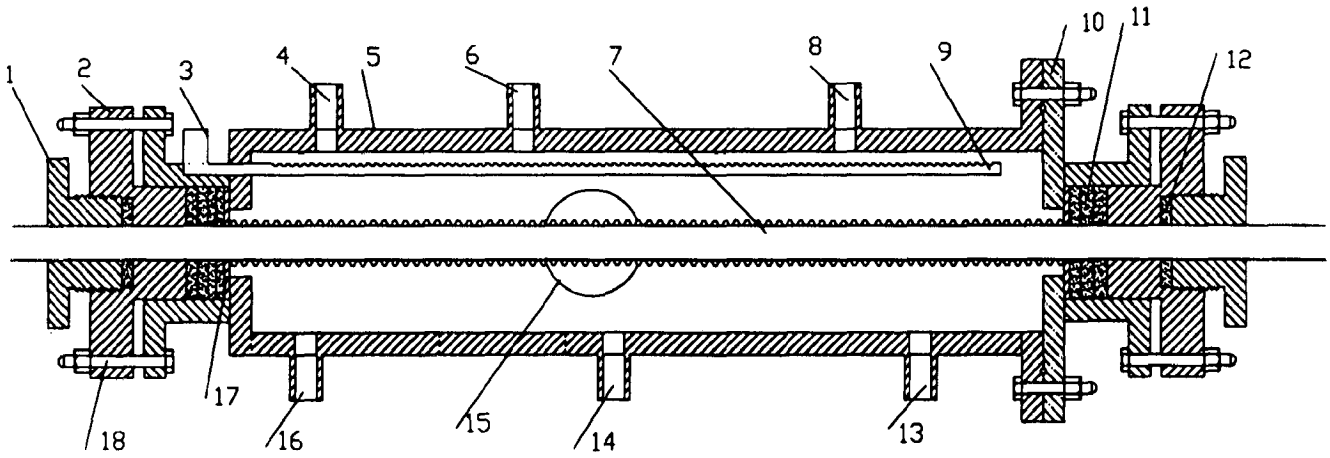

1.nut, 2.piston flange, 3.vapour inlet port, 4.adopter for compressor, 5.test-condenser wall, 6.auxiliary condenser port, 7.test-section, 8.pressure gauge port, 9.perforated tube, 10.cylinder flange, 11.hardened rubber packing, 12.lead rope packing, 13.condensate exit port, 14.thermocouple exit port, 15.viewing window, 16.condensate exit port, 17.washers, 18.nut-bolt

Figure 3.6

Schematic diagram of test-condenser [set-up #2]

The test-condenser was a mild steel cylinder of 100 mm diameter and 410 mm length. The vapour of refrigerant was supplied through a dead end pipe(9) of 350 mm length and 6.5 mm diameter. This pipe had equally spaced 125 holes of 1.0 mm diameter each, in a straight line facing top wall of the test-condenser. This arrangement served two purposes. First, the vapour was distributed uniformly along the length of the test-section and secondly, the initial momentum of vapour was made to decrease after it strikes the roof of the test-condenser, thereby, minimising the possibility of vapour

shear. The test-section was fixed inside the test-condenser with the help of a chuck nut assembly, which ensured a leak proof horizontal fixing of test-section as well as easy change over of the test- section when desired. As illustrated in Figure 3.6 the chuck nut assembly consisted a cylinder-piston arrangement. A mild steel washer(17) was provided inside the cylinder to facilitate an internal support to the packing(11). The centre of piston had a hole equal to the out side diameter of the test-section. Hardened rubber packing rings(11) were provided between the piston and the washer. The rubber was pressurised by tightening four bolts(18) connecting the flanges of the piston and that of cylinder. The compressed rubber sealed the tube and prevented any leakage of the vapour to the atmosphere. However, to make the assembly further leak proof a lead rope packing(12) was provided on the air side of piston flange. This packing prevented any chance of leakage between the tube surface and the piston. The packing was tightened with the help of a chuck nut(1).

The thermocouples inside the test-condenser were taken out through the thermocouples exit port(14). This arrangement consisted of a U-bend of a copper pipe fixed at the bottom of the test-condenser wall with a union and flare nut. After taking out the thermocouple wire through this pipe. The pipe was filled with epoxy resin and was sealed. At the bottom of test-condenser two receiver valves were fixed (in ports 13 and 16 respectively) to remove the condensate from the test-condenser. A pressure-gauge was also installed in port (8) to measure the pressure inside the test-condenser. The excess vapour inside the test-condenser was removed by a valve fixed in a port(6).

3.3.4 Test-Section

One plain tube and eight finned tubes were installed inside the test-condenser one at a time. The test-section was a horizontal tube of 18.42 mm inside diameter and 417 mm length. It was placed below the dead end perforated tube inside the test-condenser to have an uniform vapour distribution. Like the set-up #1, upstream and downstream calming sections of $50D_i$ and $20D_i$ were provided in the set-up #2 also. At the end of the downstream calming section an inverted U-bend was fixed to ensure that the test-section remained fully flooded with water for all the coolant flow

rates. The calming sections were insulated to avoid any heat exchange with the atmosphere. To measure the temperature rise of the cooling water, thermopiles was installed before and after the calming section at the inlet and outlet of test-section. Prior to installation the tubes were cleaned with hot detergent and subsequently rinsed with distilled water and dried. The thermocouples (copper-constantan) of 36 gauge were embeded on the outer surface of the test-section in the top, side and bottom positions at the mid point along the length of the tube in a vertical plane.

3.3.5 Auxiliary Condenser

As shown in Figure 3.4 the auxiliary condenser(10) was connected to the test-condenser(15). It was a horizontal cylinder of 100 mm inside diameter and 150 mm length. The water was circulated inside the auxiliary condenser through a copper tube to condense residual vapour flowing out from the test-condenser. The condensate from the auxiliary condenser was also returned to the evaporator via valve (V10). The cooling water flow rate inside the auxiliary condenser was kept higher than that in the test-condenser. This arrangement helped in keeping the auxiliary condenser at the lowest pressure in the entire experimental set-up. The primary function of the auxiliary condneser was to keep the test-condenser free from non-condensables. Since, air is lighter than the refrigerant, it intends to accumulate at the top portion of the set-up which includes the test-condenser. Therefore, the auxiliary condenser was fixed approximately 100 mm above the test-condenser. On the top of the auxiliary condenser a purge valve(V8) was fixed to remove the air from the system. Since, air is lighter than the refrigerant the purging point was located at the highest point of experimental set-up.

3.3.6 Leakage Testing and Refrigerant Charging

The leakage testing-unit incorporated a reciprocating compressor(1) capable of generating 2MPa absolute pressure and a vacuum of 600 mm Hg inside the experimental set-up. The vacuum was created by reversing the compressor inlet and outlet connections.

A refrigerant charging unit was developed to charge refrigerants of desired quantity in the experimental set-up. As shown in Figure 3.4, this unit consisted, a vertical iron frame with a hook at the top. A spring balance(9) was fixed in this hook and the refrigerant cylinder(8) was hanged from the hook in up side down position. The outlet value of the refrigerant cylinder(V6) was connected to the evaporator.

3.3.7 Cooling Water Supply System

Cooling water was circulated inside the test-section by a centrifugal pump(2) shown in Figure 3.4. A concentric tube of $80D_i$ length was fixed inside the test-section on the cooling water side to increase to temperature rise of the cooling water by creating the turbulence in the cooling water. The same practice was also adopted by Webb and Marawski[91]. A tube of length more then $50D_i$ was fixed on the upstream side of the test-section and a tube of length more than $20D_i$ was fixed on the down stream side of test-section. The inside diameter of these tubes was that of the test-section. This arrangement ensured a fully developed flow inside the test-section as discussed in Section 2.6. The thermopile was fixed between the calming sections to measure the temperature rise of cooling water from the inlet to outlet of the test-section. Two rotameters, one between the centrifugal pump and the inlet of calming section of test-condenser and another between the centrifugal pump and inlet to auxiliary condenser were employed to measure cooling water flow rates. At the out let of centrifugal pump ,a water filter was provided to remove foreign particles from the cooling water. The cooling water emerging out from the test-condenser and the auxiliary condenser was sent back to the cooling tower.

3.3.8 Cooling Tower

A cooling tower, not shown in the Figure 3.4, was used to remove the heat from the hot water emerging from the test-condenser and auxiliary condenser. After removal of heat from the hot water, it was again sent back to the centrifugal pump(2).

3.4 GEOMETRY OF TEST-SECTIONS

In order to manufacture the circular integral fin tube(CIFT), the fins of different configurations were cut on the outer surface of the test-section, basically a tube. The geometry of the test-sections has been shown in the Table-3.1.

The specially enhanced tubes consists of the spined integral-fin tubes(SIFTs) and the partially-spined circular integral-fin tubes(PCIFTs). The spines on the tube surface were generated by cutting axial slots on the tube surface of CIFTs. The SIFT-1 was manufactured by cutting forty axial slots along the length of CIFT-1. The depth of slots was purposely kept less then the height of the fin to ensure proper drainage of the condensate from the tube surface. The partially-spined circular integral-fin tubes, PCIFT-1 and PCIFT-2, were manufactured by cutting twenty axial slots along the length of a CIFT-1 on half of the tube surface. The dividing plane lied on the axis of the tube. The spines on SIFT-2 were generated by cutting sixty axial slots on the surface of CIFT-4. The partially-spined circular integral-fin tubes, PCIFT-3 and PCIFT-4 were manufactured by cutting thirty axial slots on the upper half and the lower half of the tubes respectively. The Photographs of all the tubes tested in the present investigation have been illustrated in Photo 3.4 and Photo 3.5. The schematic diagrams of CIFTs and SIFTs have been shown in Figure 3.7 and Figure 3.8.

Table- 3.1

geometry of test section-tubes

fluid	tube-no	tube type	fin density fpm	D_o mm	D_r mm	P_f mm	tt mm	tb mm	ef mm	θ degree
steam	tube-1	plain tube	-	22.10	-	-	-	-	-	-
	tube-2	CIFT-1	390	24.97	22.77	2.57	1.11	1.11	1.10	0
	tube-3	SIFT-1	390	24.98	22.87	2.56	1.11	1.11	1.11	0
	tube-4	PCIFT-1	390	24.94	23.03	2.58	1.15	1.15	0.96	0
	tube-5	PCIFT-2	390	24.94	23.03	2.58	1.15	1.15	0.96	0
R-12	tube-6	plain tube	-	21.35	-	-	-	-	-	-
R-134a	tube-7	plain tube	-	21.35	-	-	-	-		-
	tube-8	CIFT-2	934	23.82	22.40	1.07	0.12	0.94	0.80	30
	tube-9	CIFT-3	1250	23.72	22.32	0.80	0.11	0.69	0.70	22.5
	tube-10	CIFT-4	1560	24.68	23.08	0.63	0.10	0.52	0.80	15
	tube-11	CIFT-5	1875	24.78	23.58	0.53	0.08	0.43	0.60	15
	tube-12	SIFT-2	1560	24.18	22.62	0.64	0.11	0.53	0.78	15
	tube-13	PCIFT-3	1560	23.62	22.10	0.63	0.10	0.51	0.76	15
	tube-14	PCIFT-4	1560	23.62	22.10	0.63	0.10	0.51	0.76	15

geometry of spines on the circumference of SIFTs and PCIFTs

fluid	tube no.	tube type	P_{fc} mm	tt_c mm	tb_c mm	es mm	θ_c degree
steam	tube-3	SIFT-1	1.97	1.07	1.07	0.93	0
	tube-4	PCIFT-1	1.96	1.04	1.04	0.89	0
	tube-5	PCIFT-2	1.96	1.04	1.04	0.89	0
R-134a	tube-12	SIFT-2	1.27	0.58	1.13	0.68	22.5
	tube-13	PCIFT-3	1.24	0.59	1.11	0.66	22.5
	tube-14	PCIFT-4	1.24	0.59	1.11	0.66	22.5

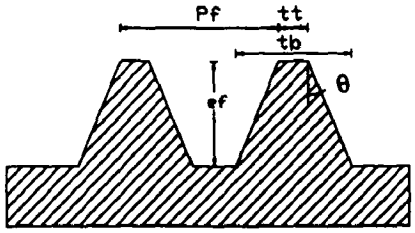

fin geometry

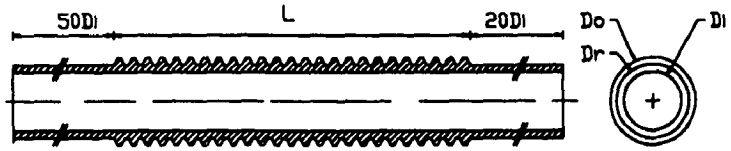

end view

Circular Integral-Fin Tube

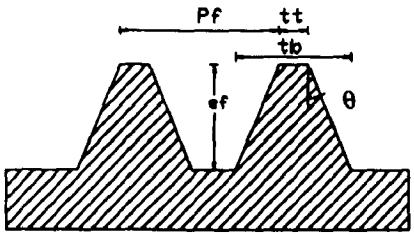

fin geometry

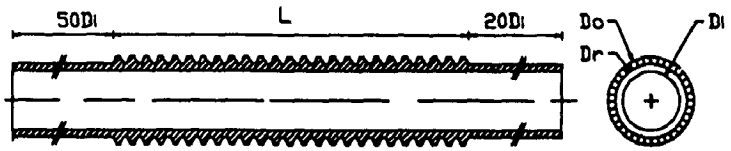

end view

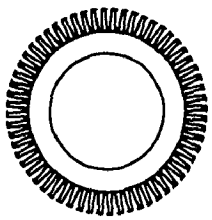

end view

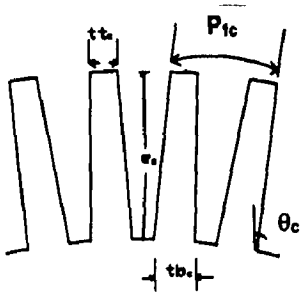

details of spine fins

Spine Integral-Fin Tube

Figure 3.7

Geometry of CIFT and SIFT

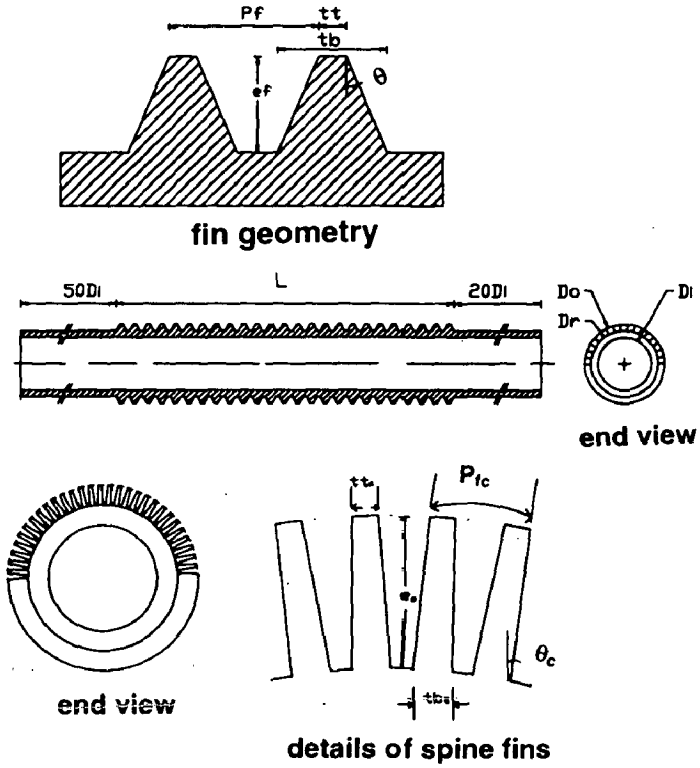

Partially-Spined Circular Integral-fin Tube(PCIFT-1&3)

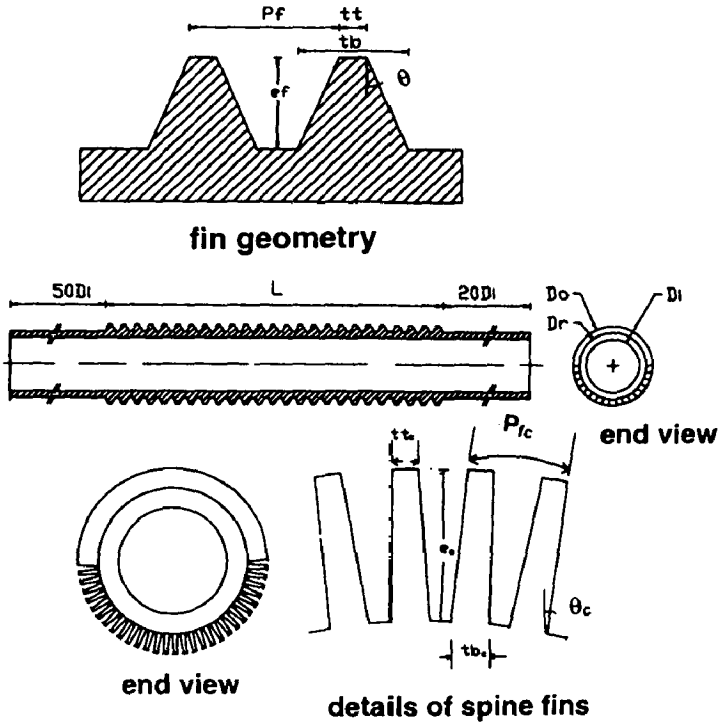

Partially-Spined Circular Integral-fin Tube(PCIFT-2&4)

Figure 3.8

Geometry of PCIFTs

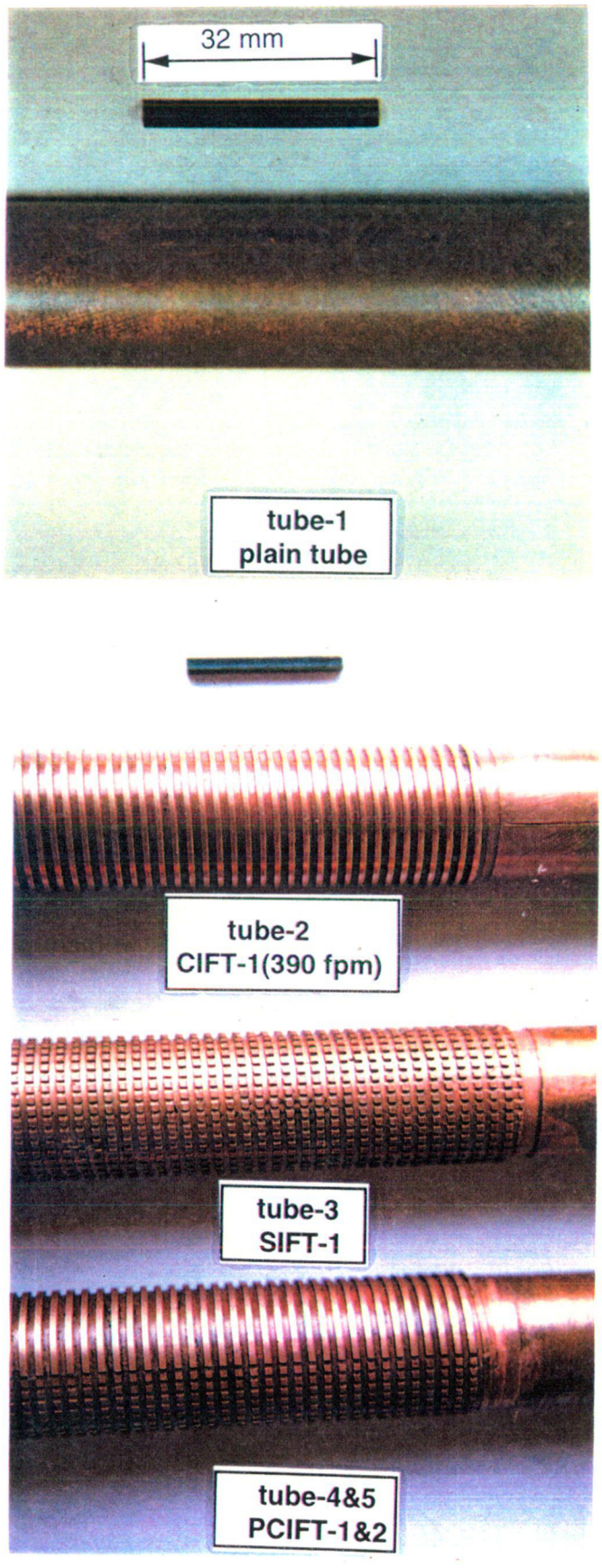

Photo 3.4 Test-section for the condensation of steam

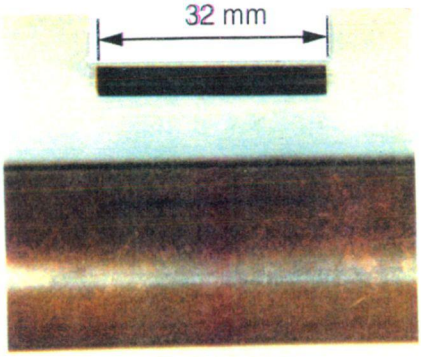

tube-6&7
plain tube

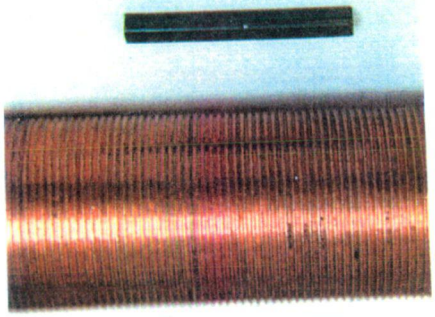

tube-8
CIFT-2(934 fpm)

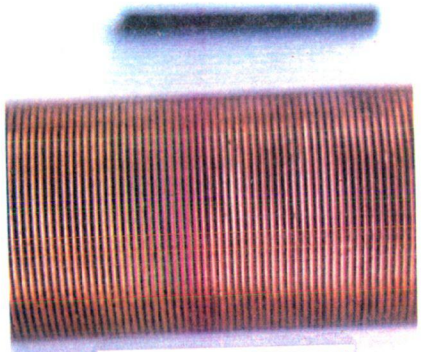

tube-9
CIFT-3(1250 fpm)

tube-10
CIFT-4(1560 fpm)

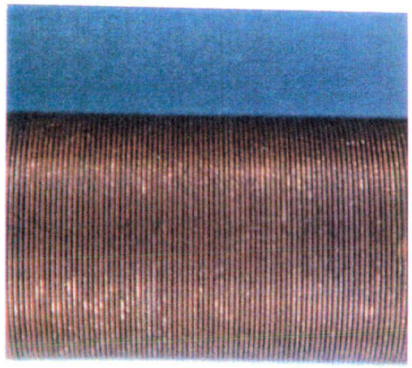

tube-11
CIFT-5(1875 fpm)

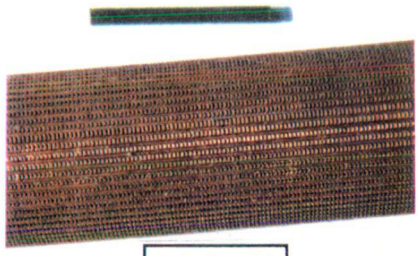

tube-12
SIFT-2

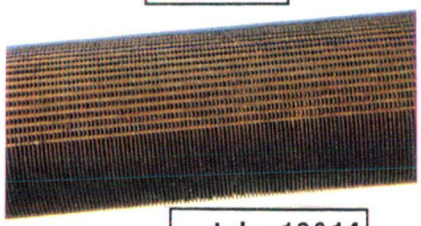

tube-13&14
PCIFT-3&4

Photo 3.5 Test-section for the condensation of refrigerants

3.5 INSTRUMENTATION

In the present investigation the temperatures, coolant flow rate, energy input to the evaporator, and the pressure of condensing vapour are required to be measured. The instruments employed for the measurement of some parameters have been discussed below.

3.5.1 Measurement of Temperature

The temperature measurement is one of the most significant activity of the present investigation and demanded maximum precision and care. The temperature measurement includes the measurement of the condensing vapour temperature, surface temperatures of the test-section and the temperature rise of cooling water.

The measurement of the surface temperature of the test-section was the most sensitive job due to fluctuations in the tube wall temperature. The tube wall temperature fluctuated because of the periodic wrapping of the tubes surface by the condensate layer followed by the condensate drainage from the bottom of the test-section in the form of drops under gravity. Hence, the thickness of the condensate layer varied with time resulting in a variable condensate film thermal resistance, and thus, the outcome was the variable tube wall temperature. The situation demandend an on-line temperature integration and averaging facility to measure the temperature.

Teflon coated copper- constantan thermocouples were fixed on the tube surface in the inter-fin spacing. At each predetermined position a hole of 0.5 mm depth was drilled on the root diameter in the inter-fin space with a 1.0 mm drill bit. In order to fix the thermocouple beads the tube was heated and the hole was filled up with solder. The thermocouple bead, already coated with solder was inserted into the hole with the help of a hot soldering iron. When the bead entered the molten solder in the hole, the solder present in the hole was displaced and oozed out of the hole. The protruded portion of the bead was given a curvature similar to that of the tube by the emery paper and hot needles. In fact, the installation of the thermocouples and the measurement of the

temperature by these were carried out as detailed in Singh[79]. To prevent any contact of vapour with the thermocouple wires they were insulated right up to the beads by further coating the wires of the thermocouples with teflon tape and the epoxy resin.

The thermocouple readings were noted with the help of a Kiethley 177 Model DMM, connected to an on-line hardware integrator and a frequency counter to record the time averaged values of thermo-emf signals. The hardware integrator was designed around a precision V/F converter and was suitable for integrating low level signals for different integration periods. The frequency counter gave the output of the integrated signals in term of counts which was subsequently converted into thermo-emf.

3.5.2 Measurement of Pressure

The pressure of condensing vapour was measured with the help of a dial type pressure gauge fixed with the test-condenser. In the experimental set-up #2 a pressure gauge was also fixed to the evaporator to avoid any disproportionate rise in the vapour pressure.

3.5.3 Measurement of Cooling Water Flow Rate

The cooling water flow rate was measured with the help of rotameter fixed before the test-section.

3.5.4 Measurement of Energy Input

The energy input to the immersion heaters was measured with a watt meter.

CHAPTER #4

Experimental Procedure and Data Acquisition

The experiments for the condensation of steam and refrigerants (i.e. R-12 and R-134a) over horizontal plain and finned tubes have been conducted on experimental set-up #1 and set-up #2 respectively. The photographic and the schematic views of the set-up #1 are shown in Photo 3.1 and Figure 3.1 respectively. The Photo 3.3 and Figure 3.4 show the photographic and schematic views of set-up #2 which is used for the condensation of refrigerants i.e. R-12 and R-134a. The data acquisition procedure during condensation of steam and refrigerants i.e. R-12 and R-134a on horizontal plain tubes and finned tubes has been discussed below in details:

4.1 CALIBRATION OF MEASURING INSTRUMENTS

All the measuring instruments viz. pressure gauges, rotameters, thermocouples and watt meter fixed in the experimental set-up #1 and set-up #2 were calibrated prior to conducting experiments. The rotameters were also calibrated after every change of the test-section. The calibration of instruments was accomplished to mitigate the error of measurements, which finally leads to uncertainty in the experimental results.

4.1.1 Calibration of Pressure Gauges

All the pressure gauges fixed in the experimental set-ups were calibrated prior to installation using a dead weight pressure gauge testing machine.

4.1.2 Calibration of Rotameters

The rotameters have been employed to measure the cooling water flow rate for the determination of heat transfer rate. An error analysis in Appendix-B (Figure A-1 and Figure A-3) shows that the heat transfer rate contributes the maximum uncertainty in the heat transfer coefficient, and hence, affects the experimental results to a great extent. The heat transfer rate has been determined by measuring the cooling water flow rate and the rise in the cooling water temperature. Therefore, the rotameters were calibrated carefully several times, before and during the experimentation to assure the reliability and reproducibility of the measured flow rate. The calibration of rotameters was done by maintaining a constant flow rate of cooling water through the rotameter for a stipulated time and the quantity of coolant discharged was measured. With this technique true discharge at different indicated flow rates was determined and a calibration chart was prepared. The scale of rotameter was marked for different desired flow rates and during experimentation the flow rate was maintained at these marks only.

4.1.3 Calibration of Thermocuples

The teflon coated thermocouples (manufactured by Omegaclad, USA) were used for the temperature measurement and were calibrated in a constant temperature bath. The constant temperature bath was a container filled with the lubricating oil. The container was insulated to maintain a constant temperature of the oil. The temperature of the oil bath was measured by a standard thermometer with 0.1°C accuracy. The standard thermometer was also tested by measuring the boiling temperature of triple distilled water at atmospheric pressure and the temperature of melting ice. The calibration chart was also prepared for thermocouples.

4.1.4 Calibration of Watt Meter

The watt meter was calibrated with an electrodynamic calibrator with 10 watts least count, manufactured by the Cambridge Instruments Co. Ltd., England.

4.2 EXPERIMENTAL PROCEDURE FOR THE CONDENSATION OF STEAM

Experiments for the condensation of steam were carried out on experimental set-up #1 shown in Photo 3.1 and Figure 3.1. The experimental procedure involved the following steps.

4.2.1 Leakage-Testing

The experimental set-up was tested against any leakage. To check the leak the system was pressurised up to 300 kPa (gauge) and joints were checked using soap water solution. Once, the pressure inside the set-up remained constant for a period of 24 hours followed by a vacuum of 300 mm of Hg for the same duration of time, the set-up was considered as leak proof.

4.2.2 Removal of Dirt and Air

The steam required for the present investigation was generated in an oil fired boiler with the demineralised feed water to have minimum non-condensables in steam. However, the presence of traces of non-condensables in the steam can not be ruled out. Before starting the experiments the dirt and air were removed from the steam pipe line as per steps given below:

step-1 First of all each valve in the experimental set-up was closed properly.

step-2 The cooling water tank(3) was filled with the cooling water and then it was circulated inside the test-condenser(5) with a centrifugal pump(18) . The flow of cooling water was controlled with the valve V10.

step-3 The valve V9 was opened and the steam from the boiler was routed through a drain-pipe(17).

step-4 When the stream draining out from drain pipe(17) became free form dirt the valve V9 was closed and valve V8 was opened to drain the condensate continuously from the steam line through a steam trap(21).

step-5 The condensate formed in the steam pipeline was drained from the bottom part of the U-bend through the drain-pipe(13). Thus, through this line only, the condensate generated in the upstream pipe is drained to atmosphere.

step-6 The steam was allowed to enter the test condenser(5) by opening valves V1 and V3 after setting the pressure regulator(1) at a predetermined value.

step-7 To displace all the air inside the test-condenser(5) the valves V4 to V7, V15 and V17 were opened. The steam entering the test-condenser pushed the air out to the atmosphere.

step-8 The valve V6 allowed the steam, air and the condensate to enter the condensate vessel(16), from where the condensate was drained off via valve V15. The steam and air did not drain off, but remained inside the vessel. A part of these non-condensables was escaped to atmosphere via valve V7 and the leftover entered the auxiliary condenser(11).

step-9 Valve V4 was also held open to allow constant purging of steam from the condenser and the valve V13 was intermittently opened to

knock out any residual air(non-condensible) collected in auxiliary condenser(11).

step-10 The readings of the thermocouples fixed inside the test-condenser to measure the vapour temperature were intermittently recorded. The test-condenser was considered free from non-condensable only when the readings of these thermocouples were the same and equal to the saturation temperature corresponding to the steam pressure inside the test-condenser.

When the condensation started inside the test-condenser a low pressure zone was created around the test-section. Therefore, the traces of air and carbon dioxide which come with the steam accumulated around the test-section with time and after a few hours grew to a proportion which could affect the performance of the test-section. As the air and carbon dioxide are heavier than steam these settle down at the lower portion of the test-condenser. Most of the non-condensables were purged out from the lower half of the test-condenser through the perforated pipe connected to the purging port. Remaining traces of non-condensables were automatically driven to the auxiliary condenser due to the steam flow to it and were subsequently removed from there. Approximately twenty percent of steam was condensed inside the auxiliary condenser.

4.2.3 Data Recording

When it was assured that the set-up has become free from dirt and non-condensables, the data for the condensation of steam were acquired as per Table-4.1 in the following steps:

step-1 The gauge pressure inside the test condenser was maintained at 9.8 kPa(374.3 K) gauge pressure. The cooling water flow rate was set at 8.0 lpm. It took 20-30 minutes to attain the steady state. At this

juncture the readings of rotameters, pressure gauge and thermocouples were recorded.

step-2 The experiment was repeated three times to check steady state condition and reproducibility of the experimental data.

step-3 For a given steam pressure the data were acquired for cooling water flow rates varied from 8.0 lpm to 28.0 lpm in five steps with an increment of 4.0 lpm, leading to total six test-runs.

Table- 4.1

operating parameters for the condensation of steam

S.No	tube	saturated steam		cooling water flow rates litre per minute(lpm)	
		gauge* pressure kPa	saturation temperature K	range lpm	increment lpm
1	plain	9.8-107.9	374.5-394.0	8.0-28.0	4.0
2	CIFT-1	9.8-107.9	374.2-394.2	8.0-28.0	4.0
3	SIFT-1	9.8-107.9	374.3-394.0	8.0-28.0	4.0
4	PCIFT-1	9.8-107.9	374.3-393.7	8.0-28.0	4.0
5	PCIFT-2	9.8-107.9	374.5-394.2	8.0-28.0	4.0

* gauge pressure was measured in kg/cm^2

The step-3 was repeated for a higher gauge pressure of condensing steam for all the cooling water flow rates considered in the step-3 and were recorded. This was repeated until

the readings for the condensing steam pressures of 29.4, 49.0, 68.8, 88.3 and 107.9 kPa gauge were recorded. The range of operating parameters is given in Table- 4.1

First, the data were collected for the condensation over a plain tube. Later on, the plain tube was replaced by a CIFT-1(390fpm) followed by SIFT-1, PCIFT-1 and PCIFT-2. For each tube the data were collected at six pressures (or saturation temperatures). For each saturation temperature cooling water flow rate was varied from 8.0 lpm to 28.0 lpm in five steps with an increment of 4.0 lpm. Thus total 180 test-run were conducted for the condensation of steam over five tubes.

4.3 EXPERIMENTAL PROCEDURE FOR THE CONDENSATION OF R-134a

For the condensation of R-12 and R-134a an experimental set-up was designed, fabricated and tested. The set-up is shown in Photo 3.3 and Figure 3.7. The data acquisition for the condensation of refrigerants was carried out through the following steps.

4.3.1 Leakage Testing

To ensure no leakage from the experimental set-up, a pneumatic pressure of 2.0 Mpa(gauge) was kept inside the set-up for 24 hours followed by a vacuum of 600 mm Hg for same duration of time. No fall in pressure or vacuum inside the set-up testified that the set-up was leak proof.

4.3.2 Charging of Refrigerant and Removal of Air

The charging of refrigerant(R-12 and R-134a) inside the experimental set-up and removal of air from the set-up involved the following steps:

step-1 First, all the valves of the experimental set-up were closed and a vacuum of the order of 600 mm Hg was created inside the experimental set-up.

step-2 The valve V5 and valve V6 were opened and the set-up was brought to the saturation pressure of R-134a at room temperature by allowing the refrigerant vapour to enter the set-up from the refrigerant cylinder(8).

step-3 The valves V5 and V6 were closed and set-up was put under vacuum of 600 mm Hg.

step-4 The steps-1 to step-3 were repeated three times.

step-5 Finally, refrigerant was charged in the evaporator(6) to a certain level to fully submerge the heaters in the liquid refrigerant. The quantity of the charged refrigerant was noted by the spring balance(9). The level of liquid refrigerant inside the evaporator was further checked by the level indicator(4). When the desired quantity was charged in the evaporator the valve V5 and V6 were closed.

step-6 All the valves except V6, V8, V11 and V17 were opened.

step-7 After 24 hours of charging the refrigerant, valves V7 & V16 were closed and all the vapours inside the system except that in the evaporator was purged out to the ambience via purging pipe(11) by opening valve V8.

step-8 Later on, this valve was closed and the valves V7 and V16 were opened. The cooling water was circulated inside the test-section with a centrifugal pump(2).

step-9 The refrigerant inside the evaporator was heated with the electric immersion heaters(5). The vapour of refrigerant thus generated rushed to the test-condenser(15) and was subsequently condensed by coming in contact with the cold surface of test-section.

It is not possible to remove all the air inside the experimental set-up prior to charging the refrigerant. With the onset of condensation, the test-condenser and the auxiliary condenser became the low pressure zones inside the system. Therefore, air and refrigerant vapour rushed to this part of experimental set-up. The refrigerant vapour was condensed coming in contact with the cold surface of test-section but the air in traces remained uncondensed and formed a blanket around the tube. The quantity of air increased with time up to a certain limit. It is a known fact that air is lighter than the refrigerant, therefore, it started to accumulate in the upper portion of test-condenser and the auxiliary condenser. In the auxiliary condenser approximately fifty percent of the total vapour was condensed.

step-10 After thirty minutes of operation the electric supply to immersion heaters was switched off and the valves V10, V14 and V15 were closed.

step-11 The purging valve V8 was opened to discharge the refrigerant and air to the atmosphere. Again, the electric supply was restored to the pool of refrigerant and the valves were opened. The steps-10 and step-11 were repeated 3-4 times.

step-12 Most of the air was removed from the system by this method. Still, the traces of air may remain with the refrigerant. To cope with this problem the experimental set-up was kept operative and the gas inside the test-condenser and the auxiliary condenser was purged four times at an interval of four to five hours. When the refrigerant become free from

air, the temperature of refrigerant vapours above the test-section and below the test-section became equal and corresponding to the vapour saturation temperature.

Step-10 to step-12 were repeated when a new tube was fitted inside the test-section.

4.3.3 Data Recording

The data have been recorded in the following steps:

step-1 First, a plain tube was fixed inside the system and the refrigerant R-12 was charged inside the set-up and air was removed as discussed in Section 4.3.2.

step-2 The water pump was switched on and the cooling water flow was maintained at the predetermined value with valve V1.

step-3 The power supply to the immersion heaters inside the evaporator was controlled with the help of a variac of 0-270V range and was measured with a watt meter. The vapour generated inside the evaporator rushed to the test-condenser and the auxiliary condenser. As the vapour came into the contact with the cold surface of test-section, it transferred the latent heat to the test-section and was subsequently condensed.

step-4 The condensate from the tube surface was drained back to the evaporator under gravity. The flow of condensate to the evaporator was seen through a sight glass(19). The temperature of condensing vapour inside the test condenser was controlled by varying the heat to the liquid refrigerant pool.

step-5 The vapour temperature was maintained at an approximately constant value of 312.4±0.5 K. After approximately 40 minutes the steady states was attained and the temperatures of cooling water were noted. The cooling water flow rate was also noted along with the tube surface temperature and the temperature of condensing vapour.

step-6 The cooling water flow rate was set to the next higher value. This process continued for 14 flow rates of cooling water and for each flow rate the experiment was repeated two to three times.

step-7 Then, R-12 was replaced by R-134a and the air was removed from the system as per the process discussed in 4.3.2. For the condensation of R-134a first of the data were collected on the same plain tube which was used for the condensation of R-12, for the calibration of experimental set-up.

step-8 Later on, the plain tube was replaced by four CIFTs(390 fpm,1250 fpm, 1560 fpm and 1875 fpm fin density), SIFT-2, PCIFT-3 and PCIFT-4 one at a time. The data were recorded for the condensation of R-134a over each of the above tubes as per step-5&6.

Hence, alltogether eight tubes were tested for the condensation of R-134a and one tube for the condensation of R-12. For each tube the data were acquired for the 14 different cooling water flow rates leading to 126 test runs. In fact, the experimentation involved total 306 experimental test-runs for the condensation of steam, R-12 and R-134a. The range of the operating parameters for the condensation of R-12 and R-134a is given in Table -4.2.

Table-4.2

operating parameters for the condensation of R-12 & R-134a

fluid	test-section	saturation temperature of condensing vapour K	Cooling water flow rate kg/hr	
			range kg/hr	increment kg/hr
R12	plain	313.2-313.8	400-1050	50
R-134a	plain	311.9-312.9	400-1050	50
	CIFT-2	311.9-312.9	400-1050	50
	CIFT-3	311.9-312.9	400-1050	50
	CIFT-4	311.9-312.9	400-1050	50
	CIFT-5	311.9-312.9	400-1050	50
	SIFT-2	311.9-312.9	400-1050	50
	PCIFT-3	311.9-312.9	400-1050	50
	PCIFT-4	311.9-312.9	400-1050	50

4.4 LIMITATION OF EXPERIMENTS

The experiments for the condensation of steam and R-134a have been carried out subjected to a number of constrains mainly due to machining of test-section and uncertainty in the measurements. These constrains finally became the limitations of experiments. Details of these limitations are described below:

4.4.1 Manufacturing Limitation

In order to attain the optimum fin density of finned tubes, the investigations for the condensation of R-134a have been carried out on four circular integral-fin tubes (CIFTs). It was required that the fin spacing be reduced systematically with a constant fin height. Therefore, the semi-vertex angle of the fins (the fins are trapezoidal in shape) was reduced from 30° for CIFT-2(934 fpm) to 15° for CIFT-5(1875 fpm). In fact, the semi-vertex angle of fins, θ, does not affect the performance of the finned tubes as observed by Sukhatme et al.[83]. In spite of all efforts to keep the fin height constant the fin heights of CIFT-2,3,4&5 remained 0.8 mm, 0.7 mm, 0.8 mm and 0.6 mm respectively. In fact, it was difficult to maintain a constant fin height as the fin density increased, therefore, the tubes of fin density higher than 1875 fpm(CIFT-5) could not be manufactured. The test-section was made out of copper and it being a soft material the fins were found to deform as the fin density increased above 1875 fpm. Although it has been tried to manufacture the thinnest possible fins to attain higher fin density yet the fin density could not be increased more than 1875 fpm.

The SIFT-1 was manufactured by cutting rectangular slots on the surface of CIFT-1, which has rectangular shape of circular fins. In order to keep the axial thickness of the spine(tt) and the circumferencial thickness(tt_c) of spine equal, 40 axial slots were cut on the surface of CIFT-1.

Similarly, SIFT-2 was manufactured by cutting V shape 60 axial slots on the CIFT-4 surface as the shape of the circular fins of CIFT-4 is trapezoidal. The slots generated pyramidical shape spine fins on the tube surface. In fact, it was tried to have maximum spines on the tube surface and but the number of slots could not be increased more than sixty.

4.4.2 Limitation of Operating Parameters

For the condensation of steam the absolute pressure could not be increased more than 200 kPa because the steam at high pressure and temperature (393 K approximately) might have damaged the viewing window .

In the present investigation it was possible to attain the highest cooling water flow rate of 28 litres per minute(approximately 1680 kg/hr) for the condensation of steam in set-up #1 and 1050 kg/hr for the condensation of refrigerants in set-up #2.

The further increase in cooling water would have induced the high uncertainty in the experimental results. Moreover, to attain high cooling water flow rates the rotameter of higher range was to be taken. This would have reduced the accuracy of measurements and had led to the high uncertainty in the experimental results also. Therefore, the maximum cooling water flow rate for the condensation of steam was chosen 28 lpm and that for the condensation of R-134a was 1050 kg/hr.

CHAPTER #5

Results and Discussion

This Chapter covers the interpretation and discussion of results of an investigation carried out for the condensation of steam, R-12 and R-134a vapours over a horizontal plain tube and condensation of steam and R-134a over horizontal finned tubes. The finned tubes consist of the circular integral fin-tubes(CIFTs), spine integral-fin tubes(SIFTs) and partially-spined circular integral-fin tubes(PCIFTs). As discussed in Chapter #3 two separate experimental set-ups, viz. set-up #1 and set-up #2 were used to conduct experiments for the condensation of steam and refrigerants(R-12 and R-134a) respectively. First of all the integrity of experimental set-up #1 has been established by conducting experiments for the condensation of steam and that of set-up #2 by conducting experiments for the condensation of R-12. After establishing the integrity, the results for the condensation of steam and R-134a over a plain tube have been discussed. They are followed by the discussion of results for the condensation of steam and R-134a vapour over circular integral-fin tubes(CIFTs), spine integral-fin tubes(SIFTs) and partially-spined circular integral-fin tubes(PCIFTs). For each type of finned tubes, i.e. CIFTs, SIFTs and PCIFTs, the results and discussions have been presented mainly under the following subtitles:

i. effect of ΔT_f on heat flux

ii. effect of heat flux on heat transfer coefficient

iii. effect of ΔT_f on heat transfer coefficient

iv. variation of enhancement factor with ΔT_f

Later, a comprehensive study has been made to evaluate the relative performance of these tubes. The heat transfer coefficients reported in the present chapter are computed from tube wall temperature measurement. In Section 5.7 a comparison between the heat transfer coefficient computed by wall temperature measurement and that from modified Wilson plot is also included for ready reference.

The experimental results for the condensation over CIFTs have also been compared with those predicted by different analytical models. Subsequently, a generalised correlation in the form of non-dimensional numbers has been developed between the heat transfer coefficient, fin geometry and thermo-physical properties of condensing fluids.

The sample calculations and the uncertainty analysis of the experimental results is given in Appendix-A and Appendix-B respectively.

5.1 INTEGRITY OF EXPERIMENTAL SET-UP

Before the study for condensation of steam and R-134a vapours over horizontal finned tubes was carried out, the integrity of respective set-ups has been checked by conducting experiments for the condensation of vapour over a single horizontal plain tube and comparing the experimental values of the heat transfer coefficient with the earlier published work. Subsequently, the data on plain tubes thus generated, are used as reference data for the comparison of the relative performance of different finned tubes. The integrity of the experimental data on finned tube is also checked by scrutinising them as per the criteria of Yau et al.[98]. The integrity check for each experimental set-up has been discussed below:

5.1.1 Experimental Set-Up #1

The integrity of experimental set-up #1 has been checked by carrying out experiments for the condensation of steam over a plain horizontal tube. The values of condensing heat transfer coefficient from these experiments are compared with those predicted by the Nusselt's model[62], equation (5.1).

$$h_o = C_o\left(\frac{k^3\rho^2 g\lambda}{\mu D_o \Delta T_f}\right)^{0.25} \tag{5.1}$$

Where, the value of C_o for a horizontal plain tube is 0.725.

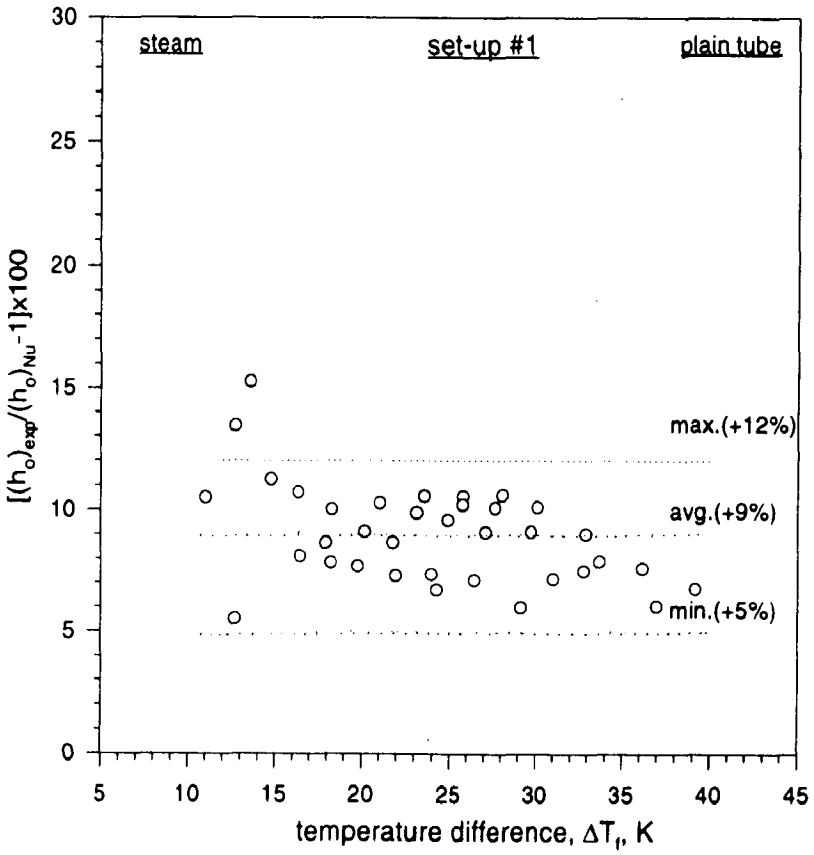

Figure 5.1
Comparison between condensing side experimental heat transfer coefficient and that predicted by the Nusselt's model for the condensation of steam over a plain tube

In Figure 5.1 a graph is plotted between the percentage deviation of the experimental values of heat transfer coefficient from the Nusselt's model versus vapour to tube wall temperature difference, ΔT_f, for the condensation of steam over the plain tube. The experimental values are approximately 5-12 percent more than those predicted by the Nusselt's model. This is in agreement with the findings of McAdams[51]. He found that the experimental values of heat transfer coefficient for the condensation of steam over a horizontal plain tube were from zero to 30 percent more than those predicted by the Nusselt's model. The experimental results of Wanniarachchi et al.[87] also agree with McAdams[51]. The higher value of condensing side heat transfer coefficient may be attributed to the thinning of condensate film on the tube surface due to a number of factors.

As described by Henderson and Marchello[19], the condensate droplets are detached from bottom part of the tube surface only when their weight is more than the balancing force exerted to retain these due to surface tension of condensate. Since, water is a high surface tension fluid (σ>0.05 N/m), the weight of the detached droplet is also high which causes the condensate film to stretch, and hence, thinning of the condensate film on the top portion of the test-section takes place. Moreover, sensible heat transfer also takes place across the condensate film. The above facts are neglected in the Nusselt's model as discussed by Henderson and Marchello[19] and Bromley[10]. Hence, in the present investigation the results for the condensation over a plain tube show an expected trend and deviation from Nusselt's model and, thus, fortify the integrity of experimental set-up #1.

5.1.2 Experimental Set-Up #2

The second set-up was fabricated and installed to carry out the study of augmentation in heat transfer coefficient during condensation of R-134a vapour over horizontal tubes. In this case also, the integrity of experimental set-up has been established by comparing the experimentally obtained condensing side heat transfer coefficients with those predicted by Nusselt's model, equation (5.1). Since, R-134a is a new refrigerant in the commercial market, there is no reported work on the experimental values of the condensing side heat transfer coefficient. Hence, a conventional refrigerant R-12, whose heat transfer characteristics are known, has been used for checking the integrity of the experimental set-up.

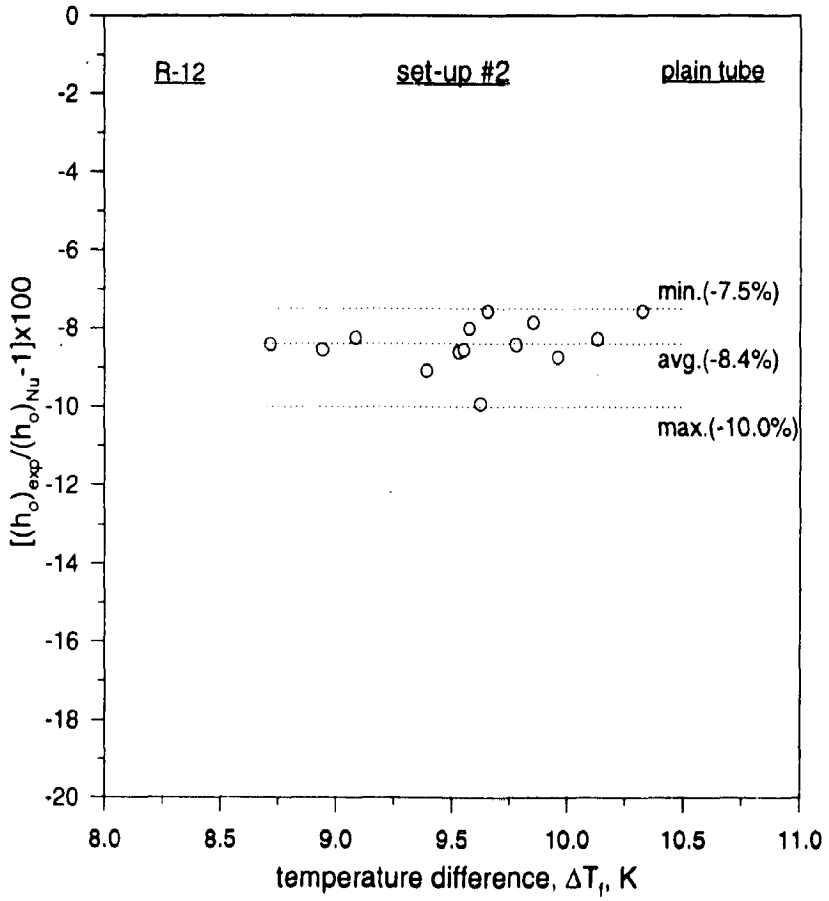

Figure 5.2
Comparison between condensing side experimental heat transfer coefficient and that predicted by the Nusselt's model for the condensation of R-12 over a plain tube

The vapour of R-12 is condensed over a horizontal plain tube inside the experimental set-up and condensing side heat transfer coefficients are compared with those predicted by Nusselt's model (equation (5.1)) as shown in Figure 5.2. In Figure 5.2 a graph is plotted between the percentage deviation of the experimental values of heat transfer coefficient from the Nusselt's model versus vapour to tube wall temperature difference, ΔT_f, for the condensation of R-12 over a plain tube. It is found that experimental values are approximately 7.5 to 10 percent less than those predicted by the Nusselt's model. This fact is in agreement with the findings of White[93], who reported that the Nusselt's model overpredicts the condensing side heat transfer coefficient for the condensation of R-12 by approximately 13 percent. It is a general observation by different investigators [51] that the heat transfer coefficient for the condensation of refrigerants on a plain tube is less than that predicted by the Nusselt's model.

The thermo-physical properties of steam, R-12 and R-134a are shown in Table-5.1. The surface tension, σ, of R-12 is much lower than that of steam (approximately one tenth of steam), therefore, the thinning of condensate layer on tube surface due to the weight of the condensate drop is not as effective as in the case of steam. The close agreement of present investigation with the findings of White[93] confirms the integrity of experiment set-up #2.

Table-5.1

thermo-physical properties of condensate

	fluid	temp. K	k W/m-K	ρ kg/m^3	λ kJ/kg	σ Pa-m x10^3	Cp kJ/kg-K	μ. Pa-s x10^6	σ/ρ N/m^2-kg x10^5	pressure kPa
1	steam	373	0.68	958.3	2256.7	56.85	4.27	282.4	5.93	101.30
2	R-12	308	0.0658	1273.6	132.8	5.88	0.96	201.9	0.46	847.23
3	R-134a	308	0.0772	1167.2	173.4	13.83	1.47	189.2	1.18	887.11

5.2 CONDENSATION OVER A HORIZONTAL PLAIN TUBE

After, the integrity of both the experimental apparatus has been established and the reliability of experimental data is ensured, the data for the condensation of the vapours of three fluids viz. steam, R-12 and R-134a over horizontal plain tubes have been further analysed as detailed below:

The variation of heat transfer coefficient during condensation of R-12 and R-134a over a horizontal plain tube with the temperature difference across the condensate layer, ΔT_f, is shown in Figure 5.3.

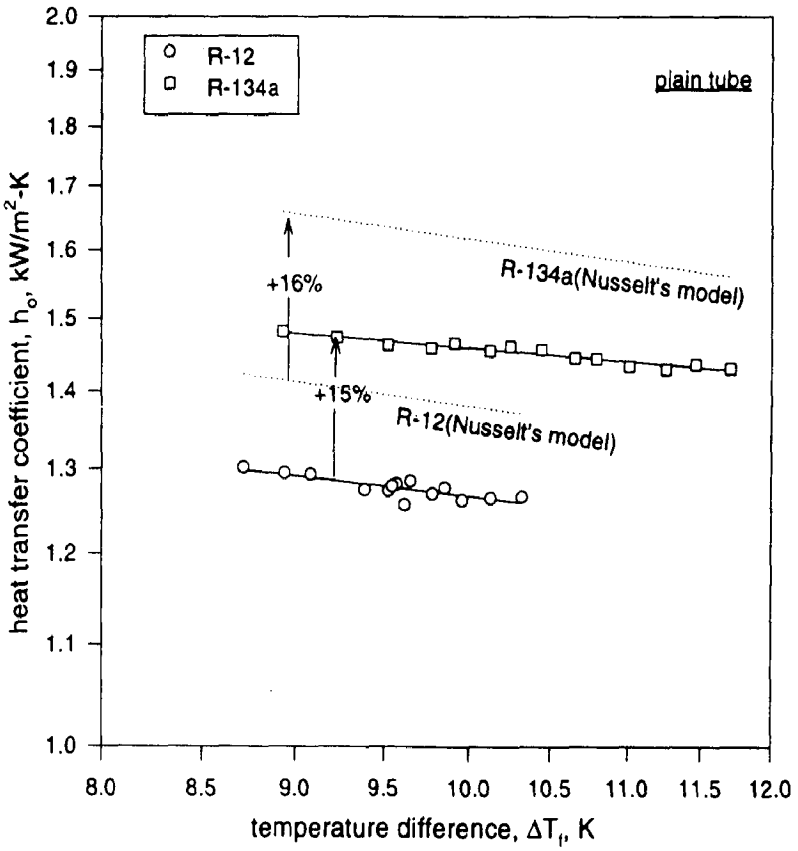

Figure 5.3
Variation of condensing side heat transfer coefficient with vapour to tube wall temperature difference for the condensation of refrigerants over a plain tube

The experimental values of heat transfer coefficient, h_o, of the plain tube for the condensation of R-134a vapour are in a range of 1.43 to 1.48 kW/m^2-K with an average value of 1.45 kW/m^2-K. However, for R-12 the value of heat transfer coefficients, h_o, are in the range of 1.26 to 1.30 kW/m^2-K with an average value of 1.28 kW/m^2-K. The coefficients, h_o, of R-134a and R-12 have also been computed by Nusselt's model, and are shown by separate dotted lines in Figure 5.3. It is inferred from the figure that the heat transfer coefficient reduces with the increase in temperature difference across the condensate layer, ΔT_f. This fact is also justified from the predictions from the Nusselt's model shown by the dotted line in the Figure 5.3.

The experimental heat transfer coefficient of R-134a is approximately 15 percent more than that of R-12. The Nusselt's model also predicts the heat transfer coefficient for R-134a about 16 percent more than that of R-12 at the same ΔT_f.

The difference in prediction of heat transfer coefficient for R-134a and R-12 is essentially due to the difference in thermo-physical properties of the condensing fluids. If the value of constant C_o in equation (5.1) is modified to 0.65, the data for the condensation of R-134a and R-12 of the present investigation are predicted within an error band of ±2 percent.

Further, if the value of C_o is modified to 0.8, the heat transfer coefficient of steam from present investigation can be predicted by the Nusselt's model within a range of ±3 percent error. Therefore, the heat transfer coefficient data of the present investigation can also be computed with high accuracy by using Nusselt's model of equation (5.1), but with modified value of C_o equal to 0.65 and 0.8 for the case of refrigerants (R-12 & R-134a) and steam, respectively.

The Nusselt's model with modified values of C_o is used in the subsequent sections as the *modified Nusselt's model* for the computation of enhancement factor, EF, (ratio of heat transfer coefficient of finned tube and heat transfer coefficient of a plain tube, at same ΔT_f). To study the heat transfer behaviour during condensation of steam, Figure 5.4 is drawn, which shows that the heat transfer coefficient for steam also reduces with the increase in ΔT_f.

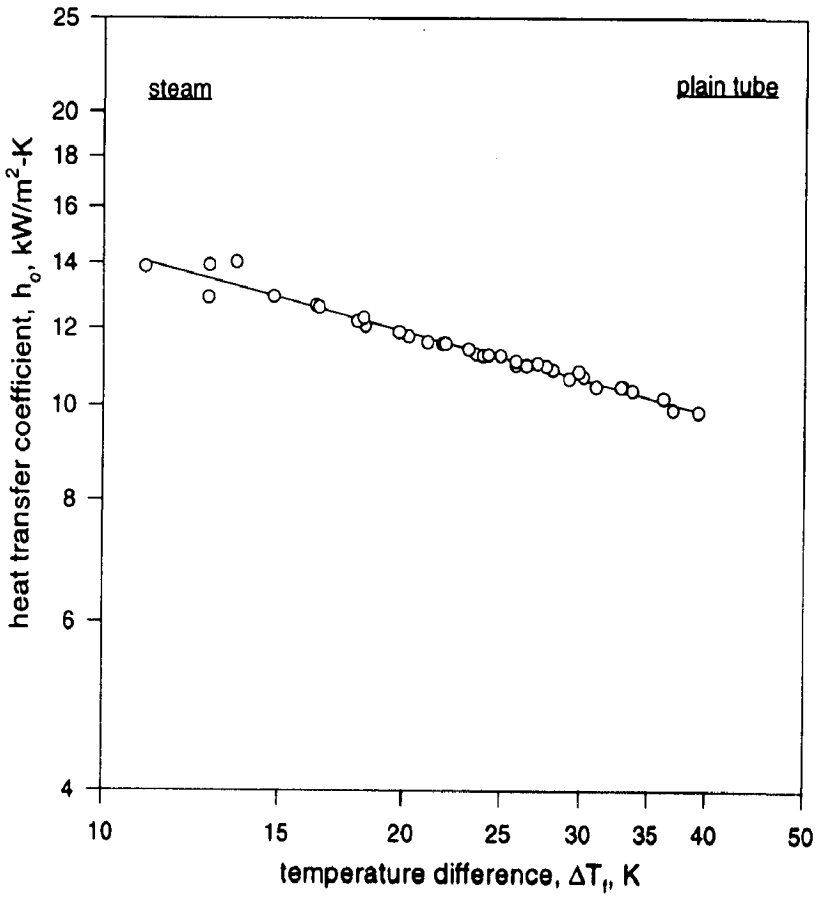

Figure 5.4
Variation of condensing side heat transfer coefficient with vapour to tube wall temperature difference for the condensation of steam over a plain tube

In case of both, refrigerants and steam, the data points tend to be on a straight line on a log-log plot and the heat transfer coefficient has reduced with the rise in ΔT_f. This is an expected trend as temperature difference across the condensate layer, ΔT_f, increases, more heat is transferred (heat flux increases) to the tube wall due to the generation of more condensate on the tube surface. This leads to the formation of a thick layer of condensate around the tube and the heat transfer coefficient decreases.

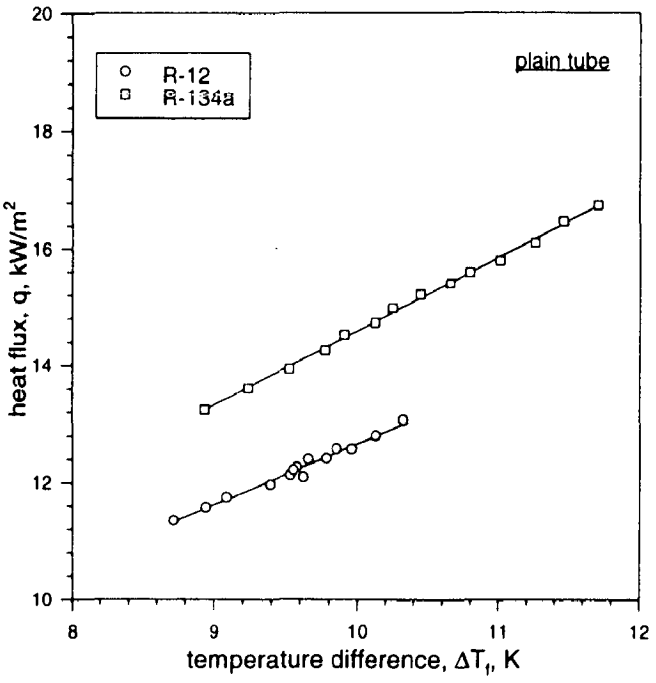

Figure 5.5
Variation of heat flux with vapour to tube wall temperature difference for the condensation of refrigerants over a plain tube

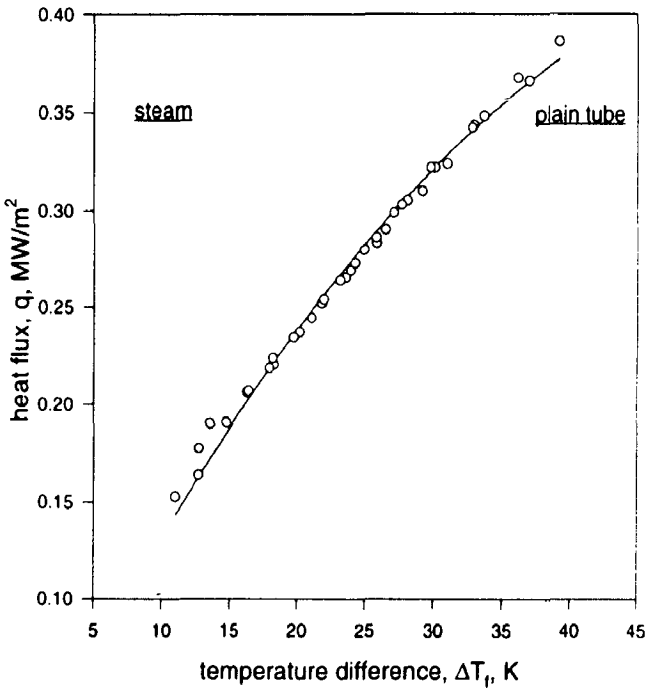

Figure 5.6
Variation of heat flux with vapour to tube wall temperature difference for the condensation of steam over a plain tube

Figure 5.5 and Figure 5.6 show the effect of ΔT_f on heat flux for the condensation of refrigerants and steam respectively. As can be seen from the figures the heat flux increases with the rise in ΔT_f. Though the rise in the value of heat flux with ΔT_f clearly indicates that, with the rise in ΔT_f the heat transfer coefficient decreases the net effect is that more heat is passed from vapour to coolant.

The facts observed in Figure 5.5 & 5.6 become more clear in the Figure 5.7 and Figure 5.8. These figures are plotted between the condensing side heat transfer coefficient and the heat flux for the condensation of refrigerants and steam respectively. The trends in these graphs clearly testify that with the rise in heat flux, the heat transfer coefficient for a plain tube decreases during condensation of steam as and well as refrigerants, though, the rate of decrease is different in both the cases. This fact is in agreement with the findings of Marto[45] for the condensation of refrigerants and Wanniarachchi et al.[88] for the condensation of steam.

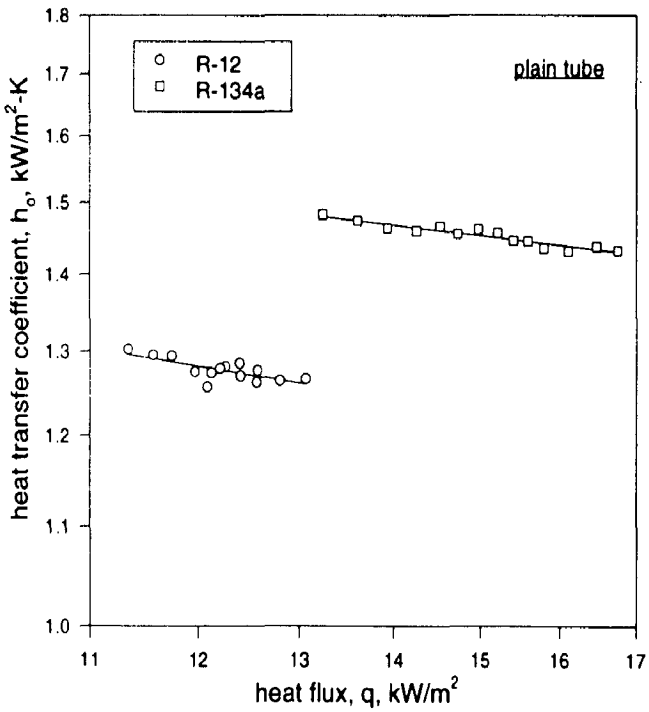

Figure 5.7
Variation of condensing side heat transfer coefficient with heat flux for the condensation of refrigerants over a plain tube

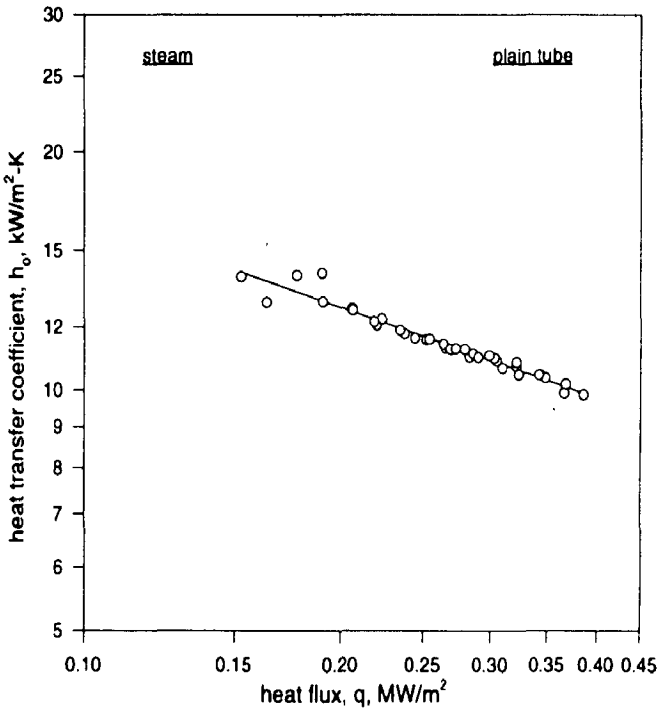

Figure 5.8
Variation of condensing side heat transfer coefficient with heat flux for the condensation of steam over a plain tube

The, following conclusions have been drawn for the condensation of steam and R-134a vapours over a horizontal plain tube.

(a) For the condensation of steam, R-12 and R-134a over a plain tube, the heat transfer coefficient reduces with the rise in ΔT_f.

(b) The Nusselt's model underpredicts the heat transfer coefficient for the condensation of steam, whereas, it overpredicts the heat transfer coefficient for the condensation of refrigerants R-12 and R-134a.

(c) For a plain tube the experimental heat transfer coefficient for R-134a is approximately 15 percent more than that for R-12 at the same vapour to tube wall temperature difference, ΔT_f.

(d) On the same horizontal plain tube the heat transfer coefficients for R-134a predicted by Nusselt's model are nearly 16 percent more than those for R-12 at a given value of ΔT_f.

(e) The modification of constant C_o(original value 0.725) in Nusselt's model[62] to 0.65 for the condensation of R-134a and R-12, and 0.8 for the condensation of steam facilitates the prediction of experimental data in an error band of ±2 percent for the condensation of refrigerants(R-12 & R-134a) and ±3 percent for the condensation of steam.

The results embodied in Section 5.2 are used as the reference results to evaluate the performance of finned tubes in subsequent sections.

5.3 CONDENSATION OVER CIRCULAR INTERGRAL-FIN TUBES (CIFTs)

Experimental studies [48,83,87,97] for the condensation over horizontal circular integral-fin tubes (CIFTs) have shown that the vapour side heat transfer coefficient is enhanced by many folds for the condensation of steam and refrigerants. The investigations have also confirmed that the enhancement in heat transfer coefficient is much more than the increase in the tube surface area due to finning [50,83]. In those cases where the vapour side film resistance is the controlling resistance, the CIFTs can reduce the size of condensers significantly for a given heat duty.

The optimum fin spacing for the condensation of steam over CIFTs has already been determined by a number of investigators [86,87,97] and it is 1.5 mm. In the present study the data for the condensation of steam over a horizontal CIFT with optimum fin density i.e. 390fpm and approximately 1.5 mm fin spacing has been generated to compare the performance of finned tubes like spine integral-fin tubes(SIFTs) and paritally-spined circular integral-fin tubes(PCIFTs) with that of CIFT.

For the condensation of R-134a, no reported work is available. Therefore, in the present investigation an optimum fin density for the condensation of R-134a over CIFTs has been determined by varying the fin density systematically.

The results of the present investigation are discussed below:

5.3.1 Effect of The Temperature of Condensing Vapour on Heat Transfer Coefficient- Steam

In the present investigation, for the condensation of steam, the data are collected at different saturation temperatures of steam, T_s. The cooling water flow rate has been varied in a certain range for each saturation temperature. In Figure 5.9 a graph has been plotted between the condensing side heat transfer coefficient and ΔT_f.

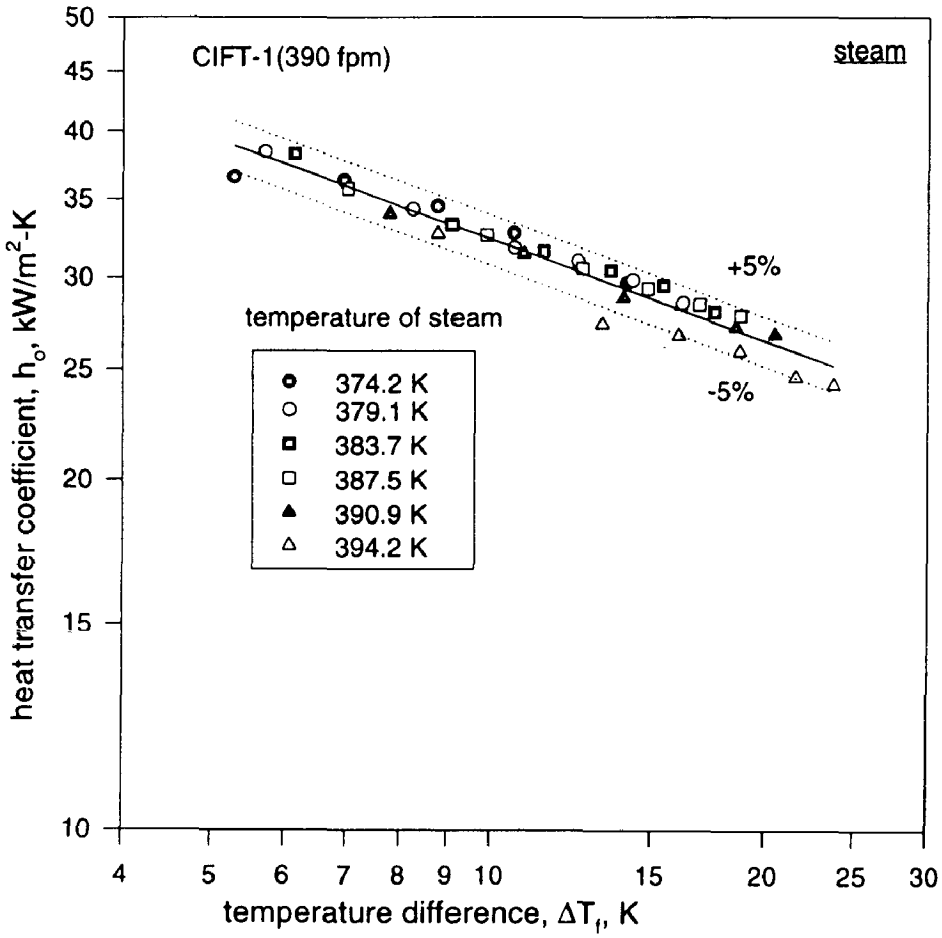

Figure 5.9
Effect of the temperature of condensing vapour on condensing side heat transfer coefficient for the condensation of steam

The following facts have been observed in this graph:

(a) The heat transfer coefficient decreases with increase in ΔT_f irrespective of the value of saturation temperature, T_s.

(b) The heat transfer coefficient is not dependent on the temperature of the condensing vapour, but the temperature across the condensate layer, ΔT_f.

It is interesting to note that a given heat flux(or ΔT_f) can be attained either by varying the saturation temperature of condensing vapour, T_s, or coolant flow rate which subsequently reduces the tube wall temperature. In other words, same heat transfer coefficient can be achieved by regulating either of the two parameters i.e. T_s and coolant flow rate. In the present investigation the saturation temperature of steam has been varied between 374.2K and 394.2K, whereas, ΔT_f has changed from 5.3K to 23.7K. For the said range of ΔT_f the condensing side heat transfer coefficient lies well within ±5% of the best fit line and 80 percent of experimental data lie in a range of ±3 percent.

As in the present experiments the uncertainty also varies up to 4%(Figure A-1 in Appendix-B), these results conclude that the condensing side heat transfer coefficient at constant ΔT_f is almost independent of the saturation temperature, T_s. No doubt that, the heat transfer coefficient seems to be independent of the fact that how a particular ΔT_f (or heat flux) is achieved, either by varying the cooling water flow rate or by increasing the condensing steam pressure. Therefore, during condensation of refrigerants i.e. R-12 and R-134a only the cooling water flow rate was altered to have different values of condensing side heat transfer coefficient at different ΔT_f. Almost all the data for R-134a were acquired at 312.4±0.5K temperature of condensing vapours which is closer to the vapour temperature inside the condenser of a refrigeration plant.

5.3.2 Effect of ΔT_f on Heat Flux

First of all trustworthiness of experimental results pertaining to the condensation of steam and R-134a over finned tubes, has been verified through the criterion given by Yau et al.[98].

It is a know fact that the heat flux across the condensate layer is proportional to the temperature difference across the condensate film, ΔT_f (the primary driving force for the transfer of heat from vapour to tube wall). The relationship between heat flux(q) and ΔT_f is

given below:

$$q = h_o \Delta T_f \tag{5.2}$$

According to Nusselt's theory[62], h_o is proportional to the $\Delta T_f^{-0.25}$, thus, the equation (5.2) for practical purposes can be written in the following form

$$q = a\Delta T_f^b \tag{5.3}$$

The equation (5.3) indicates that the heat flux, q, and ΔT_f have a non-linear relationship and heat flux increases with ΔT_f. In equation (5.3) the 'a' and 'b' are constants and in an ideal case the value of 'b' should be equal to 0.75. But, for all practical purposes, for plain tubes as well as for finned tubes the experimentally determined value of 'b' are likely to vary between 0.7 and 0.8, as pointed by Yau et al.[98]. The value of 'a' depends upon the thermo-physical properties of condensing fluid and the fin geometry.

Table-5.2

values of constants in equation (5.3)

fluid	tube	a	b	r^2
steam	plain tube	27.29	0.72	0.99
	CIFT-1(390 fpm)	65.27	0.70	0.99
R-134a	plain tube	1.98	0.86	0.98
	CIFT-2(934 fpm)	7.58	0.71	0.97
	CIFT-3(1250 fpm)	9.41	0.82	0.96
	CIFT-4(1560fpm)	11.67	0.86	0.96
	CIFT-5(1875fpm)	12.51	0.78	0.98

r^2 = Sum of the squares of residues

According to them in an experiment if the value of 'b' lies between 0.7 to 0.8, it can be safely concluded as a reliable one. The value of constants 'a' and 'b' for equation (5.2) computed from the present experimental data are tabulated in Table-5.2. The value of 'b' hovers between 0.7 to 0.85 and its value for the 80 percent of experimental data lie between 0.7 and 0.8.

Figure 5.10 and 5.11 have been drawn between the heat flux and the temperature difference across the condensate layer, ΔT_f, for the condensation of steam and R-134a respectively.

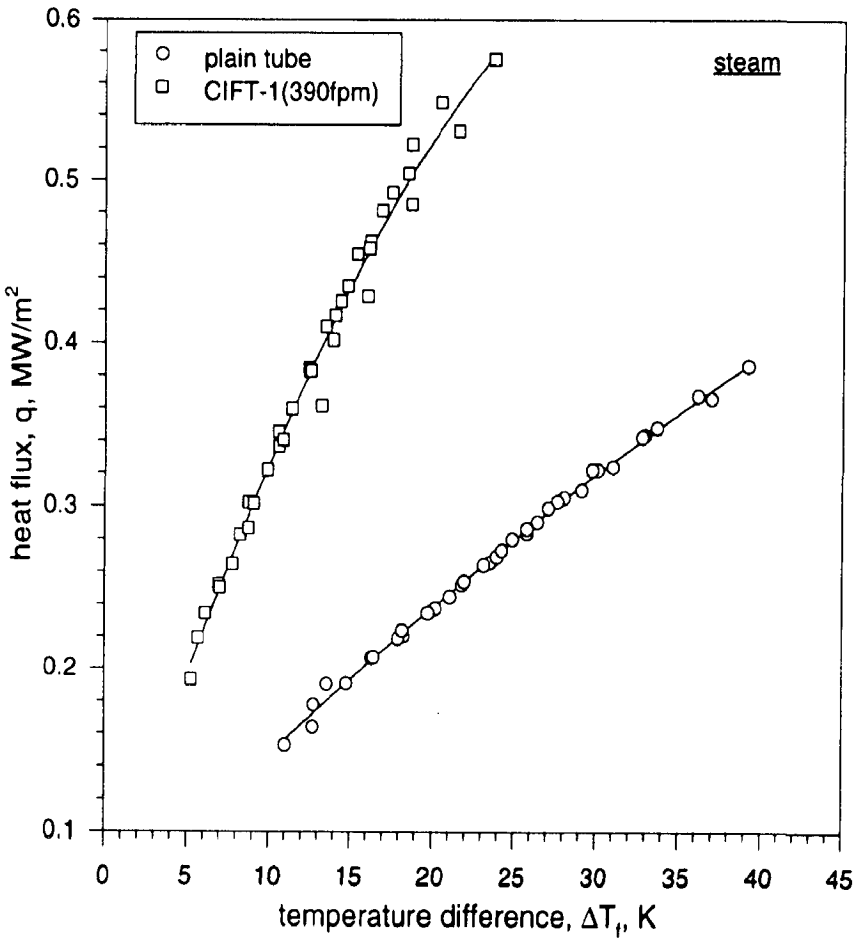

Figure 5.10
Variation of heat flux with vapour to tube wall temperature difference for the condensation of steam over CIFT-1

The scrutiny of these figures reveals the following note worthy observations:

(a) At a constant temperature difference across the condensate layer, ΔT_f, the heat flux for CIFTs is more than that for the plain tubes for the condensation of steam as well as R-134a.

(b) The heat flux increases with rise in the temperature difference across the condensate layer, ΔT_f, for the condensation of steam and R-134a.

(c) For a given value of ΔT_f, the heat flux increases up to a fin density of 1560 fpm(CIFT-4) and then decreases for the condensation of R-134a.

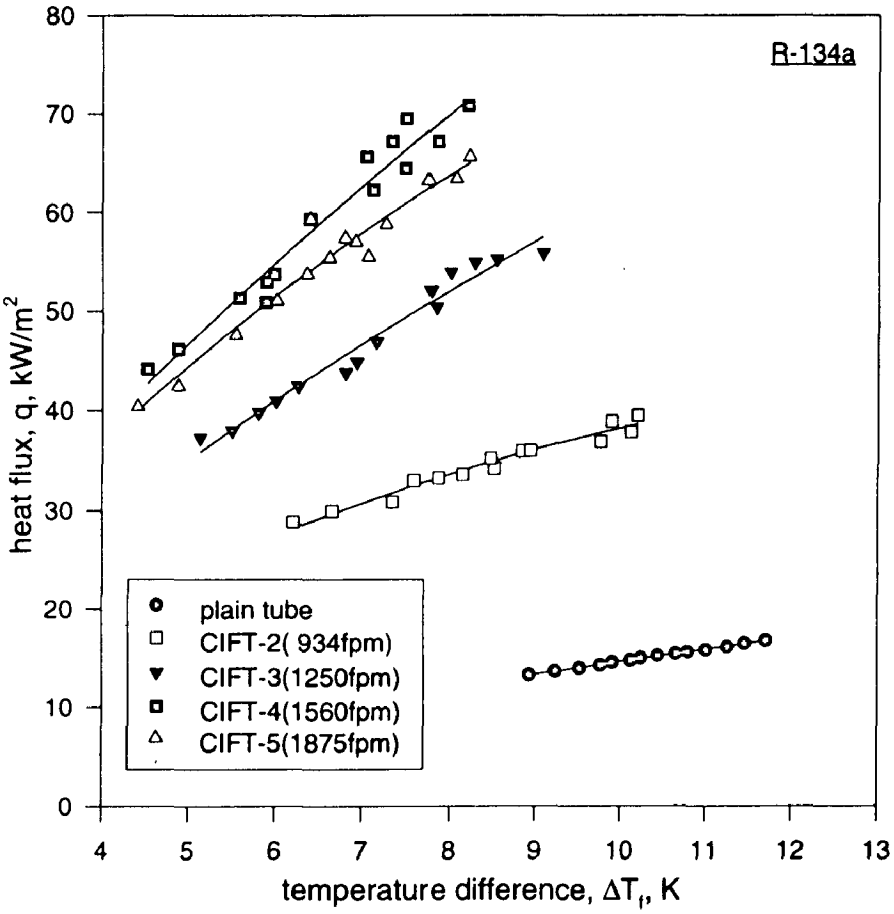

Figure 5.11
Variation of heat flux with vapour to tube wall temperature difference for the condensation of R-134a over CIFTs

The observation at point (a) clearly indicates that for a given value of ΔT_f the rate of condensation is more on a CIFT than that on a plain tube as the heat transfer coefficient for CIFT is appreciably more than that for a plain tube. This is primarily due to enhanced drainage capability of CIFT which maintain small thickness of condensate film around the tube even in face of increased rate of condensation over it [25].

The observation at point (b) can be explained on the basis of the equation (5.2). Although, an increase in the ΔT_f leads to a lower value of heat transfer coefficient, h_o, yet the system behaves in such a way that the product of h_o and ΔT_f increases with the rise of ΔT_f, thus the heat flux increases. This fact is true for all the tubes investigated i.e plain and CIFTs. According to Nusselt's equation heat transfer coefficient, h_o, is proportional to $\Delta T_f^{-0.25}$ and hence, heat flux is proportional to $\Delta T_f^{0.75}$ for a plain tube. Which clearly shows that heat flux should increase with rise in ΔT_f.

The observation in point (c) is only due to variation in heat transfer coefficient due to finning. The detailed explanation is given in Section 5.3.4.

5.3.3 Effect of Heat Flux on Heat Transfer Coefficient

The variation of condensing side heat transfer coefficient with heat flux has been illustrated in Figure 5.12 and Figure 5.13 on a log-log plot for the condensation of steam and R-134a respectively.

These figures reveal that

(a) Heat transfer coefficient of CIFTs is always more than that for a plain tube for the condensation of steam as well as of R-134a.

(b) Heat transfer coefficient reduces with heat flux for the condensation of steam and R-134a as well.

(c) In case of R-134a, for a given heat flux, the heat transfer coefficient increases with the fin density up to 1560 fpm. A further increase in fin density decreases the heat transfer coefficient.

As explained in Section 5.2, higher heat flux generates thicker condensate film around the tube which in turn reduces the condensing side heat transfer coefficient. The performance of a finned tube can also be judged by comparing the condensing side heat transfer coefficient at a given heat flux. For example, during the condensation of steam at a heat flux of 0.3MW/m^2 the condensing side heat transfer coefficient is 10.9 kW/m^2-K and 33.2 kW/m^2-K for the plain tube and CIFT-1 respectively.

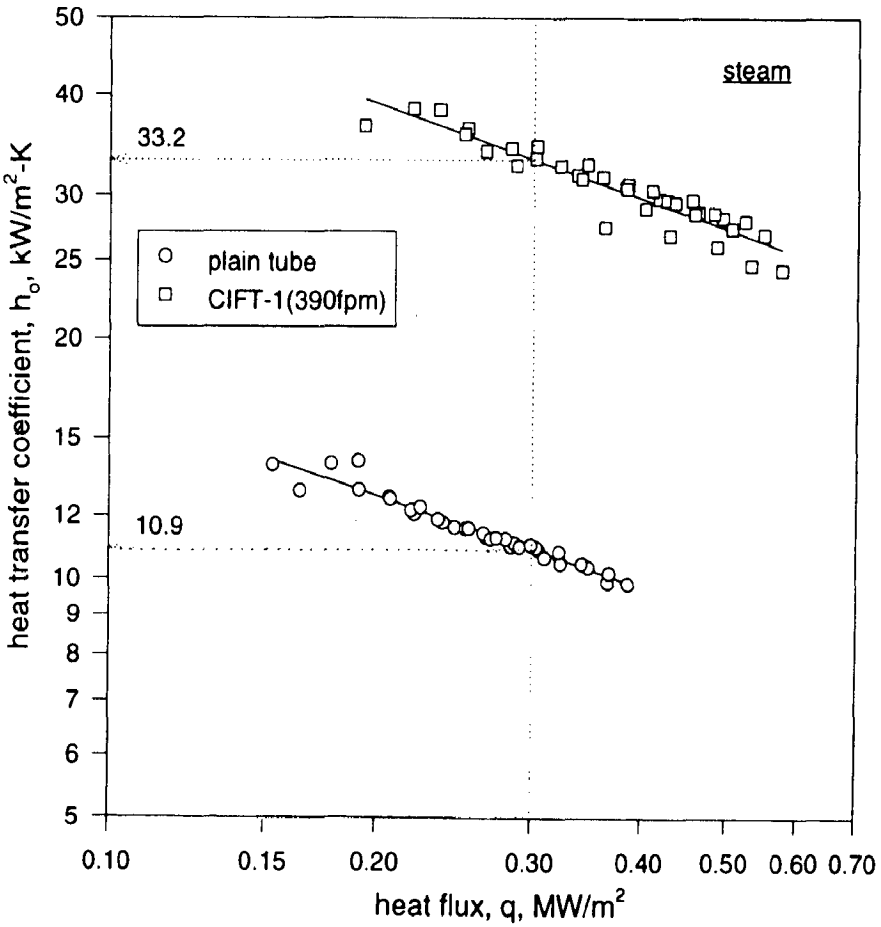

Figure 5.12

Variation of condensing side heat transfer coefficient with heat flux for the condensation of steam over CIFT-1

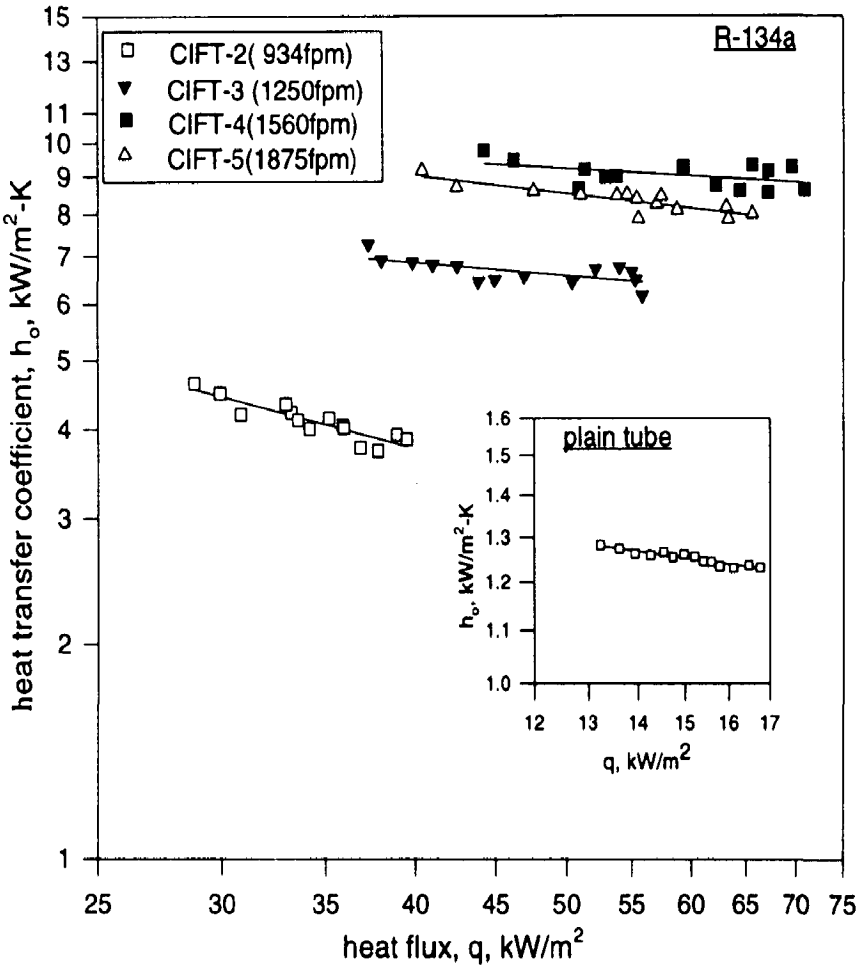

Figure 5.13
Variation of condensing side heat transfer coefficient with heat flux for the condensation of R-134a over CIFTs

These values are estimated from the best fit line. This clearly indicates that for the equal condensate loading over unit surface area (for the same heat flux) the heat transfer coefficient of CIFT-1 is almost three times higher than that of the plain tube. This is primarily due to the higher rate of drainage from finned tubes due to surface tension. The explanation of point (c) is given in Section 5.3.4.

5.3.4 Effect of ΔT_f on Heat Transfer Coefficient

During condensation over CIFTs, the effect of ΔT_f on condensing side heat transfer coefficient is again significant like that over plain tubes. To illustrate the above fact Figure 5.14 and Figure 5.15 have been plotted between the heat transfer coefficient and ΔT_f on a log-log scale for the condensation of steam and R-134a respectively.

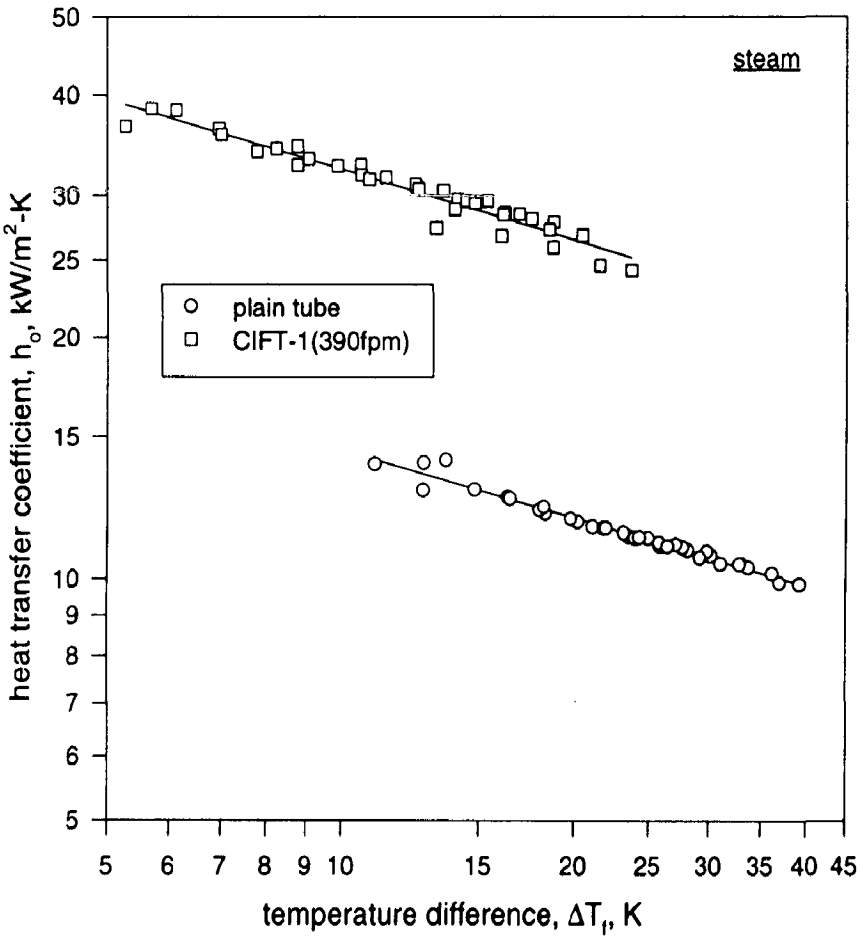

Figure 5.14
Variation of condensing side heat transfer coefficient
with vapour to tube wall temperature difference
for the condensation of steam over CIFT-1 .

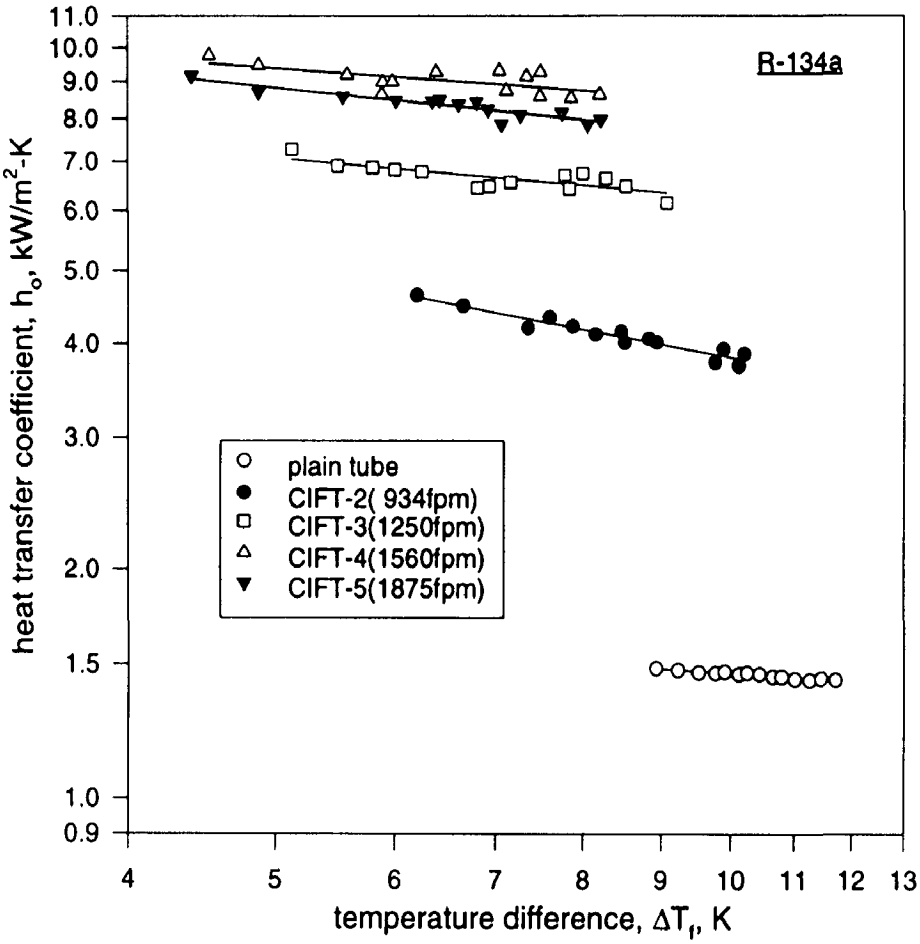

Figure 5.15
Variation of condensing side heat transfer coefficient with vapour to tube wall temperature difference for the condensation of R-134a over CIFTs

The following facts are observed in these figures:

(a) The heat transfer coefficient for the condensation of steam and R-134a over CIFTs is more than that for their condensation over plain tube in the range of ΔT_f investigated.

(b) The condensing side heat transfer coefficients for steam as well as R-134a reduce with the increase in ΔT_f.

(c) For the condensation of R-134a the condensing side heat transfer coefficient increases with fin density irrespective of the value of ΔT_f and reaches a maximum for CIFT-4 having fin density of 1560 fpm and then decreases.

The heat transfer coefficient for the condensation of steam and R-134a over CIFTs is more than that over a plain tube for all values of ΔT_f investigated. This is due to the fact that the CIFTs drain condensate at a faster rate than plain tubes leading to a thinner condensate layer on CIFTs surface. The drainage of condensate from a CIFT is surface tension and gravity dominated, whereas, from a plain tube it is only gravity dominated[25]. The change in the curvature of condensate film from fin tip to the fin root generates a force in the direction of fin root due to surface tension and thereby yield a thinner condensate film on the fin surface [73].

The behaviour of the tubes that with the rise in ΔT_f the heat transfer coefficient decreases can be explained as follows:

With the rise in ΔT_f heat flux also increases resulting in increased rate of vapour condensation on the tube surface and brings forth a thicker condensate layer around it. This layer offers higher thermal resistance to flow of heat from vapour to tube wall and in turn reduces the condensing side heat transfer coefficient.

With the increase in fin density the surface area(for heat transfer) of tube exposed for condensation increases and thus helps in increasing the rate of heat transfer. However, at the same time the increase in fin density reduces the fin pitch, P_f, and helps more and more condensate to be retained in the inter fin spacing and thereby increases the condensate retention angle, ϕ. This makes a substantial portion of tube ineffective for heat transfer. As observed by Webb et al.[92] the area flooded by condensate hampers the heat transfer from vapour to tube and contributes towards 2% of total heat transfer. Hence, the increase in heat

transfer area and decrease in inter-fin spacing due to increase in fin density, tends to counter-act each other. In fact, an optimum fin spacing is always expected when the fin density is increased systematically.

Therefore, for the condensation of R-134a over CIFTs the heat transfer coefficient increases with the fin density and attains a maximum value at 1560 fpm fin density (CIFT-4). A further increase in the fin density to 1875 fpm reduces the condensing side heat transfer coefficient. Therefore, the CIFT-4 (with 1560 fpm) turns out to be the best performing tube amongst those tested.

5.3.5 Variation of Enhancement Factor With ΔT_f

The enhancement in heat transfer coefficient due to finning on the tube surface is defined as the ratio of the heat transfer coefficient of finned tube to that for a plain tube at the same value of ΔT_f. During experimentation it is difficult to generate heat transfer coefficient data for finned tubes exactly at the same values of ΔT_f on which the heat transfer coefficient data for plain tubes were generated. In other words, to evaluate the actual performance of the finned tubes vis a vis the plain tube the heat transfer coefficient for both the tubes should be evaluated at same ΔT_f (which is experimentally difficult to obtain). The above problem has been solved by using the modified Nusselt's model (discussed in Section 5.2) to calculate the heat transfer coefficient of the plain tube exactly at the same ΔT_f values at which the experimental values of heat transfer coefficient for finned tubes are available. So, the enhancement factor, EF, in the present case is the ratio of experimental heat transfer coefficient during condensation over finned tubes and the heat transfer coefficient by the modified Nusslt's model (which has been found to predict experimental heat transfer coefficient with in an error band of ±3% for the condensation of steam and ±2% for the condensation of R-134a) as discussed in Section 5.2.

The Figure 5.16 and Figure 5.17 show the variation of enhancement factor, EF, with ΔT_f for the condensation of steam and R-134a, respectively. The Figure 5.18 is drawn to show the variation of EF and area ratio(A_F/A_r) with the fin density for the condensation of R-134a.

The salient features of these figures are as follows:

(a) For the condensation of steam as well as R-134a the enhancement factor, EF, is hardly affected by variation in the temperature difference across the condensate layer, ΔT_f for the range of ΔT_f investigated.

(b) The enhancement factor, EF, which is a measure of the heat transfer augmentation, increases with fin density and acquires a maximum value of 5.63 at 1560 fpm(CIFT-4) for the condensation of R-134a and then decreases, whereas, the area increase due to finning on this tube is only 3.06 times of the area of a plain tube with a diameter equal to the fin root diameter, D_r.

(c) The value of factor, EF, for the condensation of steam over CIFT-1(390 fpm) remains in a range of 2.04 to 2.39 and has a mean value of 2.27 and the area increase due to finning is only 1.93 times the area of a plain tube with a diameter equal to the fin root diameter, D_r.

(d) The observations given in (b) and (c) show that the enhancement in heat transfer is more than the increase in area due to finning.

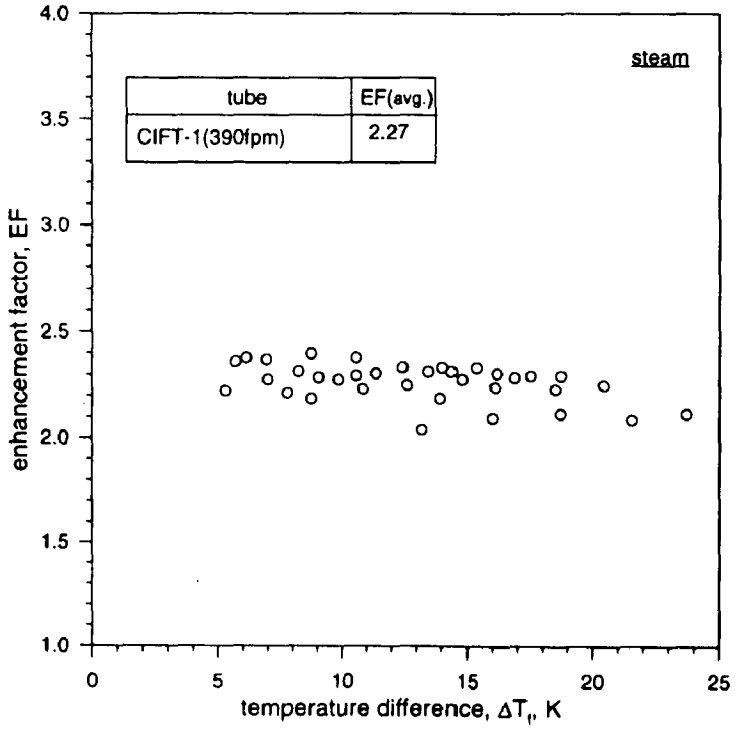

Figure 5.16
Variation of enhancement factor with temperature difference for the condensation of steam over CIFT-1

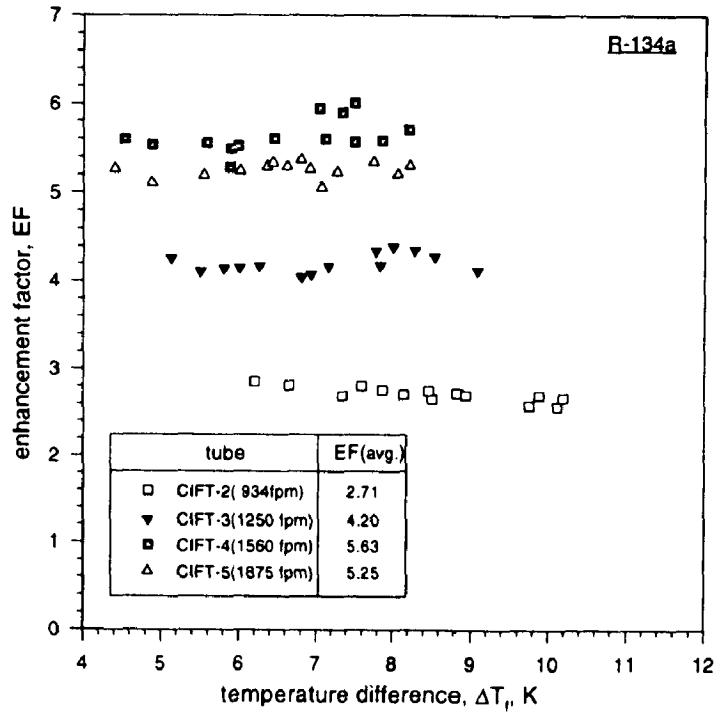

Figure 5.17
Variation of enhancement factor with tempearature difference for the condensation of R-134a over CIFTs

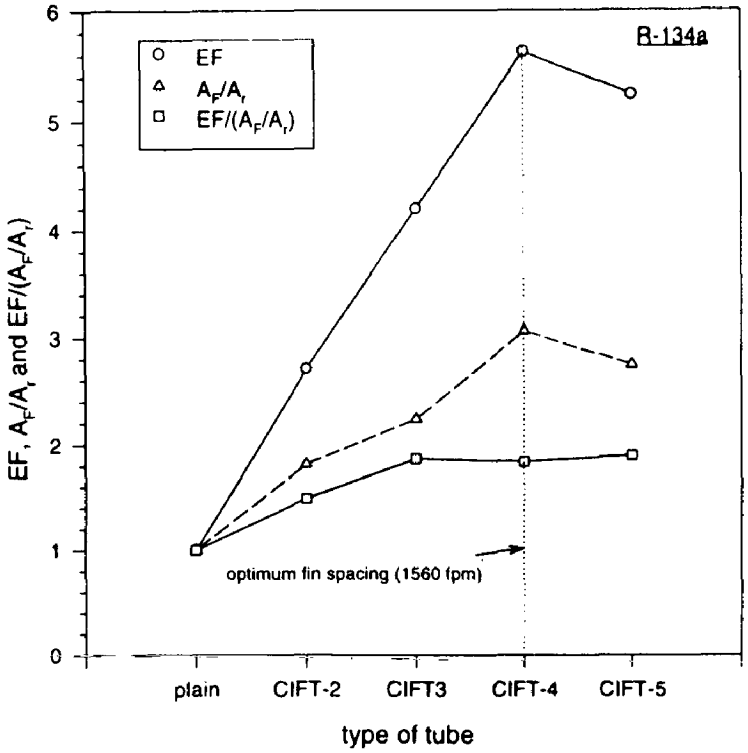

Figure 5.18
Variation of different enhancement factors with fin density for the condensation of R-134a over plain tube and CIFT's

Table- 5.3

enhancement factors of different CIFTs

fluid	tube	EF	A_f/A_r
steam	CIFT-1(390 fpm)	2.27	1.93
R-134a	CIFT-2(934fpm)	2.71	1.82
	CIFT-3(1250fpm)	4.20	2.24
	CIFT-4(1560fpm)	5.63	3.06
	CIFT-5(1875fpm)	5.24	2.75

The value of enhancement factor obtained for different tubes for the condensation of steam and R-134a can be seen in the Table 5.3. The table shows that 1560 fpm tube (CIFT-4) has the maximum value of enhancement factor and it is equal to 5.63, whereas, the area increase due to finning is only 3.06 times. Therefore, the fins not only increase the condensing side heat transfer coefficient by increasing the tube surface area but also through a heat transfer augmentation process, which has been attributed to the thinning of the condensate film over the fin surface due to surface tension. This has been observed by Marto et al.[44], Sukhatme et al.[83] and several other investigators also.

During condensation the heat flux is reported as a product of heat transfer coefficient and temperature difference, ΔT_f, and a constant heat flux can be attained with different values of heat transfer coefficient and ΔT_f. The relation between the enhancement factors at constant heat flux, EF_q, and at constant temperature difference across the condensate layer ΔT_f, $EF_{\Delta t}$, has been given by Masuda and Rose[49] in the following form (details given in Appendix-C)

$$EF_q = (EF_{\Delta T})^{4/3} \tag{5.4}$$

From equation (5.4) it can be concluded that at a constant heat flux the augmentation in heat transfer coefficient is more than that at a constant temperature difference, ΔT_f. Now, it is up to the design engineer to choose either of the values as per his design limitations and priorities. For the condensation of steam the enhancement factor at constant heat flux, EF_q, is 3.06 and enhancement factor at constant ΔT_f is 2.27. These values in equation (5.4) gives the value of 's' equal to 1.36 which is close to the theoretical value of 's'. The analysis for the condensation of R-134a over CIFTs on the same line is not possible as the range of the heat flux for the condensation over plain tube(13-17 kW/m^2) is much less than the range for the condensation over CIFTs(30-75 kW/m^2).

5.4 CONDENSATION OVER SPINE INTEGRAL-FIN TUBES (SIFTs)

Though, the CIFTs enhance the condensing side heat transfer coefficient in a significant manner a major objective of the present investigation is to study if, further enhancement of condensing side heat transfer coefficient for the condensation of steam and R-134a is attainable by horizontal spine integral-fin tubes(SIFTs). The spine fins are, in fact, three dimensional fins. It is expected that the three dimensional fins will help in further thinning the condenste film on the tube surface. Therefore, this new fin geometry is expected to display better performance than that of CIFTs and a comparison between the performance of the best performing CIFTs and SIFTs has been carried out so that viability of use of latter can be evaluated. In fact, the performance of SIFT-1 which is prepared by cutting 40 axial slots on CIFT-1 has been compared with CIFT-1, the best performing CIFT for condensation of steam. Similarly the performance of SIFT-2, which is prepared by cutting 60 axial slots on CIFT-4 has been compared with CIFT-4, the best performing CIFT for the condensation of R-134a.

5.4.1 Effect of The Temperature of Condensing Vapour on Heat Transfer Coefficient- Steam

Like CIFTs, first the effect of the temperature of condensing steam, T_s, on condensing side heat transfer coefficient at a constant ΔT_f has been investigated.

In Figure 5.19 a graph has been plotted between the condensing side heat transfer coefficient and ΔT_f at different saturation temperatures, T_s, of condensing steam. It shows that the effect of T_s on heat transfer coefficient is insignificant. The trend is similar to that for the condensation of steam over CIFT-1. As discussed in Section 5.3.1, the condensation of R-134a over SIFT-2 has been carried out at a temperature of 312.4±0.5K, which is close to the vapour temperature inside the condenser of a refrigeration plant.

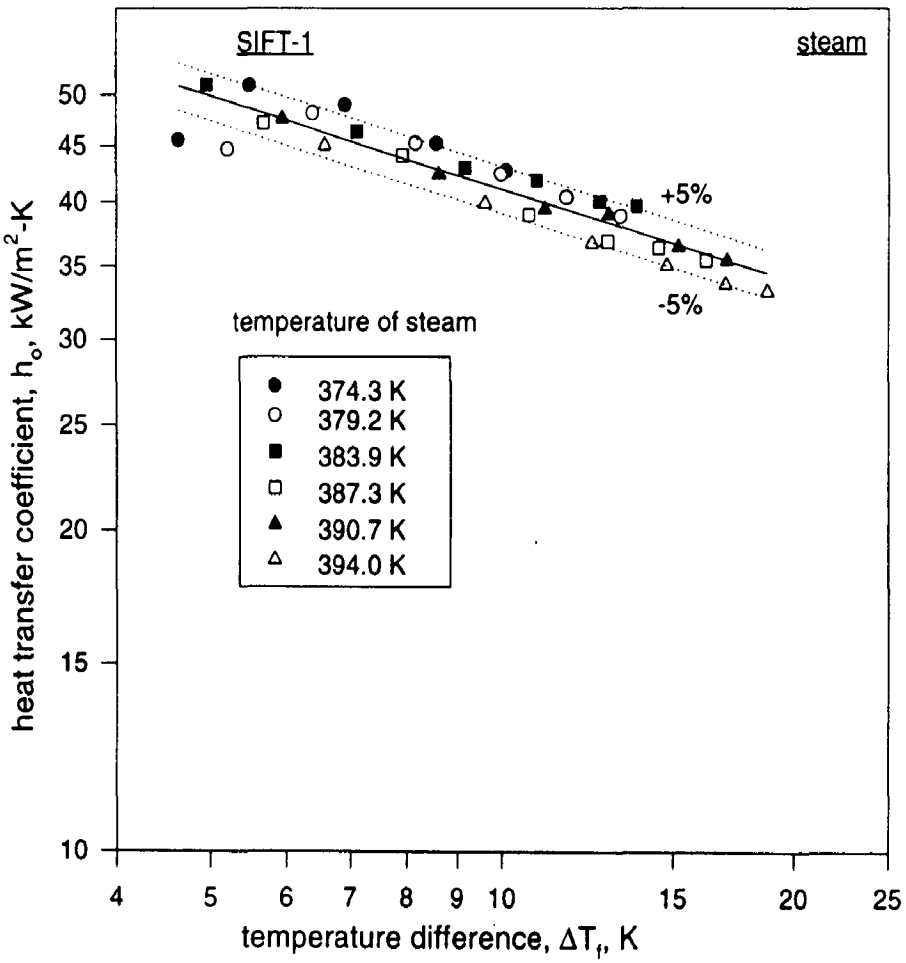

Figure 5.19
Effect of the temperature of condensing vapour on condensing side heat transfer coefficient for the condensation of steam

5.4.2 Effect of ΔT_f on Heat Flux

It is a known fact that the heat flux is equal to the product of heat transfer coefficient and the temperature difference across the condensate film, ΔT_f. In Figure 5.20 graph has been plotted between the heat flux and ΔT_f for the condensation of steam on a plain tube, CIFT and a SIFT. The Figure 5.21 illustrates the variation of heat flux with ΔT_f for the condensation of R-134a over a plain tube, the best performing CIFT i.e. CIFT-4(1560 fpm) and SIFT-2.

Following facts has been observed from these figures:

(a) At a given ΔT_f the SIFTs outperform the best performing CIFTs for the condensation of steam and R-134a, both.

(b) At lower value of ΔT_f the heat flux on SIFT-1 is marginally higher than that on the CIFT-1 for the condensation of steam.

(c) For the condensation of R-134a the proportionate increase in heat flux by SIFT-2 has reduced with rise in ΔT_f.

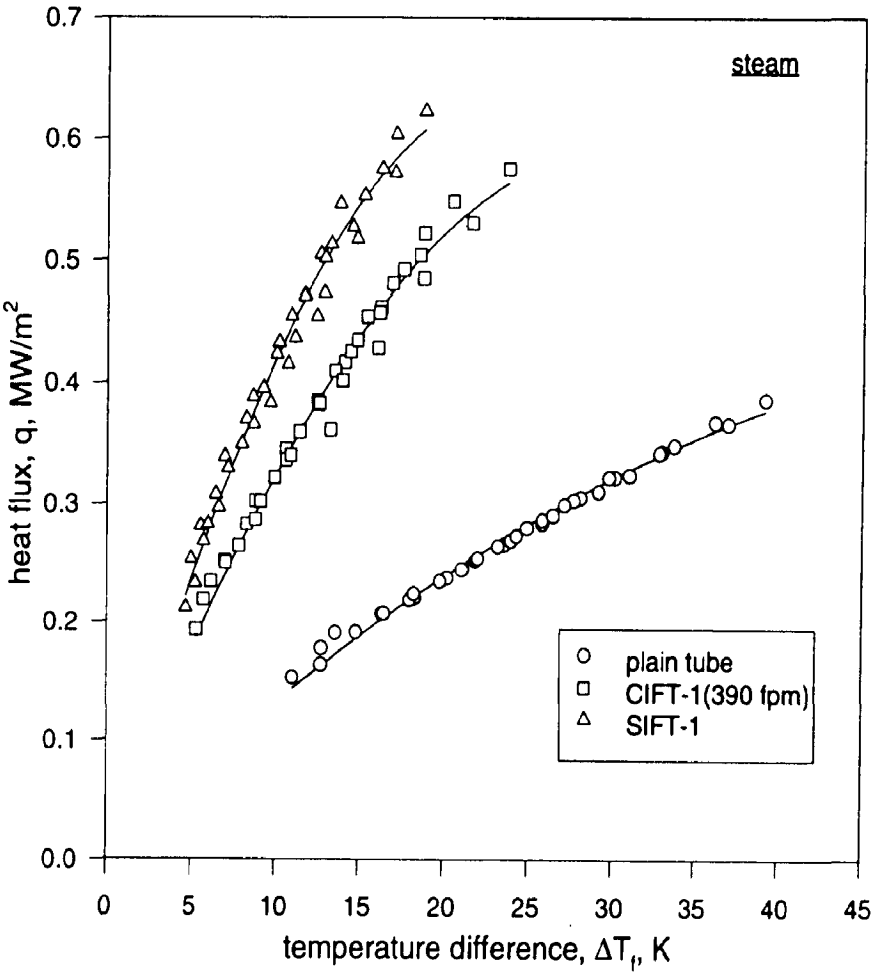

Figure 5.20
Variation of heat flux with vapour to tube wall temperature difference for the condensation of steam

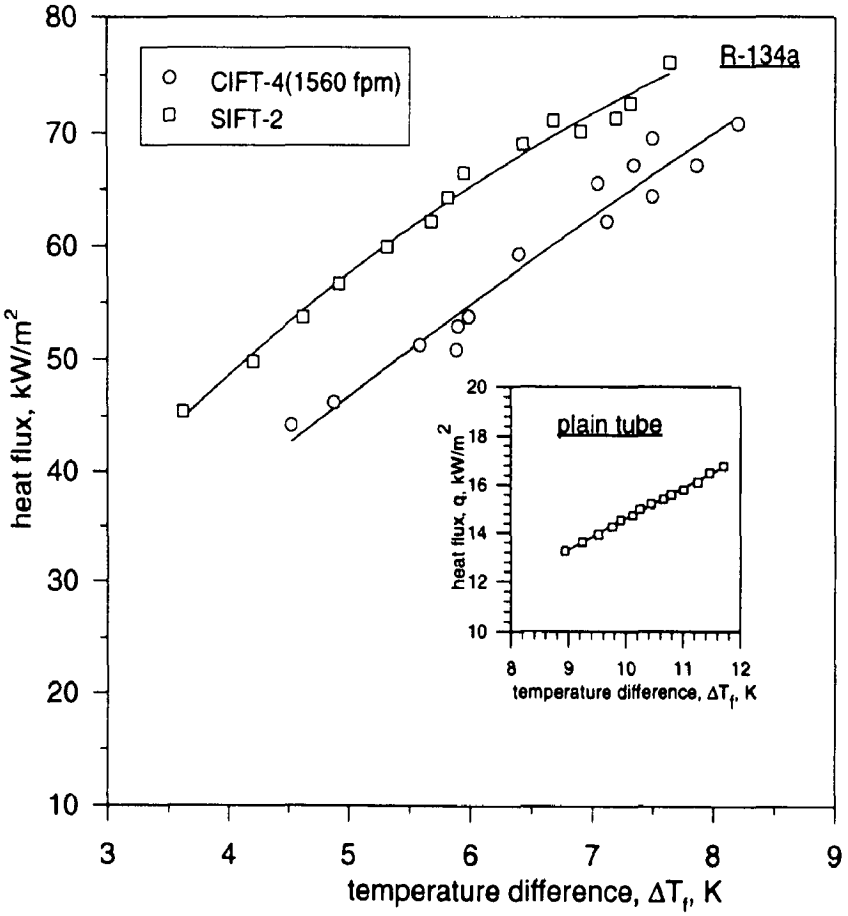

Figure 5.21
Variation of heat flux with vapour to tube wall temperature difference for the condensation of R-134a

The observation that the heat flux at a given ΔT_f is higher for the condensation of steam and R-134a over SIFTs is due to the fact that in SIFTs the drainage of condensate from the fin surface takes place in two directions. Because the spines are like pyramidical projections on the tube surface. The drainage of condensate from the fin surface is under the influence of surface tension thus the pull exerted on the condensate film is in two directions, which facilitates the thinning of condensate film on the tube surface [83].

Besides this, the condensate drainage from the bottom of the tube is faster as observed during the present experimentation and also observed by Rudy and Webb[74] as

well. Cumulative effect of these two factors is the decrease in ΔT_f due to thinner condensate film on the tube surface in comparison to CIFTs, at a constant heat flux.

As the heat flux increases the benefit of faster condensate drainage from the tube surface becomes apparent during condenation of steam. Hence, with the rise in ΔT_f the gap between the heat flux on SIFT-1 and CIFT-1 has been observed to increase. Therefore, it can be recommended that SIFT-1 is befitting for the higher value of ΔT_f for the condensation of steam. Unlike for the condensation of steam, the difference in heat flux values for CIFT-4 and SIFT-2 does not change appreciably when the value of ΔT_f is increased. The attainable heat flux over a SIFT(SIFT-2) is higher than that for the best performing CIFT(CIFT-4) at a given ΔT_f for the condensation of R-134a. Unlike for the condensation of steam, the difference in heat flux for a given ΔT_f does not change appreciably.

5.4.3 Effect of Heat Flux on Heat Transfer Coefficient

In Figure 5.22 and Figure 5.23 graphs have been plotted between heat flux and the condensing side heat transfer coefficient for the condensation of steam and R-134a respectively. These plots reveal the following typical trends:

(a) At a constant heat flux the condensing side heat transfer coefficient for SIFTs is more than that for CIFTs for the condensation of steam and R-134a both.

(b) The augmentation in heat transfer coefficient by SIFT-1 is uniform for the condensation of steam for the entire range of heat flux (0.2-0.6 MW/m^2), when compared with CIFT-1.

(c) For the condensation of steam the performance of SIFT-2 deteriorates faster in comparison to CIFT-4 as the heat flux is increased.

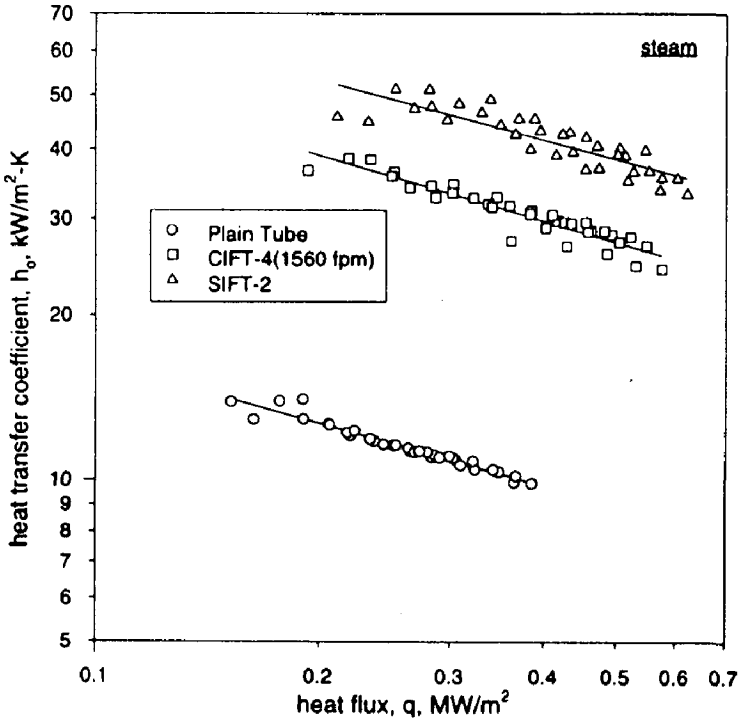

Figure 5.22
Variation of condensing side heat transfer coefficient with heat flux for the condensation of steam

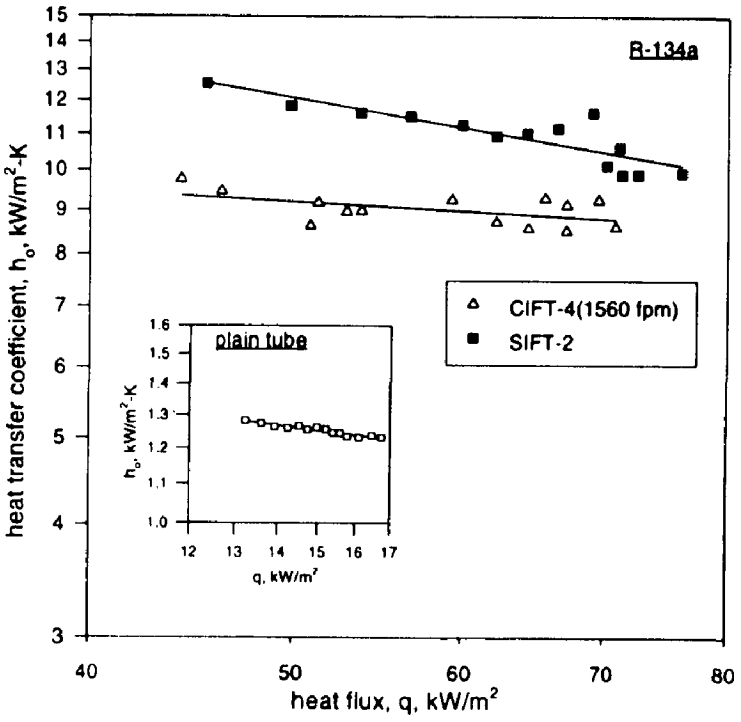

Figure 5.23
Variation of condensing side heat transfer coefficient with heat flux for the condensation of R-134a

The SIFTs give higher heat transfer coefficient in comparison to best performing CIFT at a constant heat flux, for example, for the condensation of steam at 0.35 MW/m^2 heat flux the condensing side heat transfer coefficients for plain tube, CIFT-1 and SIFT-1 are 10.27, 31.29 and 43.51 kW/m^2-K, respectively. Hence, the SIFT enhance heat flux 4.24 times in comparison to the plain tube and 1.39 times in comparison to the CIFT-1. These values are taken from the best fit lines of the graph.

For the condensation of R-134a no generalise quantitative inference can be drawn as the characteristic curves are converging. At a heat flux equal to 45 kW/m^2 the heat transfer coefficient for SIFT-2 is 36 percent more while at the heat flux of 65 kW/m^2 the heat transfer coefficient is 24 percent more than that for the CIFT-4 (1560 fpm).

The following equation has been developed to correlate the ratio of heat transfer coefficients for CIFT-4 and the SIFT-2 for a given heat flux for the condensation of R-134a.

$$\frac{(h_o)_{CIFT-4}}{(h_o)_{SIFT-2}} = 3.8q^{-0.27} \qquad (5.5)$$

5.4.4 Effect of ΔT_f on Heat Transfer Coefficient

Figure 5.24 & 5.25 are drawn to show the variation of condensing side heat transfer coefficient of SIFT with respect to vapour to wall temperature difference, ΔT_f, for the condensation of steam and R-134a respectively. For the sake of comparison curves for CIFT and plain tube are also shown in this figure.

Following are the notable features of these graphs

(a) The heat transfer coefficient decreases with increase in ΔT_f for the condensation of steam and R-134a.

(b) For a given ΔT_f the heat transfer coefficient for the condensation of steam and R-134a over SIFTs is higher than that for CIFTs.

(c) For the condensation of R-134a the performance of SIFT-2 deteriorates faster than CIFT-4 at higher ΔT_f.

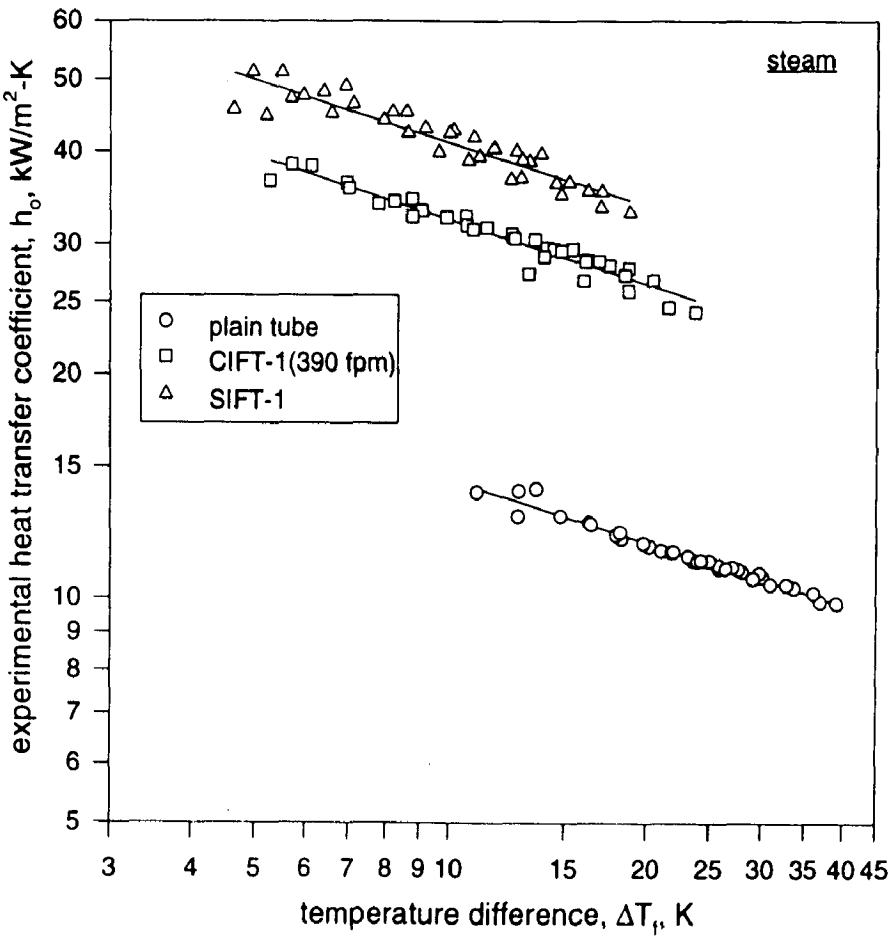

Figure 5.24

Variation of condensing side heat transfer coefficient with vapour to tube wall temperature difference for the condensation of steam

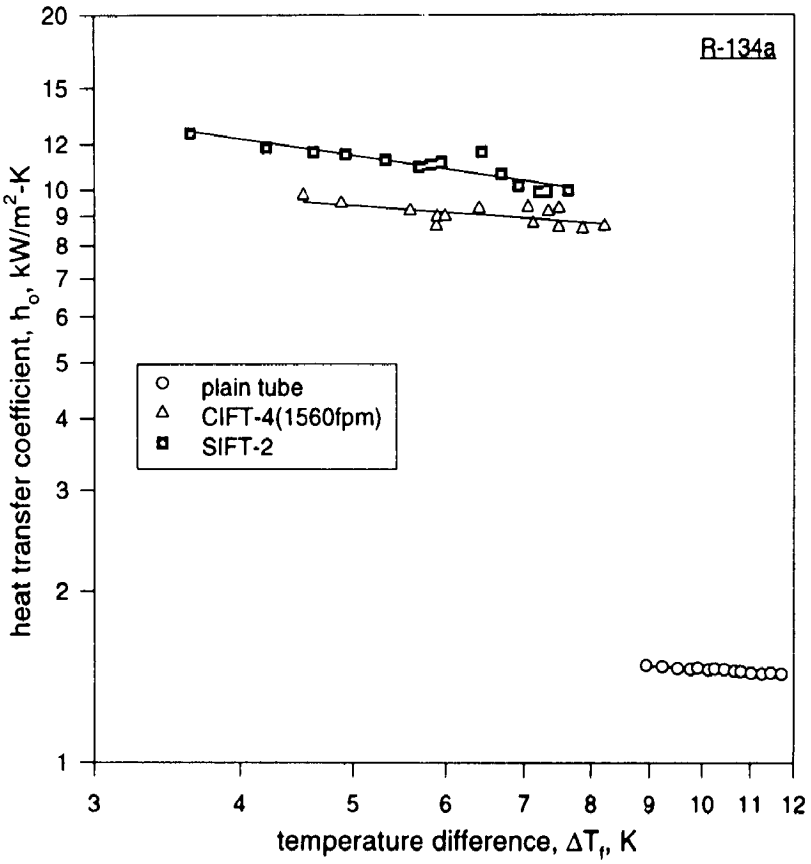

Figure 5.25
Variation of condensing side heat transfer coefficient
with vapour to tube wall temperature difference
for the condensation of R-134a

It has been observed that the spine integral-fin tube(SIFT) i.e. SIFT-1 displays better performance than plain tube and CIFT-1 for the condensation of steam. For a constant ΔT_f the condensing side heat transfer coefficient for SIFT-1 is 28 percent more than that of CIFT-1. The better performance of SIFTs at a given ΔT_f is due to thinning of condensate film on the surface of spines and faster drainage of condensate from the fin surface, this has been explained in 5.4.2.

Unlike for the condensation of steam, the characteristic curves for the condensation of R-134a are no longer parallel. In fact, they tend to converge at the higher ΔT_f. This trend indicates that the use of SIFTs is more beneficial at the lower value of ΔT_f which is usually the range

used in design of refrigerant condensers.

As in the present investigation the characteristic curves for CIFT-4 and SIFT-2 are not parallel to each other. The following equation has been developed to correlate the ratio of heat transfer coefficients for SIFT-2 and CIFT-4 with each other for the condensation of R-134a.

$$\frac{(h_o)_{SIFT-2}}{(h_o)_{CIFT-4}} = 1.55\Delta T_f^{-0.16} \tag{5.6}$$

Hence, it can be concluded that the SIFT out performs the CIFT not only for the condensation of steam but for the condensation of R-134a as well in the range of ΔT_f investigated.

5.4.5 Variation of Enhancement Factor With ΔT_f

In Figure 5.26 and Figure 5.27, graphs have been plotted between the enhancement factor, EF, and the vapour to tube wall temperature difference, ΔT_f, for the condensation of steam and R-134a respectively.

The salient features of these graphs are as follows:

(a) The enhancement factor, EF, for SIFTs is more than that for CIFTs for the condensation of steam and R-134a.

(b) The enhancement factor for SIFT becomes closer to that of CIFT for the condensation of R-134a at higher ΔT_f.

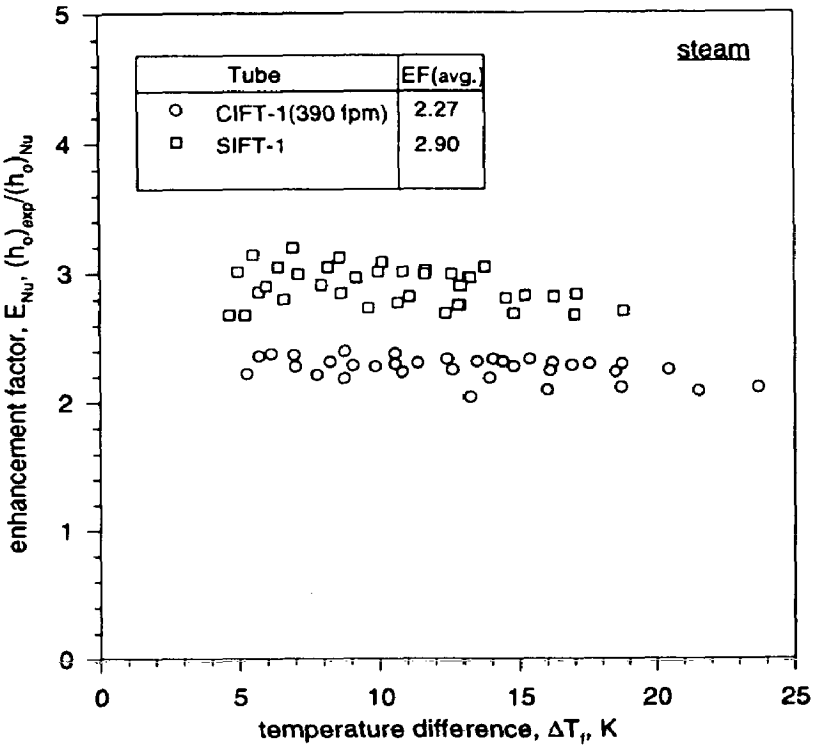

Figure 5.26
Variation of enhancement factor with temperature difference for the condensation of steam

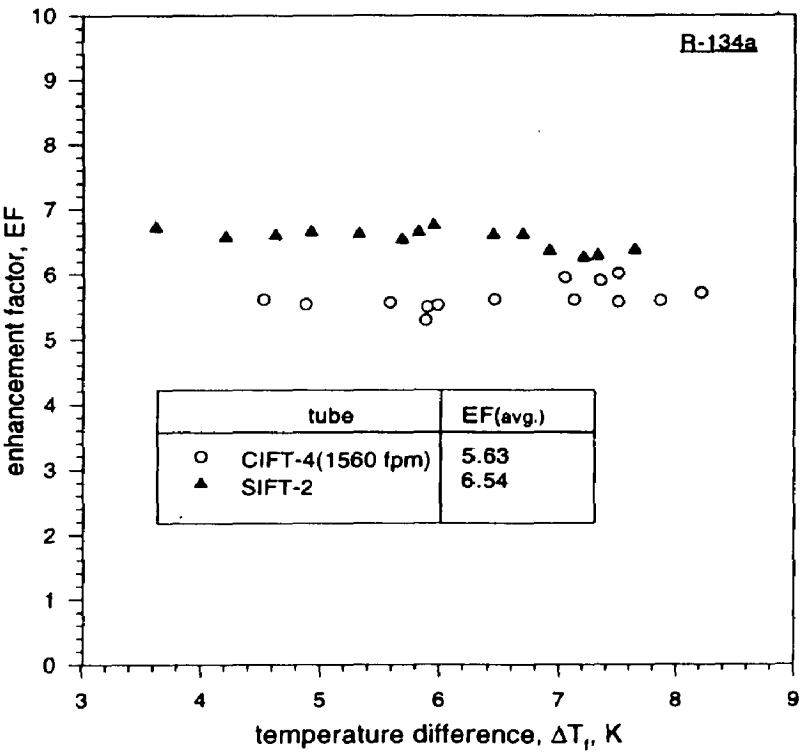

Figure 5.27
Variation of enhancement factor with temperature difference for the condensation of R-134a

The average enhancement factor of SIFT-2 for the condensation of steam is approximately thirty percent more than that of CIFT-2, hence, confirming the superior performance of SIFT over CIFT for the condensation of steam.

In the case of refrigerant, R-134a, at 4.5K temperature difference across the condensate film, ΔT_f, the EF for SIFT-2 is 24 percent more than that for CIFT-4 and at 7.5K temperature difference, ΔT_f, the EF is only 12 percent more than that for CIFT-4. However, the average EF for the condensation of R-134a over SIFT-2 is approximately 16 percent more than that for the condensation over CIFT-4.

Hence, the SIFTs are more effective for the condensation of high surface tension fluids viz. steam than the condensation of low surface tension fluids viz. R-134. Sukhatme et al.[83] also found that the SIFTs outperform the best performing CIFT by approximately twenty percent for the condensation of R-11.

5.5 CONDENSATION OVER PARTIALLY-SPINED CIRCULAR INTEGRAL-FIN TUBES (PCIFTs)

The partially-spined circular integral fin-tubes, PCIFTs, have been manufactured by cutting axial slots on half of the surface of the best performing CIFTs for the condensation of steam and R-134a. These slots generate the spines on the tube surface. The dividing plane for such tubes passes through the axis of tube. The detailed drawing of PCIFTs has been given in Figure 3.8 in Section 3.4. These tubes are machined to investigate the effectiveness of spine fins when they are either on the upper half or on the lower half positions of the tube surface.

The PCIFTs are helpful in finding the position in which the spines are most effective i.e. upper half or the lower half of a horizontal tube. This investigation into the effect of position of spine will provide a clear insight of the grounds behind the better performance of SIFTs. It will also

provide information about the best position of spines on a CIFT and may ultimately help in reducing the machining cost of the tube.

5.5.1 Need of PCIFTs

It has been established that SIFTs out perform the CIFTs for the condensation of steam and R-134a as well. The superior performance of SIFT may be contributed to the two factors. First, the three dimensional shape of spine fins, which enables the surface tension to exert pull on the condensate layer in two directions, and thereby yielding a thinner condensate film on the fin surface[83]. Secondly, the spine fins at the bottom of the tube facilitate faster drainage of condensate from the tube surface which allows a little condensate to remain on the tube surface resulting in a superior performance of SIFT[75].

Four PCIFTs have been used in this investigation. The PCIFT-1 and PCIFT-3 have spines on the upper half of the tube surface and these are used for the condensation of steam and R-134a respectively. The PCIFT-2 and PCIFT-4 have spines in the lower half of the tube and they are also used for the condensation of steam and R-134a respectively. The performance of PCIFTs in comparison to CIFT and SIFT has been discussed below:

5.5.2 Effect of ΔT_f on Heat Flux

In Figure 5.28 and Figure 5.29 the variation of heat flux with ΔT_f has been shown for the condensation of steam and R-134a, respectively. The diagrams clearly show the comparative performance of CIFTs, SIFTs, and also PCIFTs which have spines in the lower half and upper half of the tube surface.

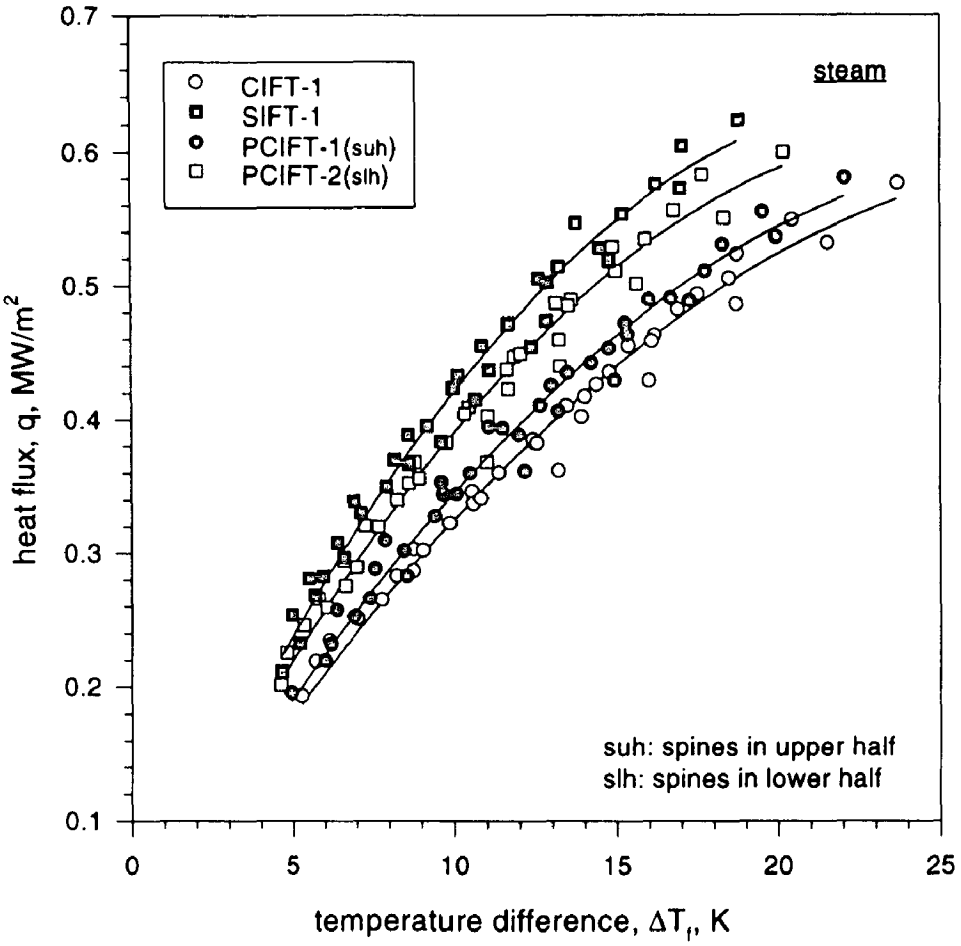

Figure 5.28
Variation of heat flux with vapour to tube wall temperature difference for the condensation of steam

The salient features of these figures are as follows:

(a) Similarly to the other tubes, the heat flux also increases with rise in ΔT_f for the condensation of steam and R-134a over PCIFTs.

(b) At a constant ΔT_f the heat flux is higher for the PCIFTs with the spines in the lower half position of the tube than those with the spines in the upper half position.

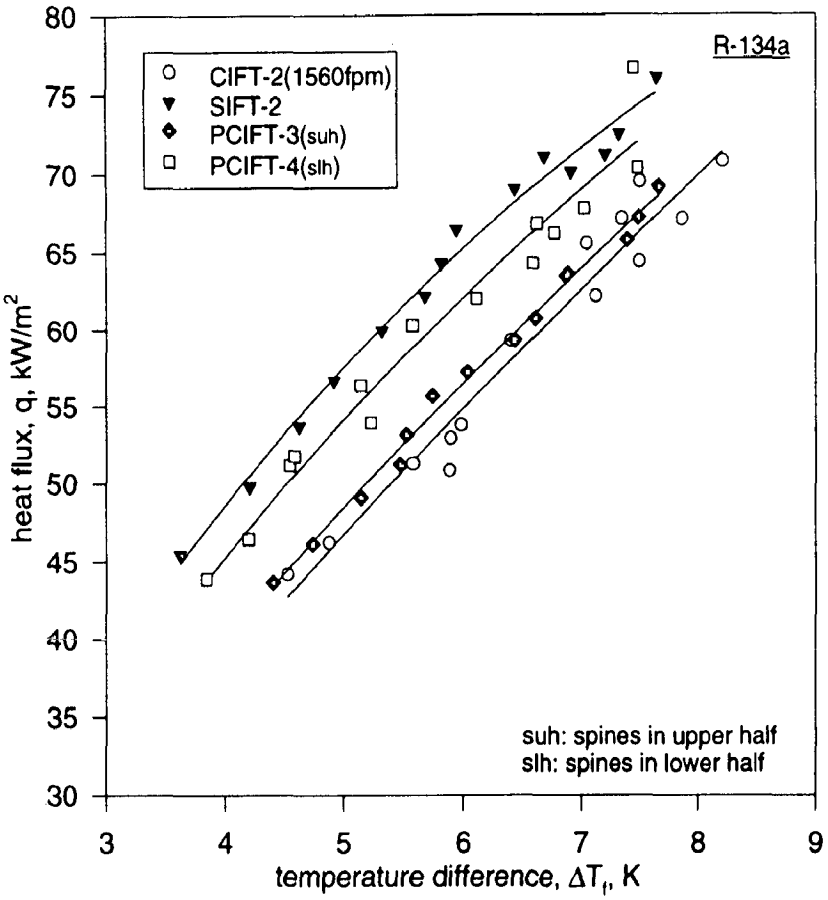

Figure 5.29
Variation of heat flux with vapour to tube wall temperature difference for the condensation of R-134a

At a constant ΔT_f the condensate drainage from the tube surface of PCIFTs is higher when the spines are kept in the downward position. The faster drainage of condensate reduces the average thickness of the condensate film on the tube surface and specially improves the thermal performance of the area which otherwise remains not as effective under condensate flooding. Although, the spines contribute to the further thinning of condensate film on the tube surface when they are in the upper half of the tube yet the average thickness of the condensate film is higher than that of the PCIFTs with spines in the lower half of the tube(PCIFT-2&4). Therefore, a constant ΔT_f the heat flux is higher for PCIFTs with spines in the lower half of the tube in comparison to the PCIFTs with spines at the top of the tube for the condensation of steam and R-134a as well.

5.5.3 Effect of Heat Flux on Heat Transfer Coefficient

Figure 5.30 and Figure 5.31 have been drawn to show the variation of heat transfer coefficient with the heat flux for the condensation of steam and R-134a respectively.

From the figures the following features are distinctly noted:

(a) The heat transfer coefficient reduces with the increase in heat flux for the condensation of steam and R-134a over PCIFTs .

(b) At a constant heat flux the PCIFTs with spines in the lower half of the tube have higher heat transfer coefficient than those with the spines in the upper half of the tube for the condensation of steam and R-134a.

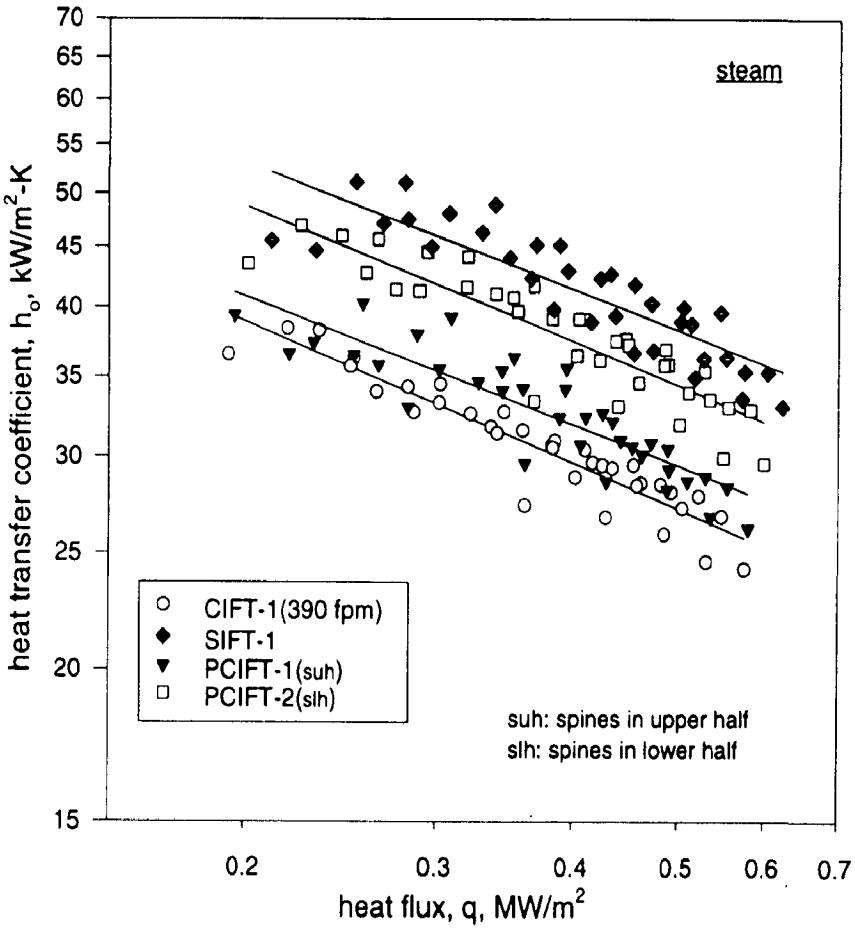

Figure 5.30

Variation of heat transfer coefficient with heat flux for the condensation of steam

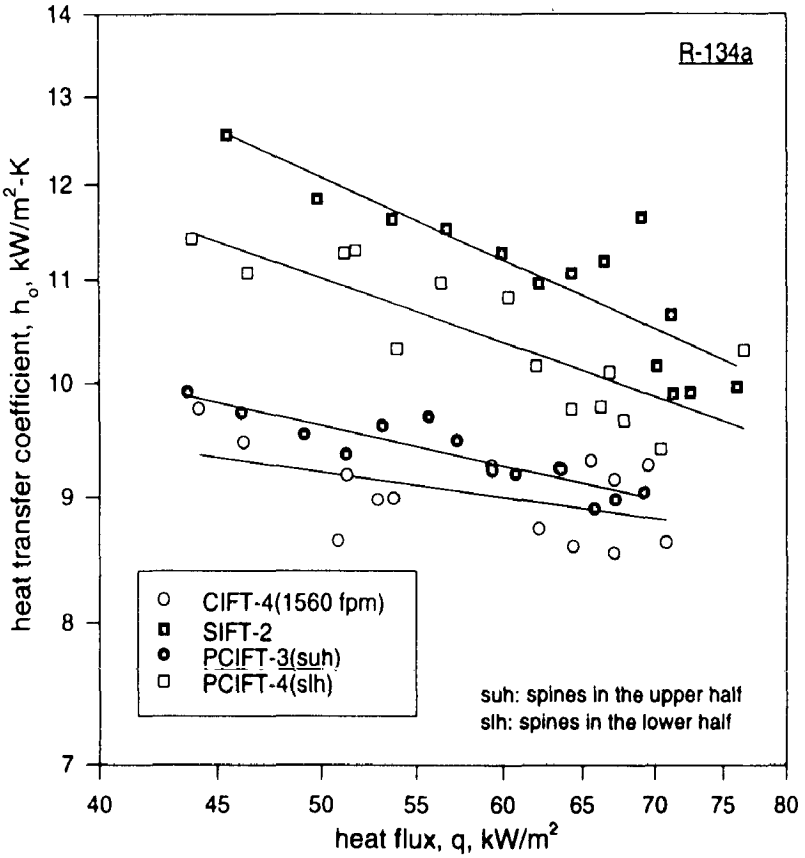

Figure 5.31
Variation of heat transfer coefficient with heat flux
for the condensation of R-134a

For the condensation of steam at a constant heat flux of 0.35 MW/m^2 the heat transfer coefficient of the PCIFT with spines in the top position (PCIFT-1) is approximately 7 percent more than that of CIFT-1 and the heat transfer coefficient for PCIFT-2(spines in the lower half) is approximately 26 percent more than that of CIFT-1, whereas, the heat transfer coefficient for spine fin tube (SIFT-1) is about 40 percent more than that of circular integral-fin tube(CIFT-1) at the same heat flux.

For the condensation of R-134a the spines in the upper half of PCIFT provide only an insignificant 4 percent increment in heat transfer coefficient at 55 kW/m^2 heat flux when compared with the CIFT-4. This increment falls in range of uncertainty of measurements. Therefore, it can not be safely concluded that spines are effective at the top position of the

tube for the condensation of R-134a, specially at constant heat flux.

When the spines are in the lower half of the tube (PCIFT-4) the increment in heat transfer coefficient at 55 kW/m^2 heat flux is about 17 percent of the best performing CIFT i.e. CIFT-4 whereas, the increment in heat transfer coefficient for SIFT-2 is 25 percent in comparison to CIFT-4, during condensation of R-134a.

5.5.4 Effect of ΔT_f on Heat Transfer Coefficient

The variation of condensing side heat transfer coefficient for the condensation of steam and R-134a has been shown in Figure 5.32 and Figure 5.33 respectively.

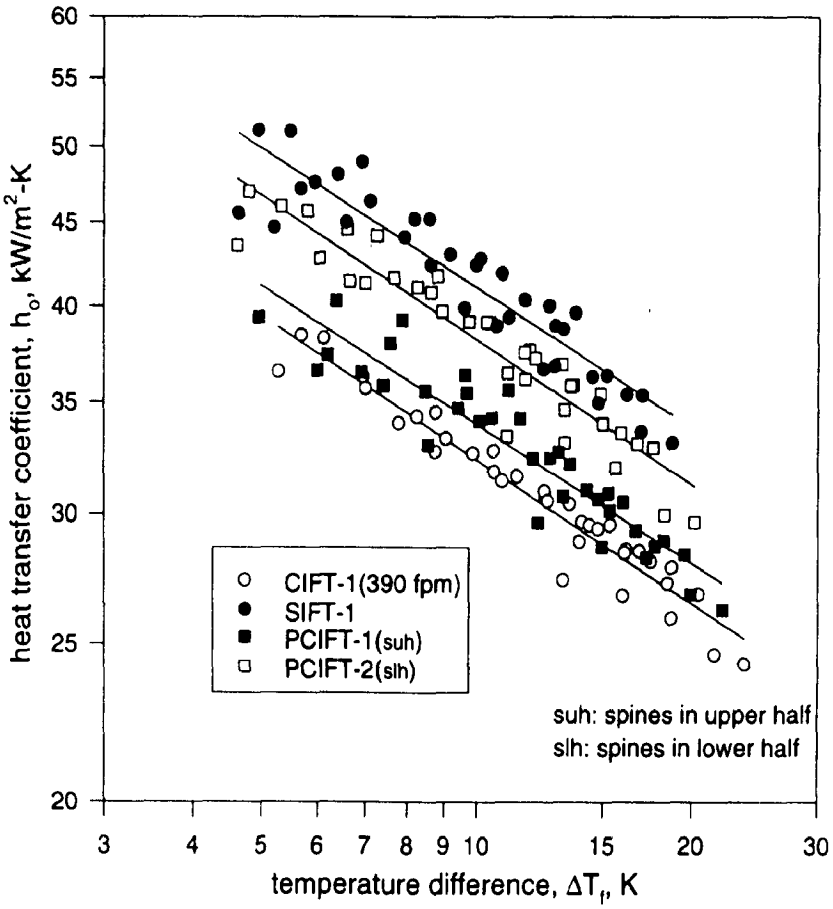

Figure 5.32
Variation of condensing side heat transfer coefficient with vapour to tube wall temperature difference for the condensation of steam

Following note worthy observations have been made in these figures:

(a) For the condensation of steam and R-134a the condensing side heat transfer coefficients for PCIFTs lie between those for CIFTs and SIFTs.

(b) PCIFT-2,4(tube with spines in the lower half) has higher heat transfer coefficient than PCIFT-1,3(tube with spines in the upper half) at a constant ΔT_f for the condensation of steam and R-134a.

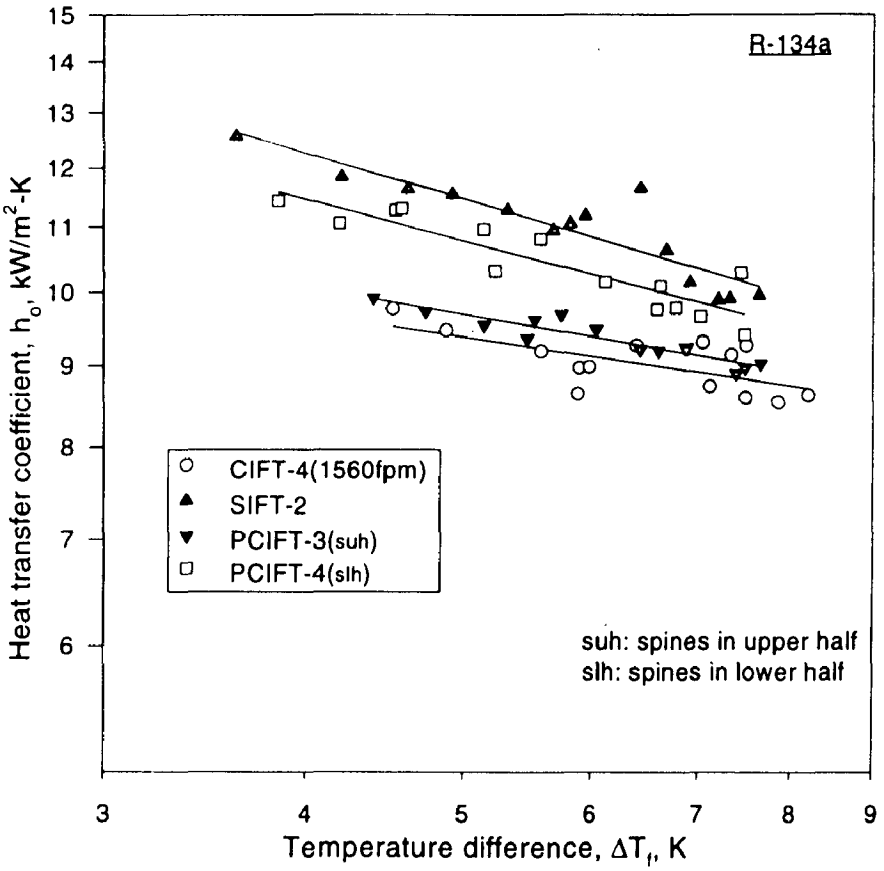

Figure 5.33

Variation of condensing side heat transfer coefficient with vapour to tube wall temperature difference for the condensation of R-134a

At a constant ΔT_f the better performance of PCIFTs with spines in the bottom position(PCIFT-2&4) than that of the PCIFT with spines in the top position(PCIFT-1&3) clearly indicates that reduction in the average thickness of condensate film on the tube surface due to faster drainage of condensate from the bottom of the tube by the spine fins is more than the reduction in the average thickness of the film on the tube surface due to surface tension when the spines are in the upper half of the tube(PCIFT-1&3).

5.5.5 Variation of Enhancement Factor with ΔT_f

Figure 5.34 &3.35 are drawn between enhancement factor and ΔT_f for the condensation of steam and R-134a respectively. Following conclusions have been drawn from the figure:

(a) For the condensation of steam the enhancement factor, EFs for PCIFTs lie between those for CIFTs and SIFTs.

(b) The average EF for PCIFTs with spines in the lower half of the tube is more than that for the PCIFTs with spines in the upper half of the tube.

As expected the EF for partially-spined circular integral-fin tubes PCIFTs lies between that of CIFTs and SIFTs for the condensation of steam and R-134a as well. For the condensation of R-134a the spines in the upper half of the tube do not seem to be effective because EF for PCIFT-3 is 5.71, which is marginally higher (only 1.4%) than that for the CIFT-1 i.e. 5.63.

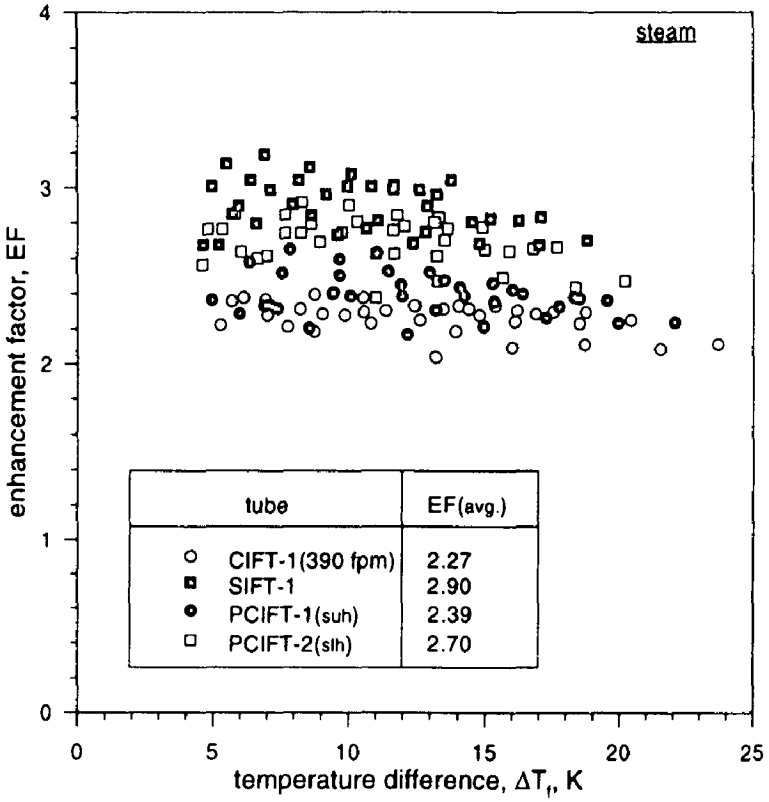

Figure 5.34
Variation of enhancement factor with temperature difference for the condensation of steam

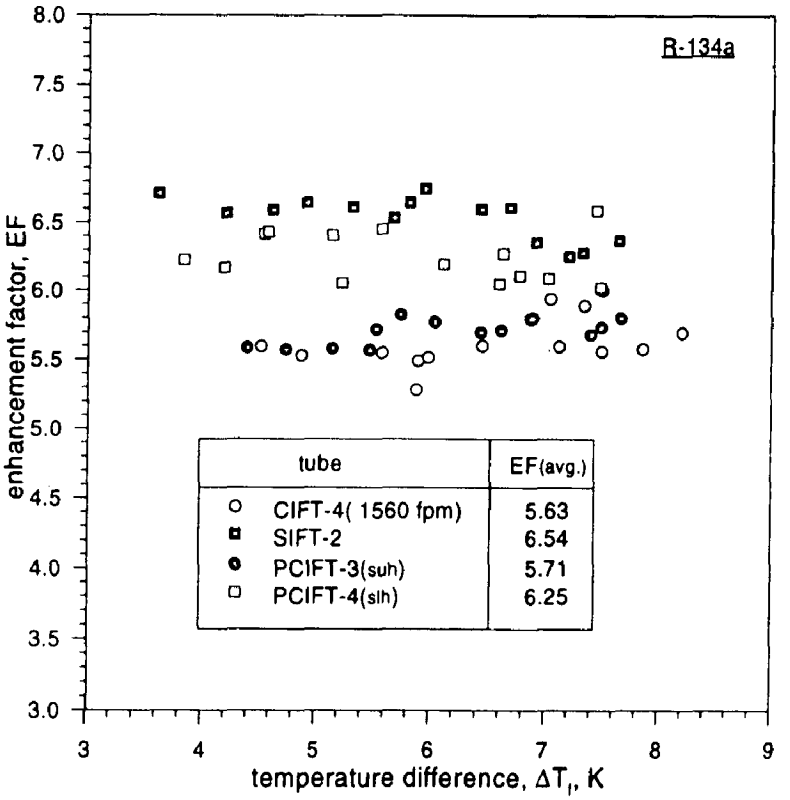

Figure 5.35
Variation of enhancement factor with temperature difference for the condensation of R-134a

Although, the spines in the upper half of the tube, by themselves are not able to augment the heat transfer coefficient appreciably, yet they seem to affect the performance of spines in the lower half of the tube and over all spines are most effective in the improvement of the heat transfer rate. It may be noted that the enhancement in heat transfer coefficient by SIFT-1 is 30% at constant ΔT_f in comparison to CIFT-1 which is more than the sum of enhancement attained by the spines independently on the upper half and lower half of the tube and same is the case for the condensation of R-134a. A comparison of the performance of CIFTs, SIFTs and PCIFTs has been given in subsequent section.

5.6 COMPARISON AMONGST THE PERFORMANCE OF DIFFERENT FINNED TUBES

In this section a comparison amongst the performance of CIFTs. SIFTs and PCIFTs has been made to evaluate the relative performance of these tubes. In the present investigation enhancement in heat transfer coefficient in comparison to a plain tube is represented by the enhancement factor, EF. In fact, the enhancement factor, EF, is a yard stick to compare the augmentation in heat transfer at a given temperature difference across the condensate layer, ΔT_f. In the Table- 5.4 a comparison of average EF and A_F/A_r has been given for the different tubes. From the information given in Table-5.4 it can be concluded that for the condensation of steam the CIFT-1 enhances the heat transfer coefficient about 2.27 times in comparison to the plain tube and the SIFT-1 further enhances the heat transfer coefficient by approximately thirty percent and thereby raising the EF to 2.9.

An investigation for the condensation of steam over PCIFTs, reveals that the spines in the lower half of the tube are quite effective and the PCIFT-2 (with spines in the lower half of the tube) has enhanced the heat transfer coefficient for the condensation of steam by approximately twenty percent, thereby raising the EF to 2.7.

Table-5.4

comparison of enhancement factors of different tubes

fluid	tube	EF(avg.)	A_F/A_r
Steam	plain tube	1.00	1.00
	CIFT-1(390 fpm)	2.27	1.93
	SIFT-1	2.90	2.14
	PCIFT-1(suh)	2.39	2.17
	PCIFT-2(slh)	2.70	2.17
R-12	plain tube	1.00	1.00
R-134a	plain tube	1.00	1.00
	CIFT-2(945 fpm)	2.71	1.82
	CIFT-3(1250 fpm)	4.20	2.24
	CIFT-4(1560 fpm)	5.63	3.06
	CIFT-5(1875 fpm)	5.25	2.75
	SIFT-2	6.54	2.31
	PCIFT-3(suh)	5.71	2.69
	PCIFT-4(slh)	6.25	2.69

suh spines in upper half

slh spines in lower half

The spines on the upper half of the tube (PCIFT-1) are less effective and augment the EF by approximately five percent in comparison to the CIFT-1. Thus, if one can forego approximately 10% enhancement in heat transfer coefficient in comparison to SIFT-1, he should use PCIFT-2 to save about 50% of machining cost required to make a SIFT out of a CIFT. The percentage enhancement by the PCIFTs and CIFTs has been shown in Figure 5.36 and Figure 5.37 for the condensation of steam and R-134a respectively.

For the condensation of R-134a the maximum attainable EF using a 1560 fpm fin density tube(CIFT-4) is 5.63. The SIFT-2 further enhances the heat transfer coefficient by approximately sixteen percent.

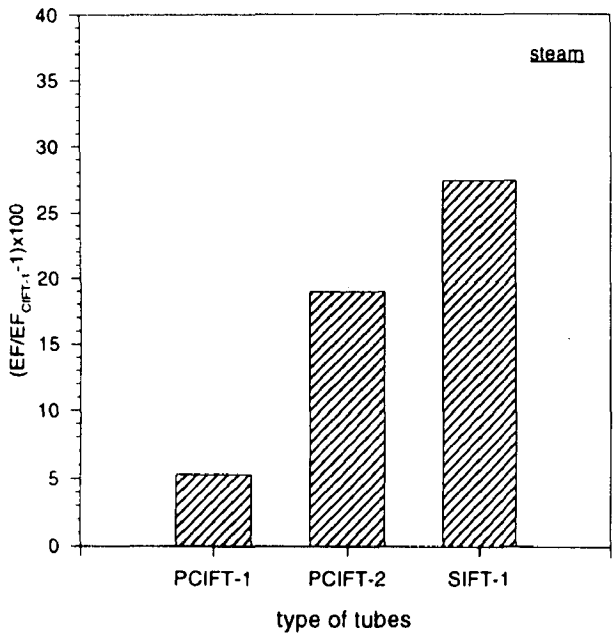

Figure 5.36
Performance of SIFT and PCIFTs in comparison to that of CIFT-1 for the condensation of steam

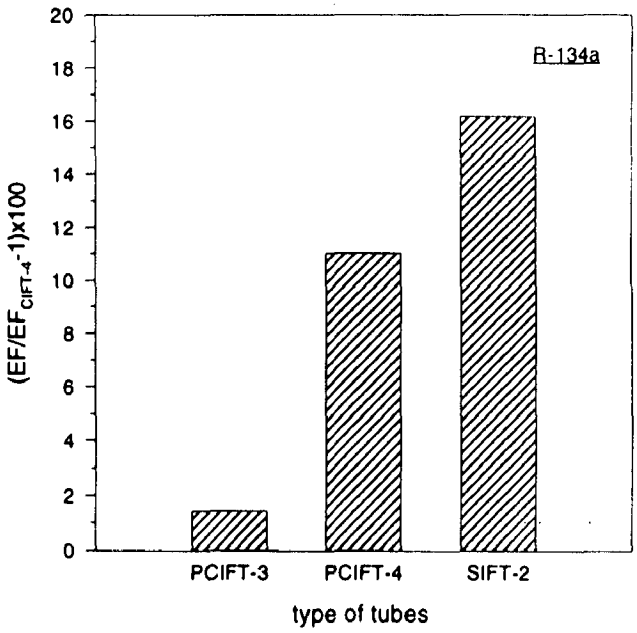

Figure 5.37
Performance of SIFT and PCIFTs in comparison to that of CIFT-4 for the condensation of R-134a

The spines in the top portion of the tube do no seem to be effective as these provide only 1.4 percent enhancement over and above CIFT-4. Therefore, spines on the bottom of the PCIFT-4 are responsible for the better performance of this tube as they improve the performance of CIFT-4 by eleven percent. In fact, the effect of faster drainage of condensate is more pronounced in case of R-134a, a low surface tension fluid. It can be seen in Table-5.4 that EFs for SIFT-2 and PCIFT-2 are 6.53 and 6.25 respectively. Therefore, for the condensation of R-134a the spines are effective only in the lower half of the tube.

It is interesting to note from Table- 5.4 that the percentage increase in area due to spines in SIFT-1 is approximately ten percent of CIFT-1 but the EF has increased approximately thirty

percent. The PCIFTs, used to study the condensation of steam have almost same surface areas that of SIFT-1 but the EFs are different.

For the condensation of R-134a the area of CIFT-4(1560 fpm) has reduced as the spines are generated on the tube surface to manufacture SIFT-2 but the heat transfer coefficient has increased by approximately fifteen percent by SIFT-2. The PCIFTs have more surface area than the SIFT-2 but the EF is less than that of SIFT-2. This clearly indicates that proper geometrical shape of the fins and its position play a deciding role in the enhancement in heat transfer coefficient.

5.7 DETERMINATION OF CONDENSING SIDE HEAT TRANSFER COEFFICIENT BY MODIFIED WILSON PLOT

The modified Wilson plot technique has been mooted as a tool to determine the condensing side heat transfer coefficient without measuring the condensing side tube wall temperature[9,94]. In this technique, only the temperature of condensing vapour, coolant flow rate and its inlet and outlet temperatures are required to be known. The method is very useful when the outside wall temperature fluctuates in case of condensation as the film thickness continuously varies due to formation of condensate and its subsequent drainage from the tube surface. The variation in the outside tube wall temperature makes the determination of heat transfer coefficient by wall temperature measurement very difficult though not impossible. Hence, in the present study the condensing side heat transfer coefficients for the condensation of steam, R-12 and R-134a are also determined by the modified Wilson plot technique(detailed in Appendix-D) in addition to that from the wall temperature measurements. A comparison between the condensing side heat transfer coefficient determined by wall temperature measurement technique and the modified Wilson plot technique for the condensation of steam and R-134a has been discussed below:

5.7.1 Heat Transfer Coefficient For The Condensation of Steam

As per the methodology discussed in Appendix-D the heat transfer coefficient during condensation of steam over a horizontal plain tube and a horizontal finned tubes has also been determined by the modified Wilson plot method.

In Figure 5.38 and Figure 5.39, graphs have been plotted to compare the condensing side heat transfer coefficient by measuring tube wall temperature and that by modified Wilson plot, for a plain tube and a finned tube respectively.

Following are the salient features of these graphs:

(a) For the condenation of steam the modified Wilson plot underpredicts the heat transfer coefficient in a range of 7.5 to 15 percent.

(b) The underprediction is high at the higher value of condensing side heat transfer coefficient or at the low value of ΔT_t.

Hence, in the present investigation the underprediction of heat transfer coefficient by modified Wilson plot technique is quite in agreement with the findings of Marto[45]. Marto has also reported the underprediction of heat transfer coefficient by modified Wilson plot technique in the same range.

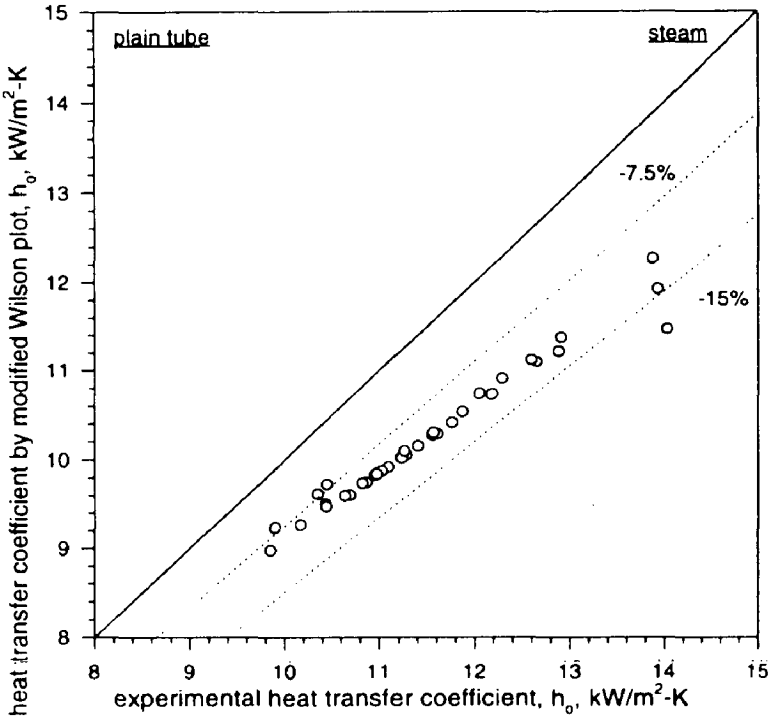

Figure 5.38

Comparison between experimental heat transfer coefficient and that predicted by modified Wilson plot for the condensation of steam over a plain tube

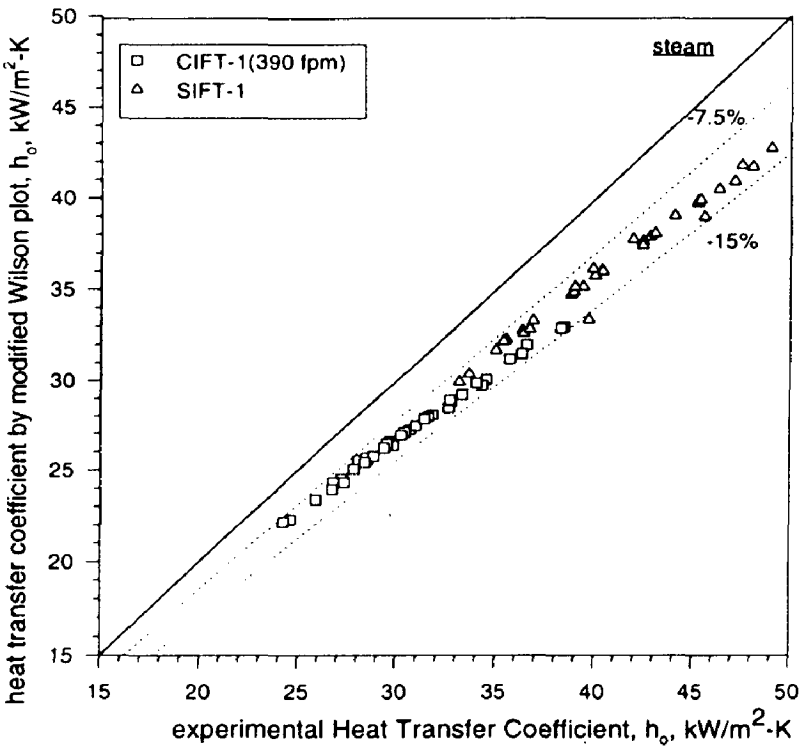

Figure 5.39

Comparison between experimental heat transfer coefficient and that predicted by modified Wilson plot for the condensation of steam over finned tubes

5.7.2 Heat Transfer Coefficient for The Condensation of R-134a

Similarly, for the condensation of R-134a, the condensing side heat transfer coefficients are also determined by the modified Wilson plot and by measuring the tube wall temperature as well.

In Figure 5.40, 5.41& 5.42 a comparison between the values of heat transfer coefficient by tube wall temperature measurement technique and by modified Wilson plot has been shown for the condensation of two refrigerants viz. R-12 and R-134a over a plain tube and R-134a over finned tubes.

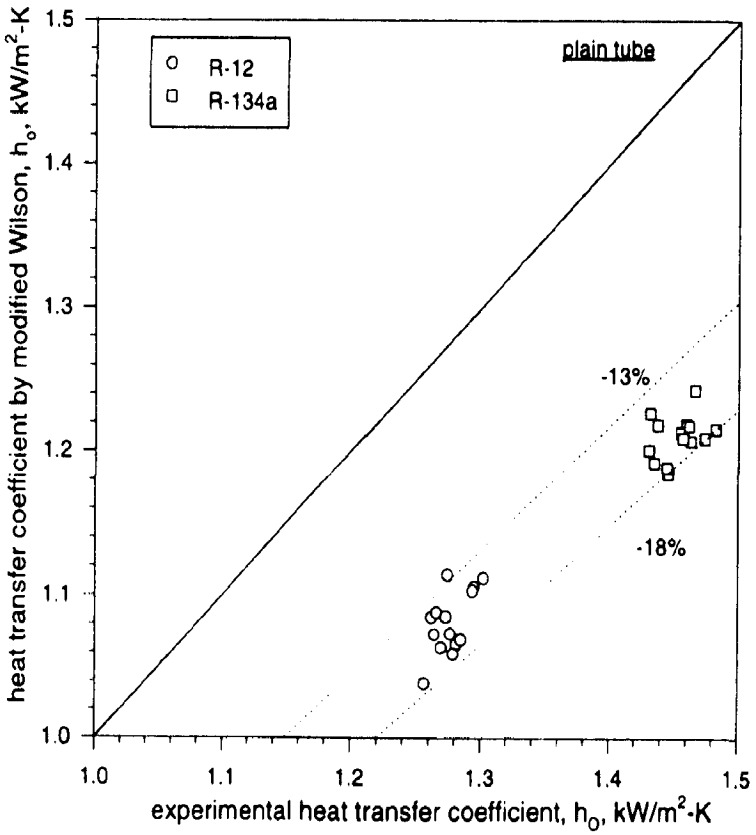

Figure 5.40

Comparison between experimental heat transfer coefficient and that predicted by modified Wilson for the condensation of refrigerants over a plain tube

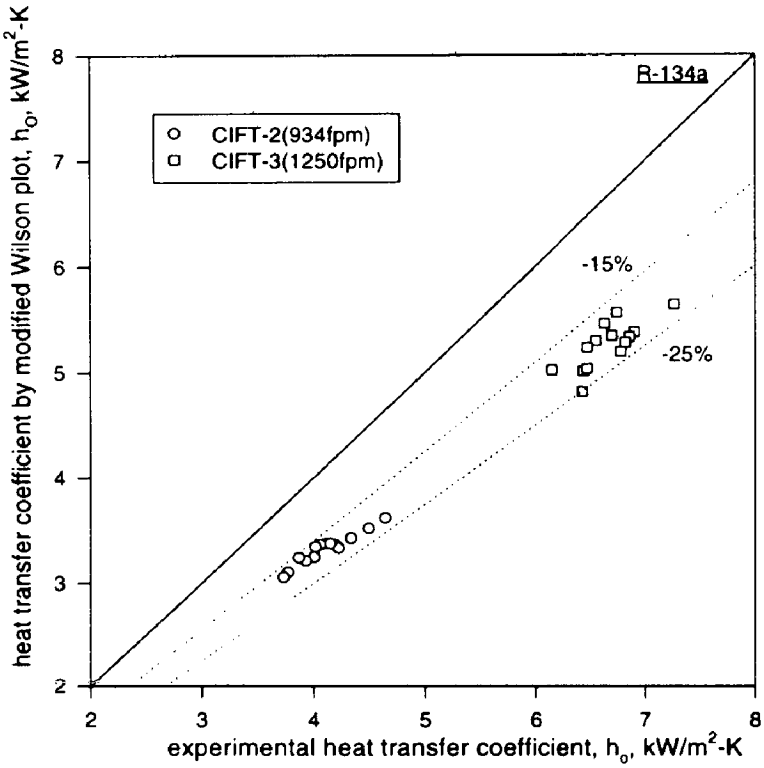

Figure 5.41
Comparison between experimental heat transfer coefficient and that predicted by modified Wilson plot for the condensation of R-134a over finned tubes

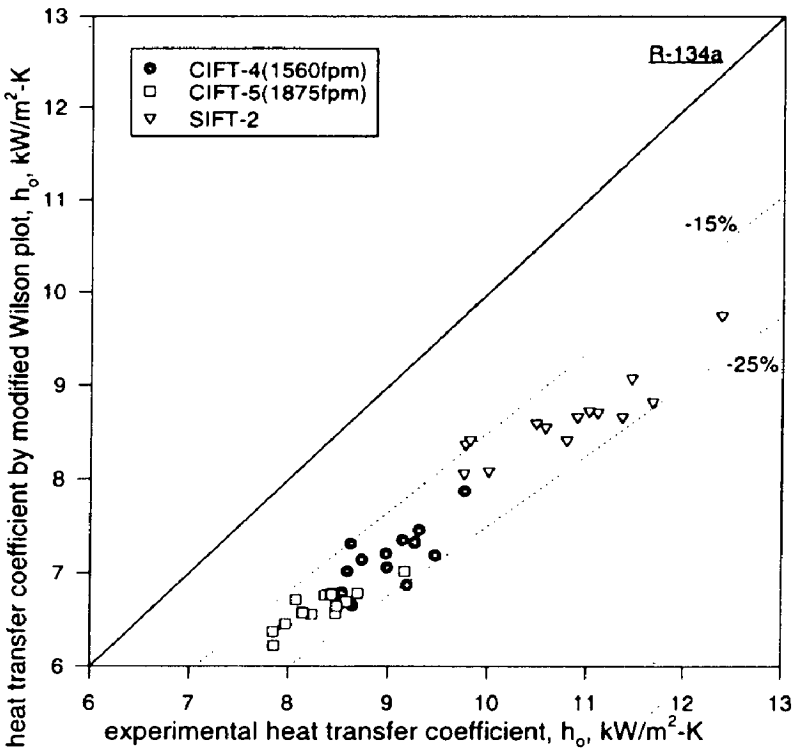

Figure 5.42
Comparison between experimental heat transfer coefficient and that predicted by modified Wilson plot for the condensation of R-134a over finned tubes

Following observation has been made out of these figures:

(a) For the plain tube the modified Wilson plot underpredicts the heat transfer coefficient in a range of 13 to 18 percent with an average value of 20 percent for the condensation of refrigerants.

(b) For finned tubes viz. CIFTs and SIFTs the modified Wilson plot underpredicts the heat transfer coefficient in a range of 15 to 25 percent is comparison to the heat transfer coefficient determined by the wall temperature measurement.

The underprediction is high for refrigerants due to the low value of ΔT_f. At low value of ΔT_f, the slight deviation in ΔT_f by the modified Wilson plot technique will alter the heat transfer coefficient significantly.

5.8 COMPARISON OF EXPERIMENTAL HEAT TRANSFER COEFFICIENT WITH DIFFERENT ANALYTICAL MODELS

Some theoretical models are available to determine the heat transfer coefficient during condensation of pure vapours over a horizontal circular integral-fin tube[13,27,31,49,71]. Whereas, no published analytical model is available for the prediction of heat transfer coefficient for SIFTs and PCIFTs. The experimental heat transfer coefficient from present investigation for CIFTs only have been compared with that predicted by some of the important analytical models.

5.8.1 Beatty And Katz Model

Beatty and Katz[4] were first to take the initiative of developing a theoretical model for the condensation of pure vapours over a horizontal integral-fin tube. In their model they calculated the heat transfer coefficient of fins by the, Nusselt's equation for vertical plates

and that of tube surface by Nusselt's model for horizontal cylinder. These heat transfer coefficients were added in proportion to their contribution in the total equivalent surface area to determine the condensing side heat transfer coefficient.

The Figure 5.43 and Figure 5.44 illustrates the percentage deviation of condensing side heat transfer coefficient by Beatty and Katz model with that from the present experimental investigations.

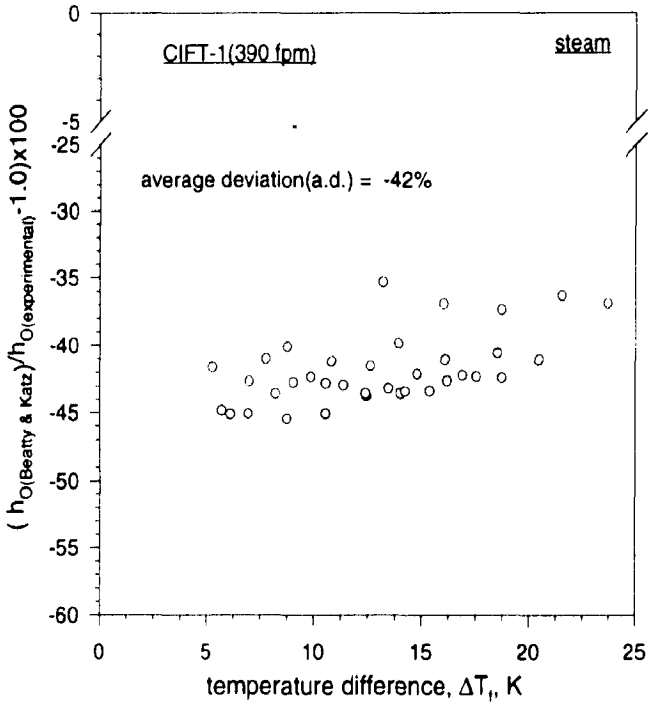

Figure 5.43
Comparison of experimental heat transfer coefficient with that predicted by Beatty and Katz model[4] for the condensation of steam over CIFT-1

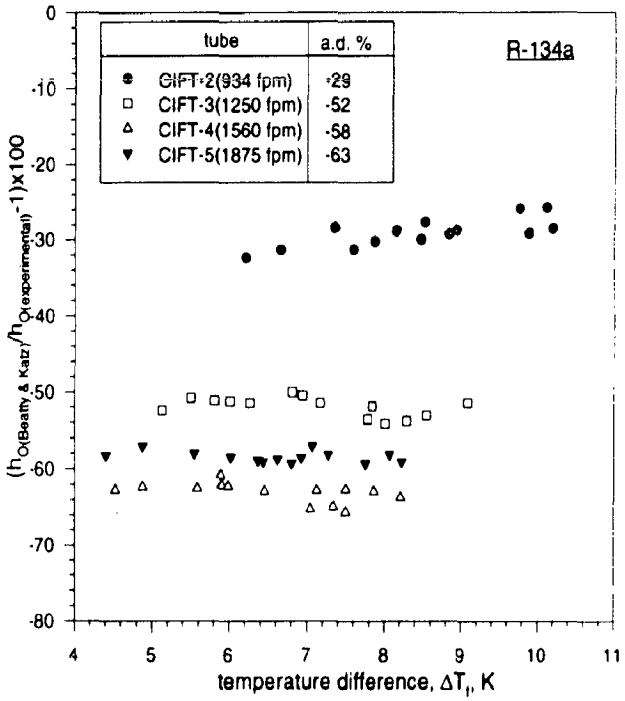

Figure 5.44
Comparison of experimental heat transfer coefficient with that predicted by the Beatty and Katz model[4] for the condensation of R-134a over CIFTs

Beatty and Katz model has underpredicted the heat transfer coefficient for the condensation of steam in a range of 35 to 45 percent with an average value of 42 percent, whereas, in the case of R-134a the underprediction ranges between 20 percent to 70 percent. In fact, the deviation has increased with the fin density. In the present study the underperdiction of heat

transfer coefficient for CIFT-5(1875 fpm) is less than that of a low fin density tube i.e. CIFT-4(1560 fpm). The reason behind such response is due to the fact that in the present study the 1560fpm(CIFT-4) tube has given the highest heat transfer coefficient. Further increase in the fin density has reduced the heat transfer coefficient. Therefore, the deviation from the predicted value for CIFT-5(1875 fpm) has lied between that for 1250fpm(CIFT-3) tube and 1560fpm(CIFT-4) tube.

In their work Beatty and Katz collected the experimental data for the condnesation of R-22 and organic vapours over a low fin density tube(630 fpm), therefore, their data matched with their model in a range of +7.2% to -10%. The model often underpredicts the condensing side heat transfer coefficient for high surface tension fluids and tubes of high fin density, as also seen in the present study. These results from the present investigation are also in agreement with the findings of Marto et al.[45].

5.8.2 Rudy And Webb Model

In Figure 5.45 and Figure 5.46 the deviation between heat transfer coefficient predicted by the Rudy and Webb[73] model and that obtained from the present investigation have been shown for the condensation of steam and R-134a respectively. The model underpredicts the heat transfer coefficient in a range of 35 to 45 percent with an mean value of 20 percent for the condensation of steam. The steam is a high surface tension fluid, therefore, the condensate retention angle, ϕ, is high for the condensation of steam.

As it is a known fact that the percentage flooding of the tube surface with the condensate is proportional to the condensate retention angle. The model has considered zero heat transfer in the flooded region of the tube and hence underpredicted the value of heat transfer coefficient in case of steam. In the case of refrigerants the model has overpredicted the

condensing side heat transfer coefficient in a range of 5 to 40 percent, as shown in Figure 5.46. The over prediction has reduced with the increase in fin density. This is in agreement with the their findings with their own data. Rudy and Webb have reported that their model overpredicted their test data of 1024 fpm tube by 25% and that of 748 fpm tube by 30% for the condensation of R-11.

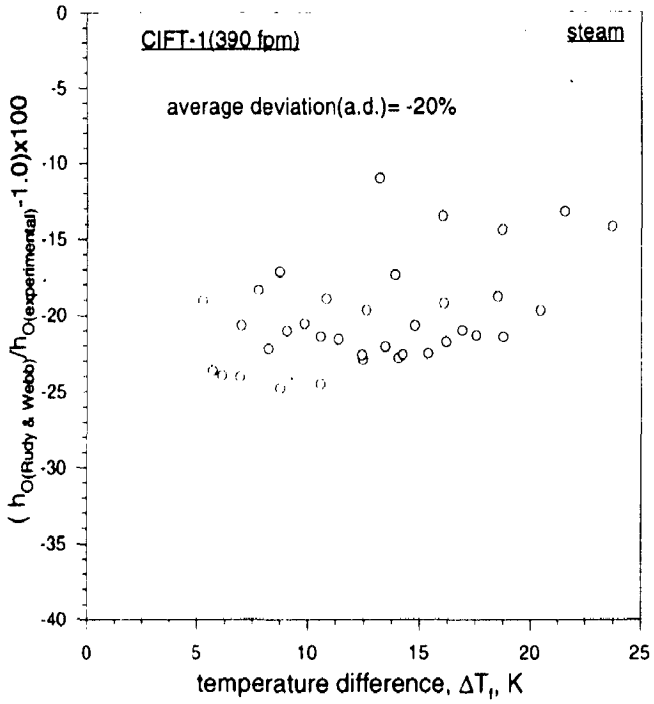

Figure 5.45
Comparison of experimental heat transfer coefficient with that predicted by Rudy and webb model[73] for the condensation of steam over CIFT-1

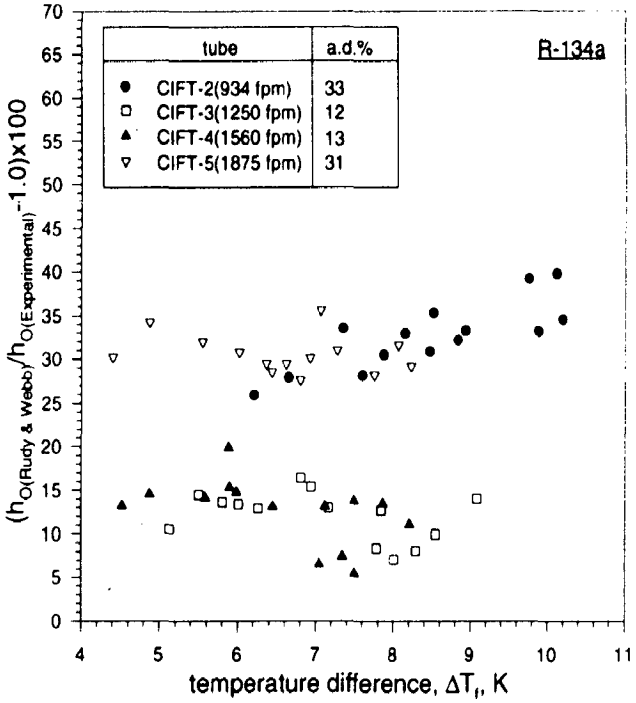

Figure 5.46
Comparison of experimental heat transfer coefficient with that predicted by the Rudy and Webb model[73] for the condensation of R-134a over CIFTs

In the present study the overprediction of heat transfer coefficient for CIFT-5(1875 fpm) is more than expected though it is a high fin density tube. The reason behind such response is due to the fact that in the present study the 1560fpm(CIFT-4) tube has given the best performance. Further increase in the fin density has reduced the heat transfer coefficient. Moreover, in the present model the fin height is a very important parameter and the CIFT-5

has the minimum fin height. Therefore, the overprediction of heat transfer coefficient by the present model for CIFT-5 is much more than expected.

5.8.3 Owen, Sardesai, Smith and Lee model

Owen et al. model[63] considered the heat transfer in the flooded portion of the tube as well, contrary to Rudy and Webb[73], who considered the flooded part of the tube to be inactive in heat transfer. But Owen et al. did not take into account the surface tension of condensing fluid as considered by the Rudy and Webb. Even then, the model underpredicts the condensing side heat transfer coefficient of present investigation in a range of 42 to 53 percent with an average value of 49 percent for the condensation of steam, as shown in Figure 5.47.

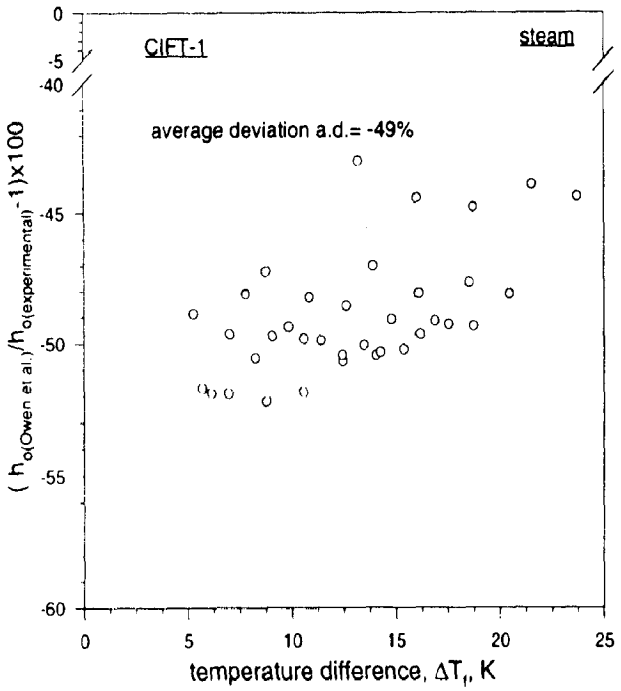

Figure 5.47
Comparison of experimental heat transfer coefficient with that predicted by Owen et al. model[63] for the condensation of steam over CIFT-1

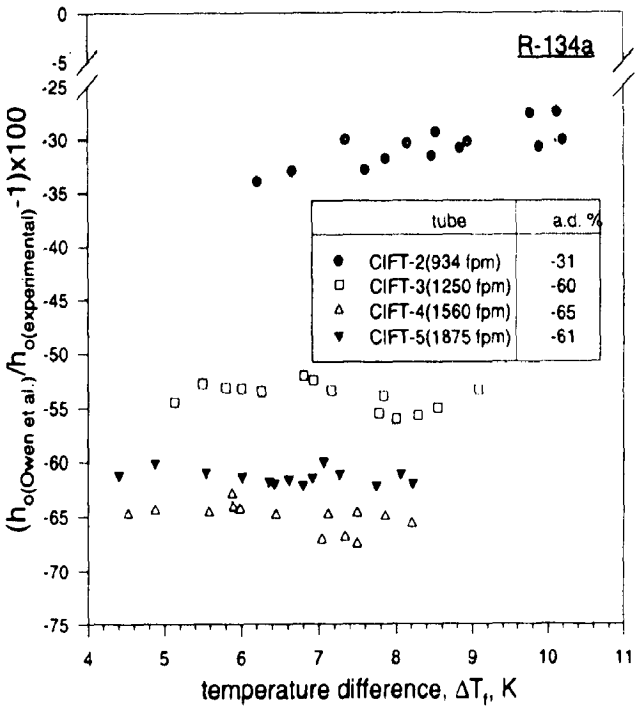

Figure 5.48
Comparison of experimental heat transfer coefficient with that predicted by Owen et al. model[63] for the condensation of R-134a over CIFTs

A similar comparison for R-134a is also shown in Figure 5.48. The model underpredicts the condensing side heat transfer coefficient in a range of 25 to 70 percent. The underprediction has increased with the fin density. By the present model also the underprediction of heat transfer coefficient has reduced after attaining a maximum value at the optimum fin density of 1560fpm(CIFT-4).

5.8.4 Webb, Rudy and Kedzierski model

In Figure 5.49 the deviations for condensing side heat transfer coefficient predicted by the Webb et al.[92] from those of present investigation have been shown.

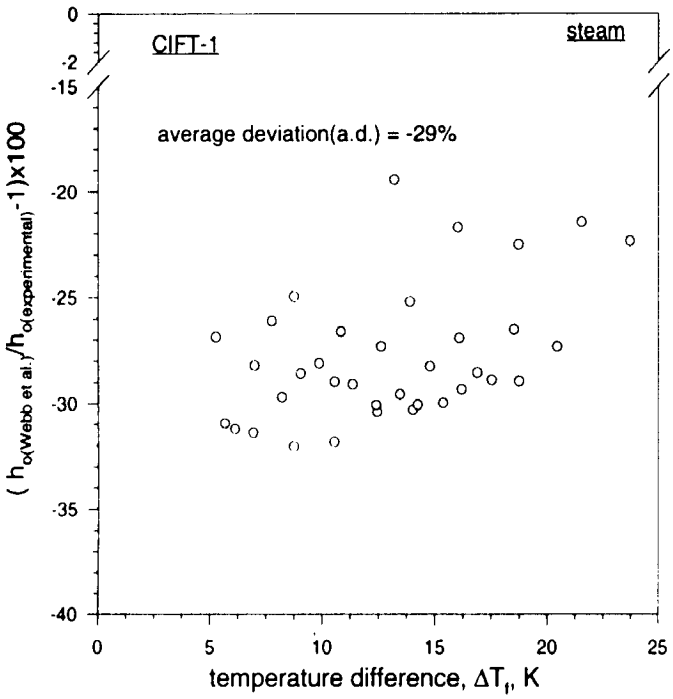

Figure 5.49
Comparison between experimental heat transfer coefficient and that predicted by Webb et al. model[92] for the condensation of steam over CIFT-1

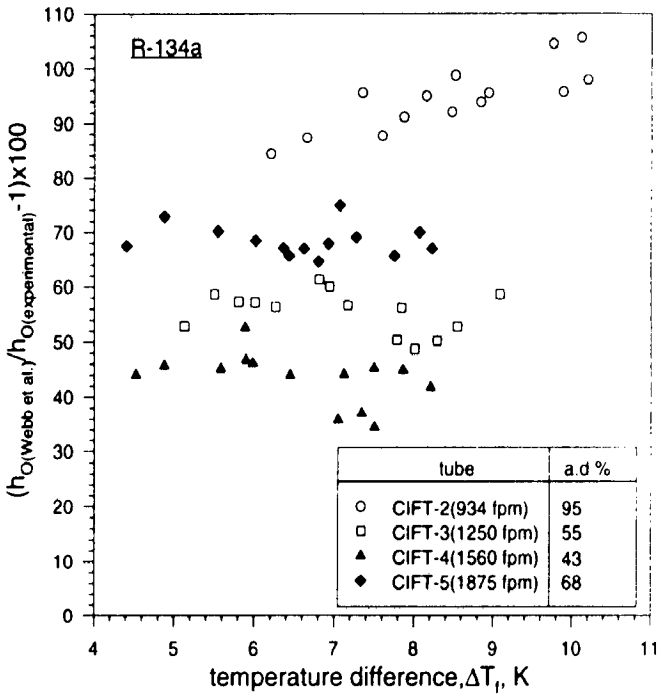

Figure 5.50
.Comparison of experimental heat transfer coefficient with that predicted by Webb et al. model[92] for the condensation of R-134a over CIFTs

For the condensation of steam the model underpredicts the condensing side heat transfer coefficient in a range of 20 to 33 percent with an average value of 28 percent. Whereas, for the condensation of R-134a, the model overpredicts the heat transfer coefficient up to 100 percent as shown in Figure 5.50. As the fin density has increased the deviation form the experimental values have reduced. At 1560fpm density(CIFT-4) the overprediction is minimum with an average value of 43 percent.

5.8.5 Honda and Nozu Model

The Honda and Nozu[25] model is a widely accepted model to determine the condensing side heat transfer coefficient for the condensation over a horizontal CIFT.

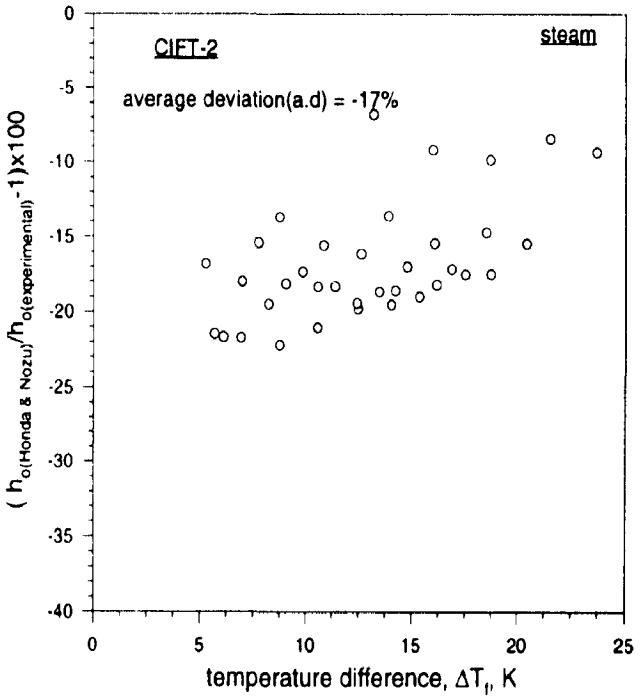

Figure 5.51
Comparison of experimental heat transfer coefficient with that predicted by Honda and Nozu model[25] for the condensation of steam over CIFT-1

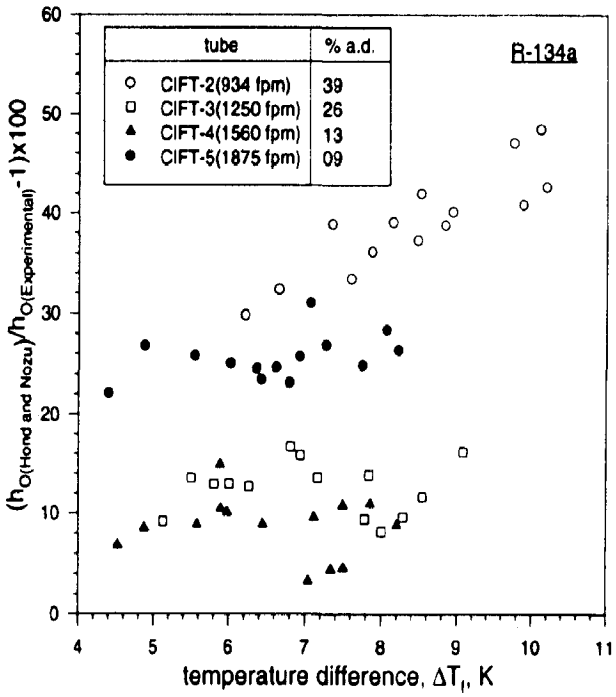

Figure 5.52
Comparison of experimental heat transfer coefficient with that predicted by Honda and Nozu model[25] for the condensation of R-134a over CIFTs

The model has been tested for twenty fluids and the twenty two tubes of different fin geometry. In all the cases most of the experimental data have agreed approximately in a range of ± 20 percent. It is a general observation that , this model underpredicts the heat transfer coefficient for high surface tension fluids and overpredict the heat transfer coefficient for the low surface tension fluids[45]. In Figure 5.51 the deviation of condensing side heat transfer coefficient predicted by this model with the experimental values for the condensation of steam has been shown. The data are underpredicted in a range of 5 to 23 percent with an average value of 17 percent.

For the condensation of R-134a the model overpredicts the data in a range of 4 to 40 percent as illustrated in Figure 5.52. In fact, the overprediction has reduced from the average value of 39 percent for CIFT-2 to 9 percent for CIFT-4 and has again increased for CIFT-5.

5.8.6 Adamek and Webb Model

In Figure 5.53 and Figure 5.54 the experimental heat transfer coefficients for the condensation of steam and R-134a over CIFTs have been compared with those predicted by the Adamek and Webb model[2]. The model has underpredicted the heat transfer coefficient for the condensation of steam with an average value of 27 percent. For the condensation of R-134a the model has overpredicted the experimental data from 9 percent to 60 percent.

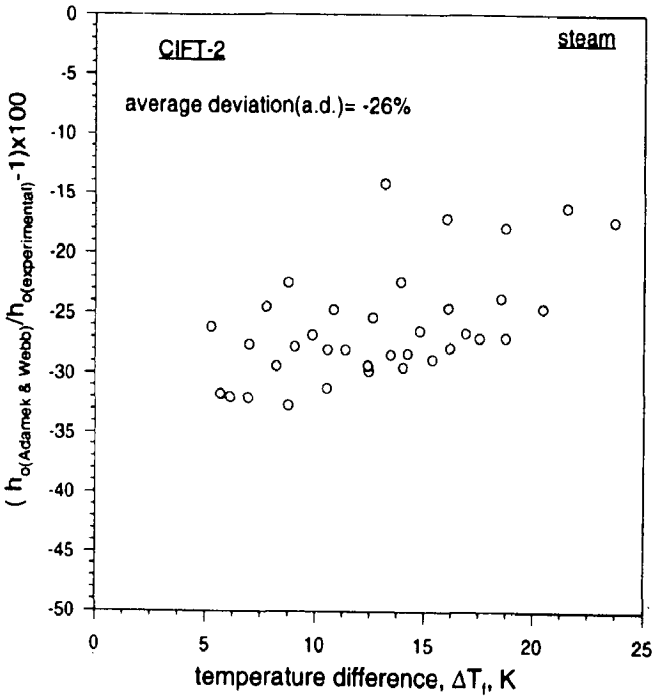

Figure 5.53
Comparison of experimental heat transfer coefficient with that predicted by Adamek and Webb model[2] for the condensation of steam over CIFT-1

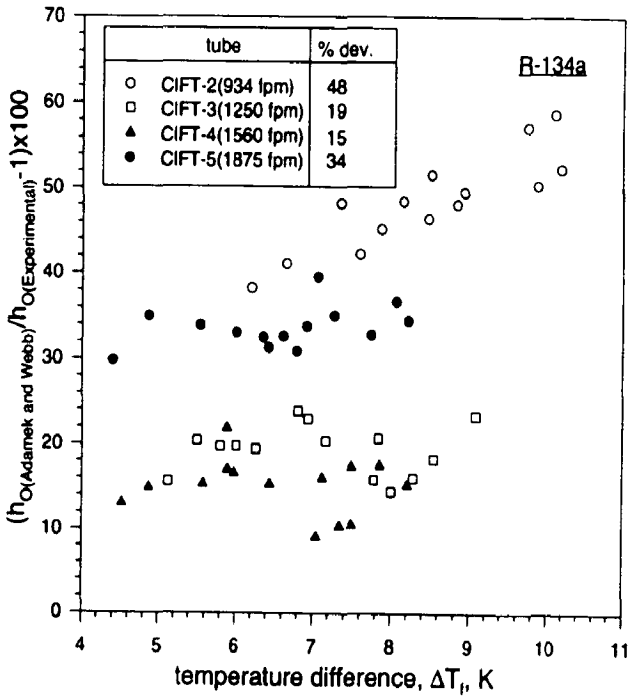

Figure 5.54
Comparison of experimental heat transfer coefficient with that predicted by Adamek and Webb model[2] for the condensation of of R-134a over CIFTs

5.9 DEVLOPMENT OF CORRELATION FOR FINNED TUBES

It can be safely concluded from the previous discussions that the condensing side heat transfer coefficient during condensation of steam and R-134a over horizontal finned tubes depends upon a number of parameters viz. heat flux, ΔT_f, thermo-physical properties of condensing fluid, fin geometry, fin density etc. It has also been observed in Section 5.8 that the predictions of different analytical models do not agree among themselves for the condensation of steam or R-134a over a particular finned tube. The order of the deviation of heat transfer coefficient predicted by these models from the experimental values also changes with the fins geometry. Moreover, no model predicts the heat transfer coefficient for the condensation over SIFTs. Therefore, it is felt necessary to develop a generalised correlation between different parameters which affect the condensing side heat transfer coefficient.

In order to develop a generalised correlation for the condensation over finned tubes, the Nusselt's equation for the condensation over a horizontal plain tube has been modified as follows:

The heat transfer across the condensate layer for a given fin pitch is expressed by the following equation

$$\dot{Q} = h_o.AF.\Delta T_f = \dot{m}\lambda \tag{5.7}$$

Where, AF is the tube surface area of a single fin pitch length, P_f

$$AF = \pi\left[\frac{D_o^{\,2} - D_r^{\,2}}{2} + D_o.tt + D_r(P_f - tb)\right] \tag{5.8}$$

The condensate flow rate ($\dot{m}$) on single pitch length, P_f, can be written as

$$\dot{m} = \rho.AF.V_f \tag{5.9}$$

The Reynolds number of condensate flow on the tube surface can be expressed as follows

$$Re = \frac{D_H \rho V_f}{\mu} = \frac{4AF}{P_f}.\frac{\rho V_f}{\mu} \tag{5.10}$$

or

$$Re = \frac{4\dot{m}}{\mu P_f} \tag{5.11}$$

The Nusselt's equation for the condensation over a horizontal tube is as given in equation (5.12)

$$h_o = C_o\left(\frac{k^3\rho^2 g\lambda}{\mu\Delta T_f D_r}\right)^{0.25} \tag{5.12}$$

The equation (5.7) and equation (5.12) will yield the following expression

$$h_o^{3/4} = C_o\left(\frac{k^2\rho^2 g}{\mu^2}\cdot\frac{\mu P_f}{4\dot{m}}\cdot\frac{4AF}{P_f D_r}\right)^{0.25} \tag{5.13}$$

or,

$$h_o\left(\frac{\mu^2}{k^3\rho^2 g}\right)^{1/3} = C_o^{4/3}\left(\frac{4AF}{D_r P_f}\right)^{1/3} Re^{-1/3} \tag{5.14}$$

For a horizontal plain tube AF/D_rP_f is equal to π and the left has side of the above expression is nothing but a non-dimensional number called Condensation number, CN

$$CN = h_o\left(\frac{\mu^2}{k^3\rho^2 g}\right)^{1/3} \tag{5.15}$$

And for a horizontal plain tube

$$CN = 1.47Re^{-1/3} \tag{5.16}$$

The Condensation number, CN, will be different for the finned tubes due the discrete values of equivalent hydraulic diameter of these tubes due to finning.

The condensate drainage from the fin surface is surface tension dominated. To account for the effect of condensate drainage from the fin surface under surface tension a dimensionless number called Weber number has been introduce which is the ratio of surface tension and the inertia force of the condensate. The Weber number for the drainage from the tube surface can be expressed as follows :

$$We = \frac{\partial p/\partial x}{\rho g} = \frac{\frac{2\sigma}{ef}\left(\frac{1}{rt}+\frac{1}{rb}\right)}{\rho g} \tag{5.17}$$

Therefore, the experimental results of heat transfer coefficient are correlated in the following equation form

$$CN = aRe^{b} We^{c} Y^{d} \tag{5.18}$$

Where, b=-1/3 and Y is equal to $\frac{AF}{D_r P_f}$

The regression of experimental data of present investigation for the condensation of steam and R-134a over respective CIFTs and SIFTs has given the following correlation by the least square method

$$\boxed{CN = 0.024 Re^{-1/3} We^{0.3} Y^{1.4}} \tag{5.19}$$

The Figure 5.55 illustrates the comparison between the experimental heat transfer coefficient and that determined by the developed correlation (given in equation (5.19)). The correlation has predicted the Condensation number in a range of ±15% for the 90 percent of experimental of steam and R-134a taken together. Although, it predicts the data for the higher fin density tube(1875 fpm) for the condensation of R-134a in a range of 0 to +15% yet it does not show the reduction in the Condensation number as observed in the experimental value of Condensation number, CN. Therefore, the developed correlation is recommended for the predictions up to a fin density of 1560 fpm for the condensation of R-134a over circular integral-fin tubes(CIFTs).

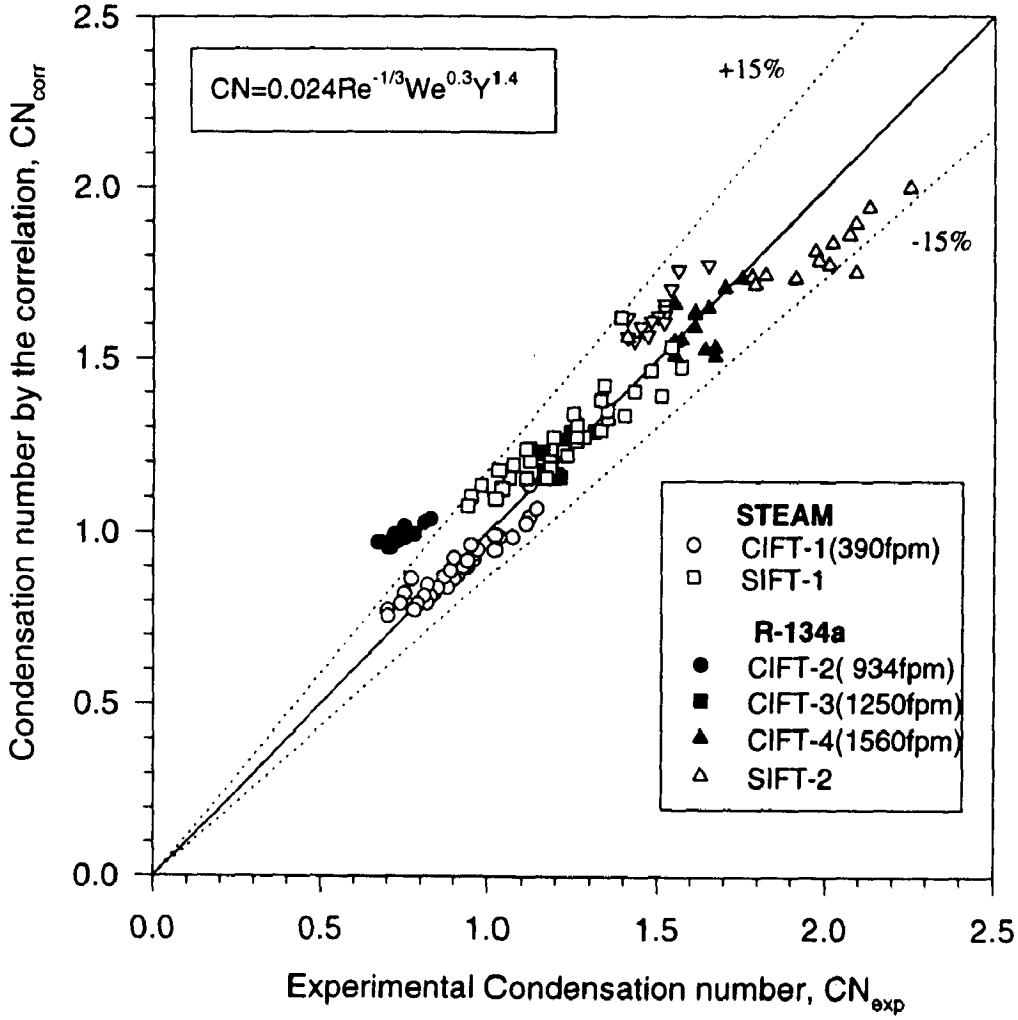

Figure 5.55

Comparison of experimental Condensation number and that predicted by the developed correlation for the condensation of steam and R-134a

5.10 VALIDATION OF CORRELATION

The correlation developed to determine the heat transfer coefficient for the condensation of steam and R-134a has been validated by comparing the experimental results of other investigators with those predicted by the correlation given in equation (5.19).

Figure 5.56 and Figure 5.57 graphs has been plotted to compare the predicted Condensation number from the correlation, equation (5.19), and the experimental Condensation numbers of a number of investigators for the condensation of steam and refrigerants respectively. The correlation has predicted the experimental data in a range of ±30 percent for the condensation of steam and in a range of ± 35 percent for the condensation of refrigerants.

A statistical analysis of the correlation represented by equation (5.19) has also been made to judge the integrity of the correlation. In Appendix-E a detailed statistical analysis of the results predicted by the correlation has been given.

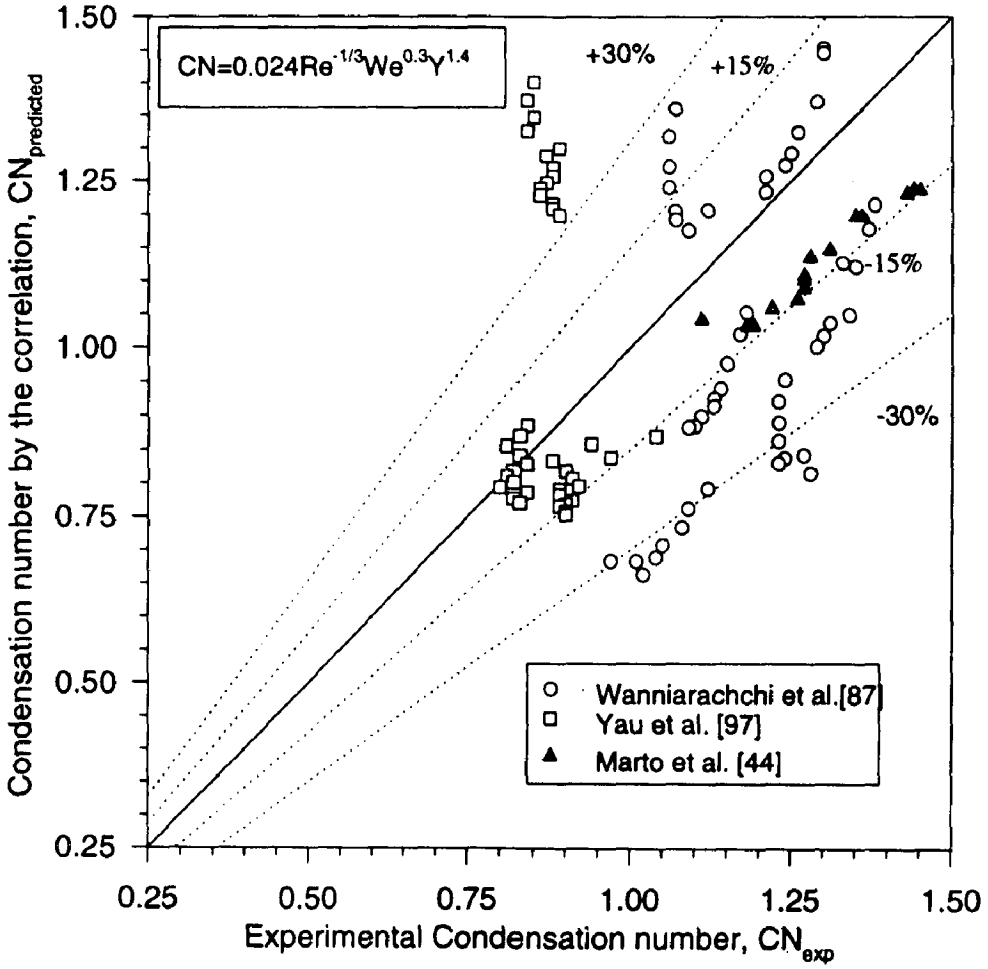

Figure 5.56

Comparison of experimental Condensation number with that by the proposed correlation for the condensation of steam over finned tubes

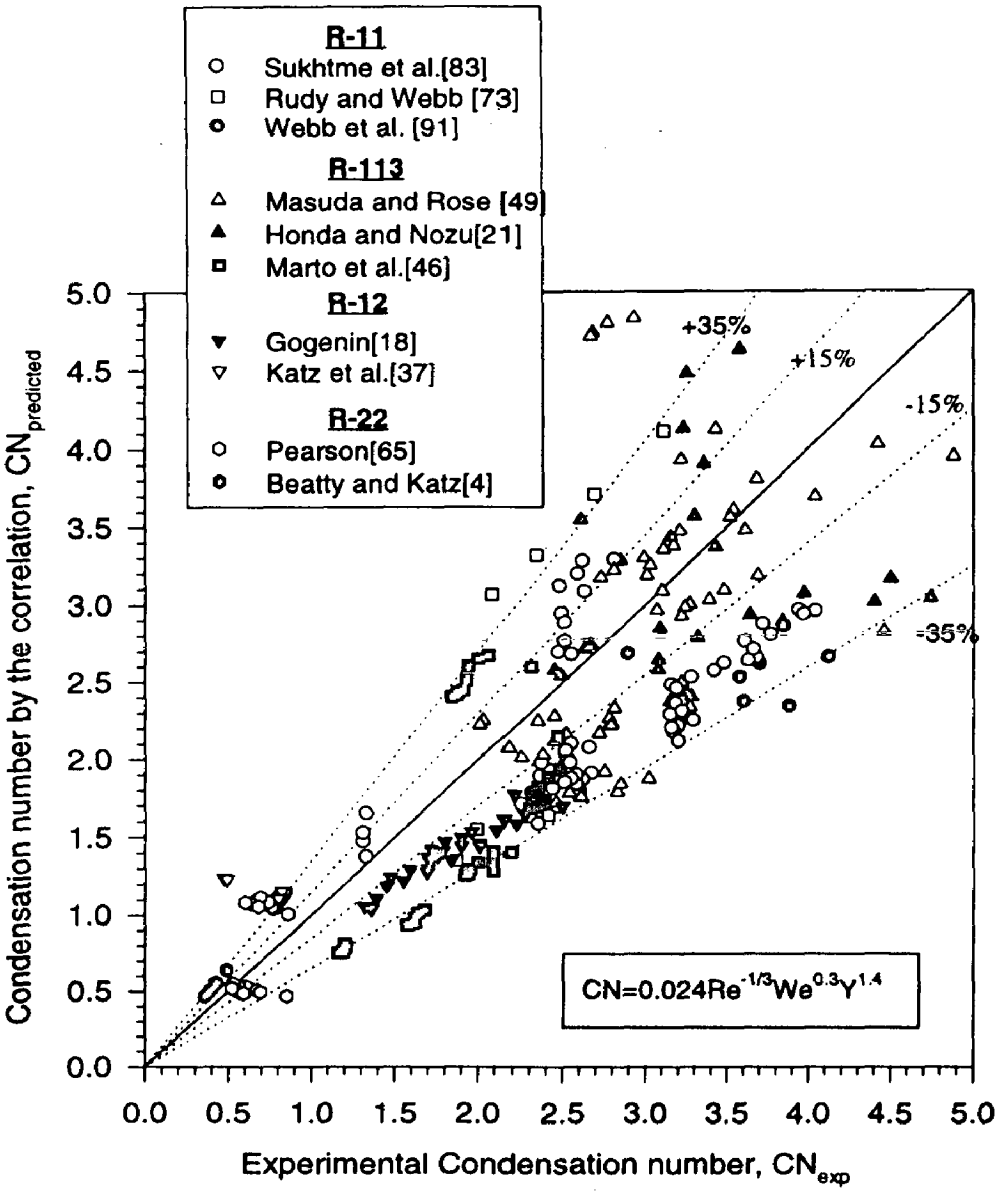

Figure 5.57
Comparison of experimental Condensation number with that by the proposed correlation for the condensation of refrigerants

CHAPTER #6

Conclusions and Recommendations

6.1 CONCLUSIONS

From the present investigation following conclusions have been drawn:

1. The proposed modified Nusselt's equation predicts the heat transfer coefficient in an error band of ±3% for the condensation of steam and ±2% for the condensation of R-12 and R-134a over a horizontal plain tube.

2. The heat transfer coefficient for the condensation of R-134a over a plain tube is 15% more than that for R-12 at the same vapour to tube wall temperature difference, ΔT_f.

3. The optimum fin density for the condensation of R-134a over a circular integral-fin tube is 1560 fins per meter. At this fin density the enhancement factor, EF, of the order of 5.63 has been achieved.

4. The spine integral-fin tube(SIFT) outperforms the best performing (with optimum fin density) circular integral-fin tube by approximately thirty percent for the condensation of steam and sixteen percent for the condensation of R-134a.

5. The spines are more effective in the lower half of the tubes for the condensation of steam and R-134a and improve the performance of best performing CIFT by approximately twenty percent for the condensation of steam and eleven percent for the condensation of R-134a.

6. For the condensation of R-134a the spines in the upper half of a CIFT(PCIFT-4) do not contribute in the enhancement of heat transfer coefficient but show 5% improvement in the performance of CIFT for the condensation of steam.

7. The experimental heat transfer coefficients for steam as well as R-134a do not show a satisfactory agreement with different models. However, the measured heat transfer coefficients are in the best agreement with those predicted by Honda and Nozu model. The model predicts 80% of experimental data in a range of ±20 percent.

8. The heat transfer coefficients for the condensation of steam have been underpredicted by the modified Wilson plot in the range of 7.5 percent to 15 percent. The underprediction of heat transfer coefficient for the condensation of R-134a and R-12 is high and remains in the range of 15 to 25 percent.

9. Following correlation has been developed between different dimensionless numbers to determine the condensing side heat transfer coefficient during condensation of steam and R-134a ove circular integral-fin tubes and spine integral fin tubes

$$CN = 0.024 Re^{-1/3} We^{0.3} Y^{1.4}$$

The 90 percent experimental data agree with this correlation in a range of ±15%. This correlation is recommended for the fin density up to 1560 fins per meter for the condensation of R-134a.

6.2 RECOMMENDATIONS FOR THE FURTHER INVESTIGATIONS

On the basis of present investigation it will be useful, for the promotion of knowledge, the following investigations are carried out:

1. In view of the wide industrial applications of the surface condensers the experimental investigations should be carried out to determine the effect of the velocity of the condensing vapours of steam and R-134a on the performance of finned tube viz, SIFTs and PCIFTs.
2. The investigations should also be carried out for the different shape of spine fins on the tube surface.
3. It shall be of yet another practical importance and immediate application if experimental investigations are carried out for the condensation of R-134a over a bundle of finned tubes with the arrangement of tubes in triangular and square pitch.

SAMPLE CALCULATION

A sample calculation to determine the heat flux and condensing side heat transfer coefficient is detailed in this section. The experimental data with accuracy of measurement for a typical test-run for the condensation of steam over CIFT-1 are given in table A-1. The table also contains the experimental data for the condensation of R-134a over CIFT-4. These data are used in the sample calculations for the condensation of steam and R-134a in the following sections:

Table A-1

sample data for the condensation of steam and R-134a

Parameters		Steam	R-134a	Accuracy
geometry of test-section	diameter at fin tip, D_o	24.97mm	24.68mm	0.02mm
	diameter at fin root. D_r	22.77mm	23.08mm	0.02mm
	inside tube diameter, D_i	18.42mm	18.42mm	0.02mm
	test-section length, L	340mm	417mm	1.0mm
cooling water flow rate		16.0 lpm	700 kg/hr	0.25lpm & 20kg/hr
cooling water temperature rise(T_{co}-T_{ci})		8.4°C	2.2°C	0.1°C
cooling water temperatures	test-section inlet, T_{ci}	23.3 °C	15.8 °C	0.1°C
	test section outlet, T_{co}	31.7 °C	18.0 °C	0.1°C
temperature of condensing vapour, T_s		114.5°C	39.7 °C	0.1°C
test-section surface temperature	top position, T_{top}	105.8°C	33.8 °C	0.1°C
	side position, T_{side}	101.8°C	33.5 °C	0.1°C
	bottom position, T_{bot}	98.4°C	32.4 °C	0.1°C

A.1 SAMPLE CALCULATIONS FOR THE CONDENSATION OF STEAM

The sample calculations for the condensation of steam are given hereunder

A.1.1 Heat Transfer Area of The Tube Surface

$$A_r = \pi D_r L$$

$$A_r = \pi x 0.02277 x 0.340$$

$$A_r = 2.432 x 10^{-2}\ m^2$$

A.1.2 Cooling Water Velocity, V

$$V = \frac{f_q / 60}{\frac{\pi D_i^2}{4}}$$

From table A-1 the cooling water flow rate, f_q=16.0 lpm

$$V = \frac{\frac{16 x 10^{-3}}{60}}{\frac{\pi}{4} x (0.01842)^2}$$

$$V = 1.0\ m/s$$

A.1.3 Cooling Water Bulk Temperature

$$T_{cb} = \frac{(T_{co} + T_{ci})}{2}$$

$$T_{cb} = \frac{(31.7 + 23.3)}{2}$$

$$T_{cb} = 27.5\ ^{\circ}C$$

A.1.4 Cooling Water Properties at The Cooling Water Bulk Temperature

viscosity, μ_b = $8.5195 x 10^{-4}$

density, ρ_b = $996.25\ kg/m^3$

specific heat Cp_b = 4.1786 kJ/kg-K

A.1.5 Heat Flow Rate

$$\dot{Q} = \frac{f_q \rho_c C_{pb} (T_{co} T_{ci})}{60x1000} \text{ kW}$$

$$\dot{Q} = \frac{1}{60x1000} x16x996.25x4.1786x(31.7-23.3)$$

$$\dot{Q} = 9.325 \text{ kW}$$

A.1.6 Heat Flux

$$q = \frac{\dot{Q}}{A_r}$$

$$q = \frac{9.325}{2.432x10^{-2}}$$

$$q = 383.429 \text{ kW/m}^2$$

$$q = 0.383 \text{ MW/m}^2$$

A.1.7 Temperature Difference Across the Condensate Layer, ΔT_f

Average outside temperature of test-section

$$T_{wo} = \frac{1}{4}(T_{top} + 2.0T_{side} + T_{bot})$$

$$T_{wo} = \frac{1}{4}(105.8 + 2x101.8 + 98.4)$$

$$T_{wo} = 101.95 \text{ °C}$$

$$\Delta T_f = (T_s - T_{wo})$$

$$\Delta T_f = (114.5-101.9)$$

$$\Delta T_f = 12.55 \text{ °C}$$

A.1.8 Condensing Side Heat Transfer Coefficient

$$h_o = \frac{q}{\Delta T_f}$$

$$h_o = \frac{383.429}{12.55}$$

$$h_o = 30.55 \text{ kW/m}^2\text{-K}$$

A.2 SAMPLE CALCULATIONS FOR THE CONDENSATION OF R-134a

A sample of the calculations for the condensation of R-134a are given hereunder

A.2.1 Heat Transfer Area of The Tube Surface

$$A_r = \pi D_r L$$

$$A_r = \pi x 0.02308 x 0.417$$

$$A_r = 3.024 x 10^{-2} \text{ m}^2$$

A.2.2 Cooling Water Bulk Temperature

$$T_{cb} = \frac{(T_{co} + T_{ci})}{2}$$

$$T_{cb} = \frac{(18.0 + 15.8)}{2}$$

$$T_{cb} = 16.9 \text{ °C}$$

A.2.3 Cooling water properties at the cooling water bulk temperature

viscosity, μ_b = $1.0975 x 10^{-3}$

density, ρ_b = 998.696 kg/m^3

specific heat, Cp_b = 4.1912 kJ/kg-K

A 2.4 Heat Flow Rate

$$\dot{Q} = \frac{f_m}{3600} C_{pb}(T_{co} T_{ci})$$

From table A-1 the cooling water flow rate, f_q= 700 kg/hr

$$\dot{Q} = \frac{1}{3600} x700x4.1912x(18.0-15.8)$$

$$\dot{Q} = 1.793 \text{ kW}$$

A.2.5 Heat Flux

$$q = \frac{\dot{Q}}{A_r}$$

$$q = \frac{1.793}{3.024x10^{-2}}$$

$$q = 59.29 \text{ kW/m}^2$$

A.2.6 Temperature Difference Across The Condensate Layer, ΔT_f

Average outside temperature of test-section

$$T_{wo} = \frac{1}{4}(T_{top} + 2.0T_{side} + T_{bot})$$

$$T_{wo} = \frac{1}{4}(33.8 + 2x33.5 + 32.4)$$

$$T_{wo} = 33.3 \text{ °C}$$

$$\Delta T_f = (T_s - T_{wo})$$

$$\Delta T_f = (39.7-33.3)$$

$$\Delta T_f = 6.4 \text{ °C}$$

A.2.7 Condensing Side Heat Transfer Coefficient

$$h_o = \frac{q}{\Delta T_f}$$

$$h_o = \frac{59.29}{6.4}$$

$$h_o = 9.264 \text{ kW/m}^2\text{-K}$$

APPENDIX-B

ERROR ANALYSIS

The present investigation is aimed to augment the heat transfer during condensation over horizontal finned tubes by increasing the condensing side heat transfer coefficient at a constant ΔT_f. In order to attain the experimental data some measurements have been made viz. cooling water flow rate, temperatures of cooling water, condensing vapour and tube surface temperature, electric energy input to the heaters etc. These measurements owing to the limitation of the instruments used for the purpose and method employed give rise to some degree of inaccuracy. When a number representing the magnitude of physical quantity is obtained by experimental methods, only through sheer luck the measured value will coincide exactly with the true value and even then, this is extremely unlikely event to occur if so, it would go unnoticed. The magnitude of true value can be approached but , in the rigid sense, never evaluated. The difference between the true value(known) and the result(best experimentally obtained value) is the *error*, Since we never know the magnitude of the error is never known, hence, it is often termed as *uncertainty*. Uncertainty is the best estimate of the magnitude of the known error. Typical procedure involved for the calculation of uncertainty is explained for a function in the following section.

B.1 TREATMENT OF UNCERTAINTY

If a given function f(x) is expanded by the Taylor's series the following expression is attained

$$f[(x1+\Delta x1), (x2+\Delta x2)...(xn+\Delta xn)] = f(x1, x2, ..x_n) + \Delta x1 \frac{\partial f}{\partial x1} + \Delta x_2 \frac{\partial f}{\partial x2} \quad ....\Delta x_n \frac{\partial f}{\partial xn} \qquad (B1)$$

Where, xn 's are variables and Δxn's are determined or assumed incremental variations(uncertainties) in the respective xn's . The equation (B1) can be rewritten as -

$$f[(x1+U_{x1}), (x2+U_{x2}).....(xn+U_{xn})] - f(x1,x2,.....xn) = [U_{x1}\frac{\partial f}{\partial x1}+U_{x2}\frac{\partial f}{\partial x2}.....U_{xn}\frac{\partial f}{\partial xn}] \quad (B2)$$

or

$$U_f = (U_{x1}\frac{\partial f}{\partial x1}+U_{x2}\frac{\partial f}{\partial x2}.....U_{xn}\frac{\partial f}{\partial xn}) \quad (B3)$$

Equation (B3) evaluates the over all maximum uncertainty of the function. It is not likely, however, that we should expect the maximum value to be attained. A more reasonable value corresponds to the Pythagorean summation of the discrete uncertainties i.e.

$$U_f = \left[\sum_{i=1}^{n}\left\{\left(\frac{\partial f}{\partial xi}\right)U_{xi}\right\}^2\right]^{0.5} \quad (B4)$$

xi= nominal values of variables

U_{xi}= discrete uncertainties associated with xi variable

U_f= overall uncertainty associated with function

For the present investigations the uncertainty in the measurements has been determined for the condensation of steam and R-134a as follows

B.2 Uncertainty in The Measurements During Condensation of Steam and R-134a

An error analysis has been carried out of all the test-runs for the condensation of steam and R-134a. A sample calculation of typical test-run data from Table A-1 is given hereunder

B.2.1 Error in The Surface Area of The Condenser Tube

Since, $A_r = \pi d_r L$

Error in the determination of the area of the tube, E_{Ar}

$$E_{Ar} = [(\pi L E_{dr})^2 + (\pi d_r E_L)^2]^{1/2}$$

Where, E_{dr} and E_L denote the error associated with diameter and length, respectively.

Hence, for the condensation of steam and R-134a the error in surface area is as follows:

steam	R-134a
$A_r = \pi x 0.02277 x 0.34$	$A_r = \pi x 0.02308 x 0.417$
$= 2.432 x 10^{-2}\ m^2$	$= 3.024 x 10^{-2}\ m^2$
$E_{Ar} = [(\pi x 0.340 x 0.00002)^2 + (\pi x 0.02277 x 0.001)^2]^{1/2}$	$E_{Ar} = [(\pi x 0.417 x 0.00002)^2 + (\pi x 0.02308 x 0.001)^2]^{1/2}$
$= 7.466 x 10^{-5}\ m^2$	$= 7.7 x 10^{-5}\ m^2$

B.2.2 Error in The Estimation Of Heat Flow Rate

steam	R-134a
Error in coolant flow rate, E_{fq} = 0.25 lpm	Error in coolant flow rate, E_{fm} = 20 kg/hr
Uncertainty in coolant flow rate = $\frac{0.25}{16.0} x 100$	Uncertainty in coolant flow rate = $\frac{20}{700} x 100$
= 1.56%	= 2.86%
Temperature rise of coolant, ΔT_c	Temperature rise of coolant
$\Delta T_c = (T_{co} - T_{ci})$	$\Delta T_c = (T_{co} - T_{ci}) = 2.2°C$
= 31.7-23.3	The accuracy of temperature measurement has
= 8.4 °C	been increased by using a thermopile of four

Error in the temperature rise of coolant

$$E_{\Delta T_c} = [(E_{Tco})^2 + (E_{Tci})^2]^{0.5}$$

$$E_{\Delta T_c} = [(0.1)^2 + (0.1)^2]^{0.5}$$

$$= 0.141^{\circ}C$$

Uncertainty in the temperature rise

$$= \frac{E_{\Delta T_c}}{\Delta T_c} x100$$

$$= \frac{0.141}{8.4} x100 = = 1.68\%$$

Heat flow rate is taken from A.1.5 in Appendix-A

$$\dot{Q} = 9.325 \text{ kW}$$

Error in heat flow rate

$$E_{\dot{Q}} = \frac{\rho_b C_p}{60x1000} [((T_{co}-T_{ci})E_{fq})^2 + (f_q E_{\Delta Tc})^2]^{0.5}$$

$$E_{\dot{Q}} = \frac{0.001x996.25x4.1786}{60} \begin{bmatrix} \{(31.7 - 23.3)x0.25\}^2 \\ + \{16.0x0.141\}^2 \end{bmatrix}^{0.5}$$

=0.2138 kW

213.8 W

Uncertainty in heat flow rate, $\dot{Q}$

$$= \frac{E_{\dot{Q}}}{Q} x100 = \frac{0.2138}{9.325} x100$$

= 2.3%

thermocouples for the measurement of temperature rise as suggested by [16], therefore, the error in measurement of temperature rise has reduced to $0.1^{\circ}C$.

Uncertainty in the temperature rise

$$= \frac{E_{\Delta T_c}}{\Delta T_c} x100$$

$$= \frac{0.1}{2.2} x100 = 4.54\%$$

Heat flow rate is taken from A.2.4 in Appendix A-1

$$\dot{Q} = 1.793 \text{ kW}$$

Error in heat flow rate

$$E_{\dot{Q}} = \frac{C_p}{3600} [((T_{co}-T_{ci})E_{fm})^2 + (f_m E_{\Delta Tc})^2]^{0.5}$$

$$E_{\dot{Q}} = \frac{4.1912}{3600} \left[\{(18.0 - 15.8)x20\}^2 + \{(700x0.1)\}^2 \right]^{0.5}$$

$$E_{\dot{Q}} = 0.09625 \text{ kW}$$

$$= 96.25 \text{ W}$$

Uncertainty in heat flow rate, $\dot{Q}$

$$= \frac{E_{\dot{Q}}}{Q} x100 = \frac{0.09625}{1.793} x100$$

=5.37%

B.2.3 Error in The Estimation of Heat Flux

steam

Heat flux, $q = \frac{\dot{Q}}{A_r}$

$$q = \frac{9.325}{0.0243} = 383.43 \text{ kW/m}^2$$

Error in heart flux

$$E_q = \left[\left(\frac{E_{\dot{Q}}}{A_r} \right)^2 + \left(\frac{\dot{Q} E_{A_r}}{A_r^2} \right) \right]^{0.5}$$

$$E_q = \left[\left(\frac{0.2138}{0.0243} \right)^2 + \left(\frac{9.325 \times 7.466 \times 10^{-5}}{(0.0243)^2} \right)^2 \right]^{0.5}$$

$= 8.8766 \text{ kW/m}^2$

uncertainty in heat flux

$$= \frac{E_q}{q} \times 100 = \frac{8.8766}{383.43} \times 100 = 2.31\%$$

R-134a

Heat flux, $q = \frac{\dot{Q}}{A_r}$

$$q = \frac{1.793}{3.024 \times 10^{-2}} = 59.29 \text{ kW/m}^2$$

Error in heart flux

$$E_q = \left[\left(\frac{E_{\dot{Q}}}{A_r} \right)^2 + \left(\frac{\dot{Q} E_{A_r}}{A_r^2} \right) \right]^{0.5}$$

$$E_q = \left[\left(\frac{0.09625}{0.03024} \right)^2 + \left(\frac{1.793 \times 7.7 \times 10^{-5}}{(0.03024)^2} \right)^2 \right]^{0.5}$$

$= 3.1832 \text{ kW/m}^2$

uncertainty in heat flux

$$= \frac{E_q}{q} \times 100 = \frac{3.1832}{59.29} \times 100 = 5.37\ \%$$

B.2.4 Error in The Estimation of ΔT_f

steam	R-134a
$T_{wo} = \frac{1}{4}\left(T_{top} + 2.0T_{side} + T_{bot}\right)$	$T_{wo} = \frac{1}{4}\left(T_{top} + 2.0T_{side} + T_{bot}\right)$
$T_{wo} = \frac{1}{4}(105.8 + 2x101.8 + 98.4)$	$T_{wo} = \frac{1}{4}(33.8 + 2x33.5 + 32.4)$
$T_{wo} = 101.95\ ^{\circ}C$	$T_{wo} = 33.3\ ^{\circ}C$
$E_{T_{wo}} = \frac{1}{4}\left(E_{T_{top}}{}^2 + 2.0E_{T_{top}}{}^2 + E_{T_{bot}}{}^2\right)^{0.5}$	$E_{T_{wo}} = \frac{1}{4}\left(E_{T_{top}}{}^2 + 2.0E_{T_{top}}{}^2 + E_{T_{bot}}{}^2\right)^{0.5}$
$E_{T_{wo}} = \frac{1}{4}\left(0.1^2 + 2.0x0.1^2 + 0.1^2\right)^{0.5}$	$E_{T_{wo}} = \frac{1}{4}\left(0.1^2 + 2.0x0.1^2 + 0.1^2\right)^{0.5}$
$E_{T_{wo}} = 0.05$	$E_{T_{wo}} = 0.05$
$\Delta T_f = (T_s - T_{wo})$	$\Delta T_f = (T_s - T_{wo})$
$\Delta T_f = (114.5-101.9)=12.55\ ^{\circ}C$	$\Delta T_f = (39.7-33.3)=6.4\ ^{\circ}C$
$E_{\Delta T_f} = \left[(E_{Ts})^2 + (E_{Two})^2\right]^{0.5}$	$E_{\Delta T_f} = \left[(E_{Ts})^2 + (E_{Two})^2\right]^{0.5}$
$E_{\Delta T_f} = \left[0.1^2 + 0.05^2\right]^{0.5}$	$E_{\Delta T_f} = \left[0.1^2 + 0.05^2\right]^{0.5}$
$E_{\Delta T_f} = 0.11^{\circ}C$	$E_{\Delta T_f} = 0.11^{\circ}C$
Uncertainty in ΔT_f	Uncertainty in ΔT_f
$= \frac{E_{\Delta T_f}}{\Delta T_f} = \frac{0.11}{12.55}x100 = 0.88\%$	$= \frac{E_{\Delta T_f}}{\Delta T_f} = \frac{0.11}{6.4}x100 = 1..72\%$

B.2.5 Error in heat transfer coefficient

steam

heat transfer coefficient, $h_o = \frac{q}{\Delta T_f}$

$$h_o = \frac{383.43}{12.55}$$

h_o= 30.55 kW/m^2-K

$$E_{ho} = \left[\left(\frac{E_q}{\Delta T_f}\right)^2 + \left(\frac{qE_{\Delta T_f}}{\Delta T_f^2}\right)^2\right]^{0.5}$$

$$E_{ho} = \left[\left(\frac{8.8766}{12.55}\right)^2 + \left(\frac{383.43x0.11}{12.55^2}\right)^2\right]^{0.5}$$

=0.7563

uncertainty in heat transfer coefficient

$$= \frac{0.7563}{30.55} x100 = 2.48\%$$

R-134

heat transfer coefficient, $h_o = \frac{q}{\Delta T_f}$

$$h_o = \frac{59.29}{6.4}$$

h_o=9.26 kW/m^2-°C

$$E_{ho} = \left[\left(\frac{E_q}{\Delta T_f}\right)^2 + \left(\frac{qE_{\Delta T_f}}{\Delta T_f^2}\right)^2\right]^{0.5}$$

$$E_{ho} = \left[\left(\frac{3.1832}{6.4}\right)^2 + \left(\frac{59.29x0.11}{6.4^2}\right)^2\right]^{0.5}$$

E_{ho} = 0.522

uncertainty in heat transfer coefficient

$$= \frac{0.522}{9.26} x100 = 5.64\%$$

The Figure A-1 has been drawn to show the uncertainty in heat transfer coefficient for the condensation of steam over CIFT-1. The uncertainty has increased with the increase in heat transfer coefficient. There are two major factors contributing towards the uncertainty in determination of heat transfer coefficient viz. heat flux and temperature difference across the condensate layer, ΔT_f. For the entire range of heat transfer coefficient the uncertainty in heat flux has influenced the uncertainty in heat transfer coefficient to a very high extend. In the present investigation the heat flux has been determined by measuring the heat carried away by the cooling water. Hence, the cooling water flow rate and its temperature rise are required to be measured. The Figure A-2 shows the variation of the uncertainty in heat flux. For the lower heat flux the uncertainty due to cooling water flow rate is high because it has been observed that for low cooling water flow rate the heat transfer is also low. As the cooling water flow increased the temperature rise of the cooling water has reduced. This reduction led the high uncertainty in the cooling water temperature rise. . The uncertainty in the value tube surface area of CIFT-1 is 0.3% and remains constant , therefore, it is not shown in the graphs.

Similarly, for the condensation of R-134a Figure A-3 has been drawn to show the uncertainty in the experimental result of heat transfer coefficient. Hese also, the heat flux controls the uncertainty in the determination of heat transfer coefficient and the error in the temperature difference across the condensate layer, ΔT_f, has relatively much less contribution in the total uncertainty.

For the condensation of R-134a also the heat flux was computed by taking the heat carried away by the cooling water into account. The uncertainty in the test-section area was 0.25%. At the low heat flux the uncertainty was mainly due to the error in the coolant flow rate. As the coolant flow rate was increased the error due to the coolant temperature rise became predominant. As shown in Figure A-4.

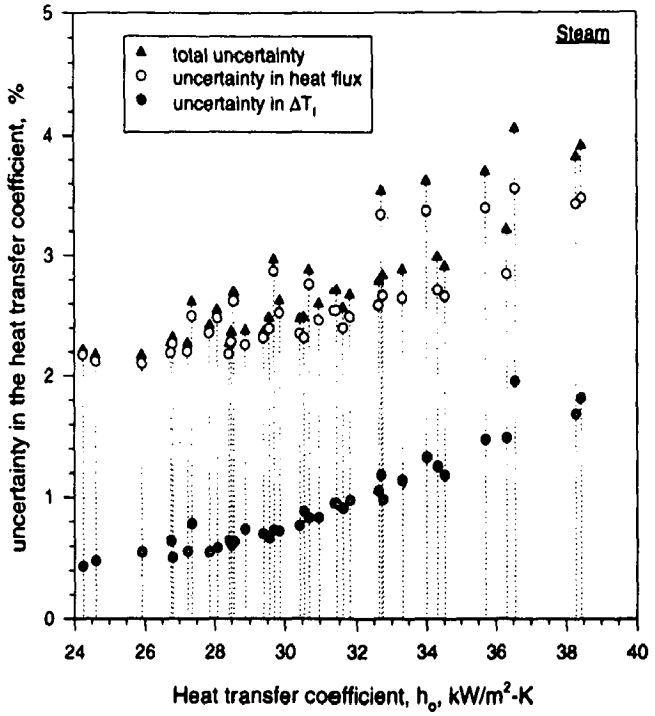

Figure A-1
Uncertainty in heat transfer coefficient for the condensation of steam over CIFT-1

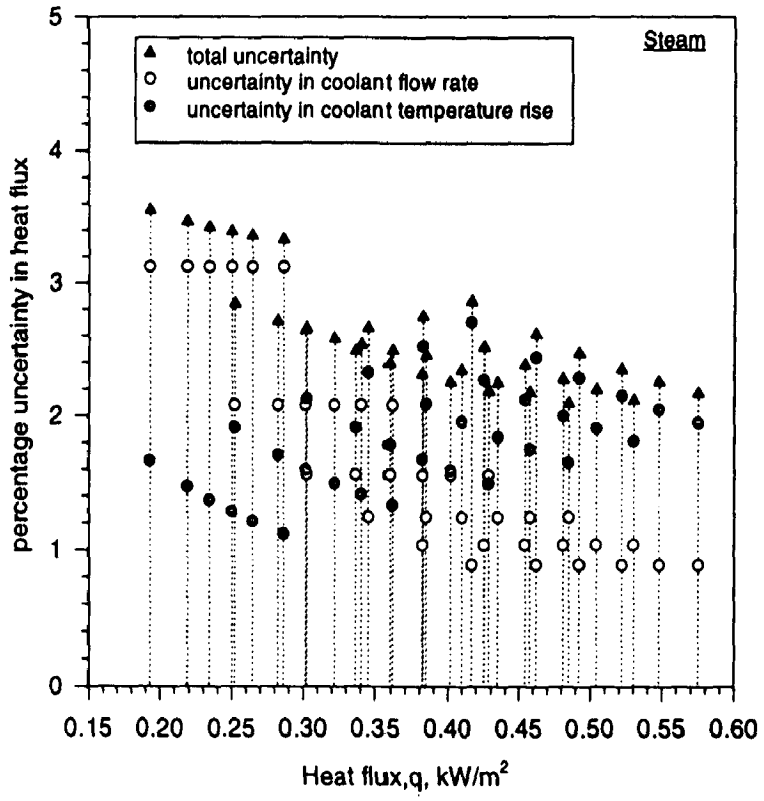

Figure A-2
Uncertainty in heat flux for the condensation of steam over CIFT-1

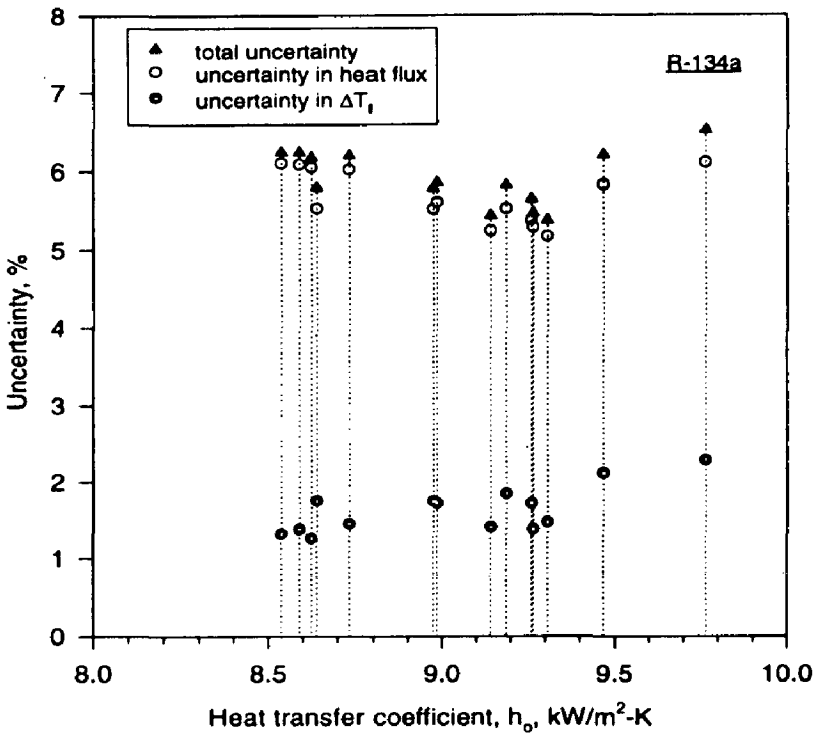

Figure A-3
Uncertainty in heat transfer coefficient for the condensation of R-134a over CIFT-4 (1560fpm)

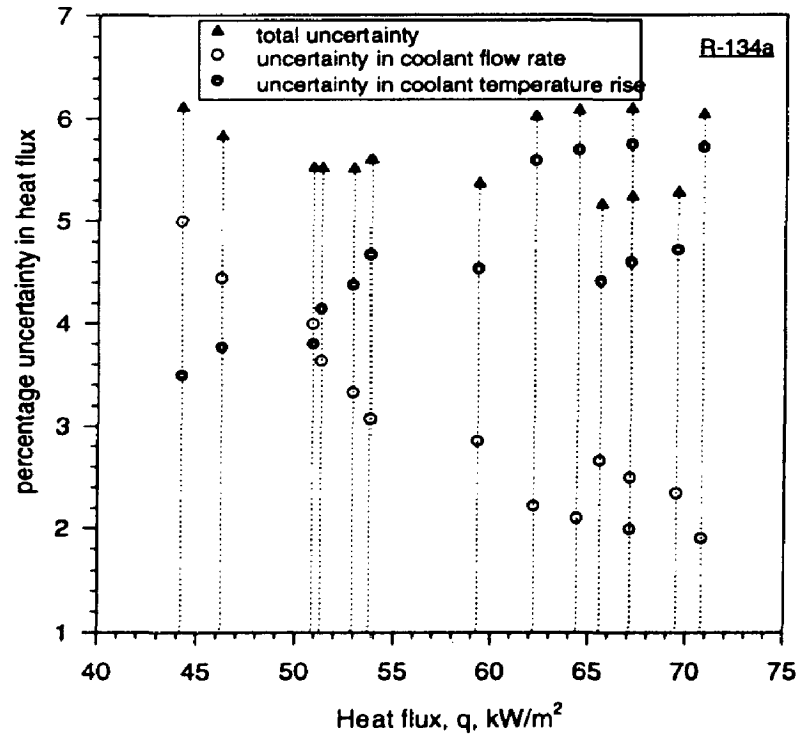

Figure A-4
Uncertainty in heat flux for the condenation of R-134a over CIFT-4(1560fpm)

Appendix-C

RELATIONS BETWEEN ENHANCEMENT FACTORS

The relation between the enhancement factor at constant temperature difference across the condensate layer, ΔT_f and at a constant heat flux can be established as follows:

Let us assume, that the enhancement factor, EF, at a constant ΔT_f is $E_{\Delta T}$ and the enhancement factor at a constant heat flux, q, is E_q for the condensation over a horizontal tube.

The condensation over a plain tube and a finned horizontal tube can be expressed by the following Nusselt's equation[62]. For different tubes the value of constant C_o will be different for finned tubes and plain tube.

$$h_o = C_o\left[\frac{k^3\rho^2 g\lambda}{\mu D_o \Delta T_f}\right]^{1/4} \tag{C1}$$

Suppose the value of C_o for a plain tube is C_a and that for the finned tube is C_b then the enhancement factor at constant ΔT_f, $E_{\Delta T}$ and the enhancement factor at constant heat flux, E_q can be expressed as follows

$$E_{\Delta T} = \frac{C_2}{C_1} \tag{C2}$$

$$E_q = \frac{C_2}{C_1}\left[\frac{\Delta T_1}{\Delta T_2}\right]^{1/4} \tag{C3}$$

At a constant heat flux

$$q = h_1 \Delta T_1 = h_2 \Delta T_2 \tag{C4}$$

or

$$\frac{h_2}{h_1} = E_q = \frac{\Delta T_1}{\Delta T_2} \tag{C5}$$

from equation (C2), (C3) and (C5) the following expression is attained

$$E_q = E_{\Delta T}(E_q)^{1/4} \tag{C6}$$

by rearranging the equation (C6) the following expression is attained

$$\boxed{E_q = (E_{\Delta T})^{4/3}} \tag{C7}$$

MODIFIED WILSON PLOT

Employing the process discussed by Briggs and Young[9], the condensing side heat transfer coefficient during condensation of steam and R-134a has been determined by the modified Wilson plot method, in addition to that by measuring the out side tube wall temperature. The stepwise procedure is given here to determine the condensing side heat transfer coefficient by the modified Wilson plot technique, the procedure contains the following steps

1. The inside tube heat transfer coefficient was determined by using Sieder-tate equation:

$$h_i = \frac{k_b C_i}{D_i} Re_b^{0.8} Pr_b^{1/3} \left(\frac{\mu_b}{\mu_w}\right)^{0.14} = C_i F \qquad (D1)$$

$$Re_b = \frac{\rho_b D_H V}{\mu_b} \qquad (D2)$$

$$Pr_b = \frac{\mu_b Cp_b}{k_b} \qquad (D3)$$

For short tubes($L/D_i \leq 50$) the thermal boundary layers inside the test-section are not fully developed[52]. Therefore, the inside tube heat transfer coefficient for short tubes is always greater than that predicted by the equation (D1) Therefore, Al-Arabi[37] has recommended the following modification in the inside tube heat transfer coefficient

$$\frac{SF.Pr^{1/6}}{\left(L/D_i\right)^{0.1}} = 0.68 + \frac{3000}{Re_b^{0.81}} \qquad (D4)$$

and $$h_i = h_j\left[1.0 + SF\left(D_i/L\right)\right] \qquad (D5)$$

Cooling water thermo-physical properties are taken at the cooling water bulk temperature, T_{cb}. The initial value of C_i is taken equal to 0.003 and μ_b/μ_w is taken equal to 1.0.

2. The coolant side tube wall temperature is calculated by the following equation

$$T_{wi} = T_{cb} + \frac{\dot{Q}}{h_i A_i} \qquad (D6)$$

Where, $A_i = \pi D_i L$

3. The value of μ_w corresponding to T_{wi} is calculated (from equation (D6)) with the new value of μ_w. Step-1 and step-3 are repeated till the value of T_{wi} converges.

4. The outside tube wall temperature, T_{wo}, is calculated by the following equation

$$T_{wo} = T_{wi} + \frac{\dot{Q}}{2\pi k_f L} \ln\left(\frac{D_r}{D_i}\right) \qquad (D7)$$

5. The Nusselt-type expression has been used to determine the condensing side heat transfer coefficient

$$h_o = C_o\left(\frac{k^3 \rho^2 g\lambda}{\mu \Delta T_f D_r}\right)^{0.25} = C_o G \qquad (D8)$$

5. The over all heat transfer coefficient has been determined by the equation (D9)

$$q = \dot{m}_c C_p (T_{co} - T_{ci}) = (\Delta T)_{lm} . U_o \qquad (D9)$$

6. The relation between over all thermal resistance and individual thermal resistance for the heat flow from vapour to cooling can represented as:

$$\frac{1}{U_o A_r} = \frac{1}{h_i A_i} + R_w + \frac{1}{h_o A_r} \qquad (D10)$$

or,

$$\left(\frac{1}{U_o} - R_w\right) G = \frac{A_r G}{C_i A_i F} + \frac{1}{C_o} \qquad (D11)$$

In fact, the equation (D11) has a simple linear form :

$$Y = mX + c \qquad (D12)$$

Where,

$$Y = \left(\frac{1}{U_o} - r_w\right) G \qquad (D13)$$

$$X = \frac{A_r G}{A_i F} \qquad (D14)$$

$$m = \frac{1}{C_i} \qquad (D15)$$

$$c = \frac{1}{C_o} \qquad (D16)$$

Hence, C_i and C_o will be determined from the best fit line between X and Y. The value of these variables has been calculated from the experimental data at different cooling water flow rates.

The best fit values of C_i and C_o are used in equation (D1) and equation (D8) respectively to determine the inside tube heat transfer coefficient and the condensing side heat transfer coefficient respectively.

Steps 1-6 are repeated till the value of C_i and C_o converges and finally the value of condensing side heat transfer coefficient, h_o, is calculated.

STATSTICAL ANALYSIS OF THE DEVELOPED CORRELATION

A statistical analysis of correlation has been done the results are as follows

y= true value of dependent variable

f = predicted values of dependent variable from correlation

E.1 DEGREE OF FREEDOMS

E.1.1 Total Degree of Freedom

tdof=n-1

n is the number of observations and is equal to 142

tdof=142-1=141

E.1.2 Regression Degree of Freedom

rdof=n-k

rdof= 142-4=138

E.1.3 Error Degree of Freedom

edof = tdof-rdof

edof = 141-138 =3

E.2 SUM OF SQUARES OF RESIDUALS

$$SSE = \sum (y - f)^2$$

$$= 2.193$$

E.3 SUM OF SQUARES OF ERROR ABOUT THE MEAN

$$SSM = \sum (y - y_{mean})^2$$

$$= 20.055$$

E.4 SUN O SQUARE OF ERROR DUE TO REGRESSION

SSR=SSM-SSE

= 20.055-2.193

= 17.916

E.5 STANDARD ERROR OF FIT

$$se = \left(\frac{SSE}{rdof}\right)^{0.5}$$

$$= \left(\frac{2.095}{138}\right)^{0.5}$$

= 0.124

E.6 SUM OF THE SQUARE O RESIDUES

$$r^2 = \left(1.0 - \frac{SSE}{SSM}\right)$$

$$r^2 = \left(1.0 - \frac{2.139}{20.055}\right)$$

$r^2 = 0.893$

E.7 FISHER VALUE

$$F = \left[\frac{\frac{(SSM - SSE)}{edof}}{\frac{SSE}{rdof}}\right]$$

$$F = \left[\frac{\frac{(20.055 - 2.139)}{3}}{\frac{(2.139)}{138}}\right] = 385.29$$

The value of 'r^2' is closer to 0.9 signifying the strong relationship amongst the variables. This agreement may be a by chance of a fluke. Therefore, to reinforce this finding, the F-test has been carried out. Because there is a relationship among the variables if the F-observed statistic is greater than the F-critical value. For a single-tailed test, with 99% confidence level and 138 degrees of freedoms. The F-critical value is 26.1. This value of 'F' has been attained from [14].

The F-observed for the present experimental data is 385.29, which is substantially greater than the F-critical value of 26.2. Therefore, the regression equation is useful in predicting the assessed value of Condensation number and it is strongly dependent on the independent variables.

PUBLICATIONS

1. **Kumar,R.**, Varma,H.K., Mohanty,B. and Agrawal,K.N., Augmentation of Outside Tube Heat Transfer Coefficient During Condensation of Steam Over Horizontal Copper Tubes, International Communication in Heat and Mass Transfer, Vol.25, No.1, pp. 81-91, 1998.

2. Singh,S.K., Mohanty,B., **Kumar,R.**, and Varshney, B., Heat Transfer During Condensation Of Steam Over A Vertical Array Of Horizontal Integral-Fin Tubes, International Journal of Multiphase Flow (Communicated).

REFERENCES

1. Adamek,T., Analytical Model of Film Condensation on Integral-Fin Tubes, *Warme und Stoffiibertragung*, Vol.19, No.2, pp.145-157, 1985.

2. Adamek,T. and Webb,R.L., Prediction of Film Condensation on Horizontal Integral-fin Tubes, *Int. J. Heat Mass Transfer*, Vol.33, No.8, pp.1721-1735, 1990.

3. Al-Arabi,M., Turbulent Heat Transfer in The Entrance Region of a Tube, *Heat Transfer Engineering*, Vol.3, NOs 3-4, pp.76-82, 1982.

4. Beatty,K.O. and Katz, D.L., Condensation of Vapours on Outside of Finned Tubes, *Chem. Engg. Prog.*, Vol.44, No.1, pp.55-70, 1948.

5. Bergles,A.E., Some Perspectives on Enhanced Heat Transfer- Second generation Heat Transfer Technology, *Trans. ASME*, Vol.110, pp.1082-1096, 1988.

6. Berman,L.D., Heat Transfer with Steam Condensing on a Bundle of Horizontal Tubes, *Thermal Engg.*, Vol.28, pp.218-224, 1981.

7. Briggs,A. and Rose,J., Effect of Fin Efficiency on a Model For Condensation Heat Transfer on a Horizontal Integral-Fin Tube, *Int. J. Heat Mass Transfer*, Vol.37, pp.457-463, 1994.

8. Briggs,A., Wen,X.L. and Rose,J.W., Accurate Heat Transfer Measurements for Condensation on Horizontal Integral-Fin Tubes, *ASME J. of Heat Transfer*, Vol. 114, pp.719-126, 1992.

9. Briggs,D.E. and Young,E.H., Modified Wilson Plot Techniques for Obtaining Heat Transfer Correlations for Shell and Tube Heat Exchangers, *Chem. Engg. Prog. Symp. Ser.*, No.92, Vol.65, pp.35-45, 1969.

10. Bromley,L.A., Humpherey,R.F. and Murray,W., Condensation on And Evaporation From Radially Grooved Rotating Disc, *ASME J. of Heat Transfer*, Vol.88, pp. 80-86, 1966.

11. Carnavos,T.C., An Experimental Study: Condensing R-11 on Augmented Tubes, *ASME paper No.80*-HT-54, 1980.

12. Cavallini,A., Doretti,L., Longo,G.A., Rossetto,L., A New Model For Forced-Convection Condensation On Integral-Fin Tubes, *ASME J of Heat Transfer*, Vol.118, pp.689-693, 1996.

13. Chen,M.M., An Analytical study of Laminar Film Condensation Part-2: Single and Multiple Horizontal Tubes, *ASME J. of Heat Transfer*, Vol.83, pp.55-60, 1961.

14. Damodar,N.G., *Basic Economics*, Mc-Graw Hill Int. Ed., p.679, 1988.

15. Dorokhov, A.R., Experimental Study of Condensation of Flowing Freon-12 Vapour on Horizontal Finned Tubes, *Heat Transfer-Sov. Res.*, Vol.11, No.2, pp.123-127, 1979.

16. Deoblin,E.O., Measurement System, 3rd ed., McGraw Hill International Biik Co., 1983.

17. G.,J.,Epstein and Manwell,S.P., Environmental Tradeoffs Between CFCs and Alternative Refrigerants, *ASHRAE Journal*, pp.38-44, 1992.

18. Gogonin,I.I., and Dorokhov,A.R., Enhancement of Heat Transfer in Horizontal Shell-and-Tube Condensers, *Heat Transfer-Sov. Res.*, Vol.3, No.3, pp.119-126, 1981.

19. Henderson,C.L. and Marchello,J.M., Role of Surface Tension and Tube Diameter in Film Condensation on Horizontal Tubes, *AIChE Journal*, Vol.13, No.3, pp.613-614, 1967.

20. Holman,J.P., Teat Transfer, Mc Graw Hill Book Co. 1989.

21. Honda,H., Nozu,S. and Mitsumori,K., Augmentation of Condensation on Horizontal Finned Tubes by Attaching a Porous Drainage Plate, *Proc. ASME-JSME Thermal Engg. Joint Conf.*, Honolulu, Vol.3, pp.189-295, 1983.

22. Honda,H. and Nozu,S., Effect of Drainage Strips on the Condensation Heat Transfer Performance of Horizontal Finned Tubes, *Proc. Int. Symp. Heat Transfer, Beijing*, Vol.2, 1985.

23. Honda,H., Nozu,S. and Furukawa,Y., Effect of porous Drainage Strips on Film Condensation on dowenward Facing Surfaces, *Proc. Int. Heat Transfer Conference*, pp.1713-1718, 1986.

24. Honda,H., Nozu,S. and Takeda,Y., A Theoretical Model of Film Condensation in a Bundle of Horizontal Low Finned Tube, *Boiling and Condensation in Heat Transfer Equipment*, ASME, HTD-Vol.85, pp.79-85, 1987.

25. Honda,H. and Nozu,S., A Prediction Method for Heat Transfer During Film Condensation on Horizontal Low Integral-Fin Tubes, *ASME J. of Heat Transfer*, Vol.109, pp.218-225, 1987.

26. Honda,H., Nozu,S. and Takeda,Y., Flow Characteristics of Condensate on a Vertical Column of Horizontal Low Finned Tubes, Proc. *2nd ASME-JSME Thermal Engg. Joint Conference*, Eds., P.J. Marto, and I. Tanasawa, Vol.1, pp.527-524, 1987.

27. Honda, H., Nozu,S. and Uchima,B., A Generalized Prediction Method for Heat Transfer During Film Condensation on a Horizontal Low-Finned Tubes, *JSME Int. J.*, Series II, Vol.31, No.4, pp.709-717, 1988.

28. Indulkar,M.V. and Sukhtme,S.P., Effect of Fin Height on Heat Transfer During Condensation of R-11 on Horizontal Integral-Fin Tube, *Indian J. of Technology*, Vol.30, pp.387-391, 1992.

29. Isachenko,V.P. and Glushkov,A.F., Heat Transfer with Steam Condensing on a Horizontal Tube and with a Flow of Condensate from Above, *Teploenergetika*, Vol.16, pp.79-81, 1969.

30. Ishihara,K.I. and Palen,J.W., Condensation of Pure Fluids on Horizontal Finned Tube Bundles, Condensers: Theory and Practice, *IChE Symp. Ser.*, No.75, pp.429-446, 1983.

31. Ivanov,O.P., Butyrskaya,S.T. and Mamchenko,V.O., Heat Transfer Attending the Condensation of F-12 Vapour Moving at Bundles of Smooth and Finned Tubes, *Heat Transfer-Sov. Res.*, Vol.4, No.6, pp.143-149, 1972.

32. Jakob,M., Heat Transfer, *John Wiley and Sons, Inc.*, New York, Vol.1, pp.667-673, 1949.

33. Jr.Faber,M.L., Proper Measurement Techniques Reduce Thermocouple Errors, *E.D.N.*, pp.115-119, June 1982.

34. Kabov,O.A., Film Condensation of Immobile Vapours on a Horizontal Finned Cylinder, *Heat Transfer-Sov. Res.*, Vol.16, No.6, pp.76-83, 1984.

35. Karkhu,V.A. and Borovkov,V.P., Film Condensation of Vapour at Finely-Finned Horizontal Tubes, *Heat Transfer-Sov. Res.*, Vol.3, pp.183-191, 1971.

36. Katz,D.L. and Geist,J.M., Condensation on Six Finned Tubes in a Vertical Row, *Trans. ASME*, Vol.70, pp.907-914, Nov. 1948.

37. Katz,D.L., Hope,R.E., Datsko,S.C. and Robinson,D.B., Condensation of Freon-12 with Finned Tubes: Part 1, Single Horizontal Tube, *J. ASRE, Refrig. Engg.*, Vol.53, pp.211-217, 1947.

38. Kern,D.Q., Mathematical Development of Loading in Horizontal Condensers, *AIChE J.*, Vol.4, pp.157-160, 1958.

39. Kisaragi,T., Enya,S., Ochiai,J.K., Kuwahara,K. and Tanasawa,J., On the Improvement of Condensation Heat Transfer on Horizontal Tubes, *JSME paper No.*780-1, pp.1-5, 1978 (in Ref.5).

40. Kline,S.J. and McClintock,F.A., Describing Uncertainti in Single-Sample Experiments, *Mechanical Engineering*, Vol.75, No.3, 1953.

41. Kumar,R., Varma,H.K., Mohanty,B. and Agrawal,K.N., Augmentation of Outside Tube Heat Transfer Coefficient During Condensation Of Steam Over Horizontal Copper Tubes, Int. Comm. Heat and Mass Transfer, Vol.25, No.1, pp. 81-91, 1998.

42. Marto,P.J., and Wanniarachchi,A.S., The Use of Wire Wrapped Tubing to Enhance Steam Condensation in the Tube Bundle, *Heat Transfer in Heat Rejection Systems*, HTD-Vol.37, pp.9-16, 1984.

43. Marto,P.J., Recent Progress in Enhancing Film Condensation Heat Transfer on Horizontal Tubes, *Heat Transfer Engineering*, Vol. 7, pp.53-63, 1986.

44. Marto,P.J., Mitrou,E., Wanniarachchi,A.S. and Rose,J.W., Film Condensation of Steam on Horizontal Finned Tubes: Effect of Fin Shape, *Proc. 8th Int. Heat Transfer Conference*, Sanfrancisco, Vol.4, pp.1695-1700, 1986.

45. Marto,P.J., An Evaluation of Film Condensation on Horizontal Integral-Fin Tubes, *ASME J. Heat Transfer*, Vol.110, pp.1287- 1305, Nov. 1988.

46. Marto,P.J., Zebrowski,D., Wanniarachchi,A.S. and Rose,J.W., Film Condensation of R-113 on Horizontal Finned Tubes, *Fundamentals of Phase Change: Boiling and Condensation*, Ed. H.R. Jacob, ASME, Vol.2, pp.583-592, 1988.

47. Marto,P.J., Film Condensation Heat Transfer Measurements on Horizontal Tubes: Problems and Progress, *Proc. 1st World Conf. on Experimental Heat Transfer, Fluid Mechanics, and Thermodynamics*, Eds. R.K. Shah, E.N. Ganic, and K.T. Yang, pp.1049-1060, 1988.

48. Marto,P.J., Debrowski,D., Wanniarachchi,A.S. and Rose,J.W., An Experimental Study of R-113 Film Condensation on Horizontal Integral-Fin Tubes, *ASME J. of Heat Transfer*, Vol.112, pp 758-767, 1990.

49. Masuda,H. and Rose,J.W., An Experimental Study of Condensation of Refrigerant-113 on Low Integral-Fin Tubes, Proc. *Int. Symp. on Heat Transfer*, Beijing, China, Vol.2, paper 32, 1985, also in *Heat Transfer Science and Technology*, Hemisphere, pp.480-487, 1987.

50. Masuda,H. and Rose,J.W., Condensation of Ethylene Glycol on Horizontal Integral-Fin Tubes, Proc. 2nd *ASME-JSME Thermal Engg. Joint Conference*, Honolulu, Vol.1, pp.525-529, March1987; also in *ASME J. Heat Transfer*, Vol.110, pp.1019-1022, 1988.

51. Mc Adams, *Heat Transmission*, 3rd ed., Mc Graw Hill Book Inc.

52. Mikheyev.M.A., Fundamentals of Heat Transfer, *Peace Publishers*, Moscow, 1965.

53. Mills,A.F., Hubbard,G.L., James,R.K. and Tan,C., Experimental Study of Film Condensation on Horizontal Grooved Tubes, *Desalination,* Vol.16, pp.121-133, 1975.

54. Mitrou,E., Film Condensation Heat Transfer on Horizontal Finned Tubes, *M.S. Thesis,* Naval Postgraduate School, Monterey, California, 1986 (in Ref.45).

55. Moffat,R.J., Using Uncertainty Analysis in the Planning of an Experiment, *ASME J. of Fluid Engineering*, Vol.107, pp.173 178, 1985.

56. Moffat,R.J., Describing the Uncertainties in Experimental Results, *Experimental Thermal and Fluid Science*, Elsevier Science Publishing Co. Inc., New York, pp.3:1-17, 1988.

57. Mohanty,B., Condensation of Steam on Short Tubes in Horizontal Pows Placed in a Vertical Grid, *Ph.D. Thesis*, Dept. of Chemical Engg., University of Roorkee, Roorkee,-247 667, INDIA.

58. Murata,K. and HashiZume,K., Prediction of Condensation Heat Transfer Coefficient in Horizontal Integral-Fin Tube Bundles, *Experimental Heat Transfer*, Vol.5, pp.115-130, 1992.

59. Nakayama,W., Takahashi,K., Senshu,T. and Yoshida,H., Heat Transfer Analysis of Shell-and-Tube Condensers with Shell-Side Enhancement, *ASHRAE Trans.*, Vol.90, part 1B, pp.60-71, 1984.

60. Newson,I.H. and Hodgson,T.K., The Development of Enhanced Heat Transfer Condenser Tubing, Proc. 4th Int. *Symp. on Fresh Water from the sea*, Vol.1, pp.69-94, 1973.

61. Nobbs,D.W., The Effect of Downward Vapour Velocity and Inundation on the Condensation Rates on Horizontal Tubes and Tube Banks, *Ph. D. Thesis*, University of Bristol, England, 1975 (in Ref.47).

62. Nusselt,W., Die Oberflaohen-Kondensation des Wasserdampfes, *VDI Zeitung*, Vol.60, pp.541-546 & 569-575, 1916.

63. Owen,R.G., Sardesai,R.G., Smith,R.A. and Lee,W.C., Gravity Controlled Condensation on Horizontal Integral-Fin Tubes, Condensers: *Theory & Practice, Inst. of Chem. Engrs. Symp. Ser.*, No.75, pp.415-428, 1983.

64. Patil,V.B., Sane,D.K., Jaganmohan,A., and Jagadish,B.S., Condensation of Freon-11 on Plain and Low Fin Single Horizontal Tubes, *Proc. 6th National heat and Mass Transfer Conference*, I.I.T.Madras, India, pp.H51-H55, Dec.29-31, 1981.

65. Pearson,J.F. and Withers,J.G., New Finned Tube Configuration Improves Refrigerant Condensing, *ASHRAE J.*, pp.77-82, June 1969.

66. Perry,J.H., Chemical Engineering Hand Book, Fourth Edition, *McGraw Hill Book Company*, New York, 1963.

67. Prabhakaran,P., Jagadish,B.S. and Sukhatme,S.P., Parametric Study of Film Condensation of R-11 Vapour on Single Horizontal Low Integral-Fin Tubes, *Proc. 10th National Heat Transfer Conference*, R.E.C. Srinagar, India, pp.335-339, Aug. 23-25, 1989.

68. Reid,R.C. and Sherwood,T.K., The Properties of Gas and Liquids, *McGraw Hill Book Company Inc.*, 1958.

69. Rifert,V.G., Steam Condensation on Profiled Surfaces, *Heat and Mass Transfer Process in Porous Media with Phase Change*, Academy of Sciences, USSR, Misk, Ed. A.B.Lykov, pp.149-170, 1982.

70. Rifert,V.G., Baramash,P.A., Golubev,A.B., Leontiev,G.G. and Chaplinskiy,S.I., *Heat Transfer- Soviet Research*, Vol. 9, 1977.

71. Rose,J.W. and Masuda,H., Condensation of Ethylene Glycolon Horizontal Integral Fin Tube, Proc. 2^{nd}, *ASME-JSME Thermal Engineering Joint Conference*, Honululu, 1987.

72. Rudy,T.M. and Webb,R.L., Condensate Retention of Horizontal Integral-Fin Tubing, *Advances in Enhanced Heat transfer,* ASME, HTD-Vol.18, pp.35-42, Aug. 1981.

73. Rudy,T.M. and Webb,R.L., Theoritical Model for Condensation of Horizontal Integral-Fin Tubes, *AIChE, Symp. Series*, 225, Vol.79, pp.11-18,1983.

74. Rudy,T.M. and Webb,R.L., An Analytical Model to Predict Condensate Retention on Horizontal Integral-Fin Tubes, *ASME J. Heat Transfer*, Vol.107, pp.361-368, May 1985.

75. Sreepathi,L.K., Bapat,S.L. and Sukhtme,S.P., An Experimental Study on The Condensing Heat Transfer characteristic of R-123, Prog., 12th *National Heat and Mass Transfer Conference*, Bombay, pp. 459-462, 1994.

76. Shklover,G.G., Milman,O.O., Baskov,V.S. and Aukudinov,G.A., Heat Transfer in Condensation of Steam on Finely-Finned Horizontal Tubes, *Heat Transfer-Sov. Res.*, Vol.13, No.2, pp.108-114, 1981.

77. Shekriladze,I.G. and Gomelari,V.I., Theoretical Study of Laminar Film Condensation of Flowing Vapour, Int. J. Heat Mass Transfer, Vol.9, pp. 581-591, 1966.

78. Sieder,E.N. and Tate,G.E., *Industrial Engineering Chemistry*, Vol.28, pp.1429-1436, 1936.

79. Singh,S.K., Studies of Heat Transfer During Condensation of Steam on an Array of Horizontal Low Integral- Fin Tubes, *Ph.D. Thesis*, Dept. of Mech. and Ind. Eng., University of Roorkee, Roorkee- 247 667, INDIA.

80. Singh,S.K., Varshney,B.S., Mohanty,B., Prakash,R., Condensation of Steam on Array of Horizontal Low Integral Fin Tubes, *J. of Energy Heat and Mass Transfer*, Vol.14, pp 157-170, 1992.

81. Smirnov,G.F. and Lukanov,I.I., Study of Heat Transfer from Freon-11 Condensing on a Bundle of Finned Tubes, *Heat Transfer-Sov. Res.*, Vol.4, No.3, pp.51-56, 1972.

82. Sukhatme,S.P., Condensation on Enhanced Surface horizontal Tubes, ix Int. Heat Transfer Conference, Jerusalem, Vol.1, pp.305-326, 1990.

83. Sukhatme,S.P., Jagadish,B.S. and Prabhakaran,P., Film Condensation of R-11 Vapour on single Horizontal Enhanced Condenser Tubes', *ASME J. of Heat Transfer*, Vol.112, pp.229-234, 1990.

84. Sylvan,J., Isolation and Conditioning Clean up Industrial Signals, *Electronic Design*, pp.169-178, April 29, 1982.

85. Varshney,B.S., Prakash,R., Mohanty,B., and Singh,S.K., A Review of Models for Publication of Heat Transfer Coefficient of Pure Vapours Condensing on Horizontal Low Integral-Fin Tubes, 1988.

86. Wanniarachchi,A.S., Marto,P.J. and Rose,J.W., Film Condensation of Steam on Horizontal Finned Tubes, Effect of Fin Spacing, Thickness and Height, *Multiphase Flow and Heat Transfer*, ASME, HTD, Vol.47, pp.93-99. 1985.

87. Wanniarachchi,A.S., Marto,P.J. and Rose,J.W., Film Condensation of Steam on Finned Tubes-Effect of Fin Spacing, *ASME J. Heat Transfer*, Vol.108, No.4, pp.960-966, 1986.

88. Wanniarachchi,A.S., Marto,P.J. and Rose,J.W., Filmwise Condensation of Steam on Externally Finned Tubes, *Fundamentals of Phase Change: Boiling and Condensation*, HTD Vol.38, Eds. C.T.Avedisian and T.M.Rudy, pp.133-141, 1984.

89. Wenn,R.L., Keswani,S.T. and Rudy,T.M., Investigation of Surface Tension and Gravity Effects on Film Condensation, *Proc. 7th Int. Heat Transfer Conference*, pp.175-180, 1982.

90. Webb,R.L., Enhancement of Film Condensation, *Int. Commun. Heat Transfer MassTransfer*, Vol.15, pp.475-508, 1988.

91. Webb,R.L. and Marawski,C.G., Row Effect for R-11 Condensation on Enhanced Tubes, *ASME J. Heat Transfer*, Vol.112, pp.768-776, 1990.

92. Webb,R.L., Rudy,T.M. and Kedzierski,M.A., Prediction of Condensation Coefficient on Horizontal Integral-Fin Tubes, *ASME J. Heat Transfer*, Vol.107, pp.369-376, 1985.

93. White,R.E., Condensation of Refrigerant Vapours Apparatus and Film Coefficient for Freon-12, *J.Soc., Refg.*, pp.375-379, 1948.

94. Wilson,E.E., A Basis for Rational Design of Heat Transfer Apparatus, *Trans. ASME*, Vol.37, pp.47-82, 1915.

95. Yanzhong,L.I. and Qinjin,W.U., Theoretical and Experimental Investigation of Condensation Heat Transfer and its Enhancement Outside a Horizontal Finned Tube, Proc. *Int. Conf. on Energy Saving in Refrigeration*, China, pp.59- 65, Sept. 17-19, 1986.

96. Yau,K.K., Cooper,J.R. and Rose,J.W., Horizontal Plain and Low-Finned Condenser Tubes-Effect of Fin Spacing and Drainage Strips on Heat Transfer and Condensate Retention, *ASME J. Heat transfer*, Vol.108, pp.946-950, 1986.

97. Yau,K.K., Cooper,J.R. and Rose,J.W., Effect of fin Spacing on The Performance of Horizontal Integral-Fin Condenser Tubes, *ASME J. of Heat Transfer*, Vol.107, pp.377-383, 1985.

98. Yau,K.K., Cooper,J.R., and Rose,J.W., Effect of Drainage Strips and Fin Spacing on Heat Transfer and Condensate Retention for Horizontal Finned and Plain Condenser Tube, *Fundamentals of Phase change: Boiling and Condensation*, ASME HTD Vol.38, Eds. C.T.Avedisian, and T.M.Rudy, pp.151-156, 1984.

99. Young,E.H. and Briggs,D.E., The Condensing of Low Pressure Steam on Vertical Rows of Horizontal Copper and Titanium Tubes, *AIChE J.*, Vol.12, pp.31-35, 1966.

100. Zozulya,N.V., Karkhu,V.A. and Borovkov,V.P., An Analytical and Experimental Study of Heat Transfer in Condensation of Vapours on Finned Surfaces, Heat Transfer- Soviet Research, Vol.9, No.2, 1977.